UNIVERSITY OF CALGARY

Influence of microRNA on Resistance to Proteasome Inhibitors in Multiple Myeloma

by

Erin Stebner Degelman

A THESIS

SUBMITTED TO THE FACULTY OF GRADUATE STUDIES

IN PARTIAL FULFILMENT OF THE REQUIREMENTS FOR THE

DEGREE OF MASTER OF SCIENCE

DEPARTMENT OF MEDICAL SCIENCE

FACULTY OF MEDICINE

CALGARY, ALBERTA

APRIL, 2012

UNIVERSITY OF
CALGARY

Abstract

Multiple Myeloma (MM) is the second most common hematological malignancy with a prevalence of approximately 2,300 new cases and 1,350 deaths in Canada deaths per year. The addition of the proteasome inhibitor Bortezomib to the therapeutic protocol in MM has led to a significant improvement in the survival of patients suffering from this disease. However, patients with MM eventually acquire resistance to Bortezomib resulting in disease progression and eventually death. A small class of genes called miRNA, have recently been shown to be important in the regulation of cancer cell behavior. We have demonstrated that miRNAs are implicated in the acquired drug resistance of MM cells and manipulation of their expression increases sensitivity to Bortezomib. Uncovering the mechanisms of drug resistance will add to our understanding of the biology of this fatal disease and ultimately improve MM patients' survival.

Acknowledgements

I would like to thank my graduate supervisor, Dr. Nizar J. Bahlis for granting me the opportunity to work in his laboratory. He has taught me the importance of the work we have done in the area of multiple myeloma and I admire his dedication not only to his research, but also to his patients. Thank you for your guidance, mentorship and the many opportunities you have provided me. I would also like to thank all of the members of the Bahlis and Bathe laboratories for making my time so enjoyable, in particular Mrs. Kathy Gratton and Dr. Paola Neri, for their support and friendship in the laboratory. Thank you to the members of my supervisory committee, Dr. Oliver Bathe and Dr. Aru Narendran for their helpful comments and guidance. Lastly, thank you to all of my mentors and colleagues within the Southern Alberta Cancer Research Institute, for sharing the passion of the work we do every day.

Dedication

I dedicate this educational journey to my supportive parents, family and friends and most importantly my husband. Thank you to my parents for encouraging me to follow my dreams and supporting my efforts through all of my education. Thank you to my husband for enduring this milestone with me – through all of the good and challenging times. I couldn't have done it without your support throughout this journey.

The best is yet to come for us!

Table of Contents

List of Tables

List of Figures and Illustrations

List of Symbols, Abbreviations and Nomenclature

Symbol	Definition
5'AZA	5'Azacytidine
Ago2	Argonaute 2
Allo-SCT	Allogeneic stem cell transplantation
AML	Acute myeloid leukemia
ASCT	Autologous stem cell transplantation
cDNA	Complementary DNA
CEP	Centromeric enumeration probe
cGy	Centigray
CLL	Chronic lymphocytic leukemia
DAPI	4′,6-diamidino-2-phenylindole
Del	Deletion
DNA	Deoxyribonucleic acid
DNAse	Deoxyribonuclease
DSS	Durie-Salmon Stage
ER	Endoplasmic reticulum
EV	Empty vector
FDA	Food and Drug Administration
FDR	False discovery rate
FISH	Fluorescent *in situ* hybridization
GEP	Gene expression profiling
GFP	Green fluorescent protein
GMR	Geometric mean ratio
GO	Gene ontology
HEK	Human embryonic kidney
HLA	Human leukocyte antigen
IARC	International Agency for Research on Cancer
IC-50	Half maximal inhibitory concentration
IgH	Immunoglobulin heavy locus
IL-6	Interleukin 6
ISS	International Staging System
LNA	Locked nucleic acid
LPH	Liposome polycation-hauronic acid
LSI	Locus specific indicator
Mb	Megabase
MGUS	Monoclonal gammopathy of undetermined significance
miR	miRNA

miRNA	microRNA
MM	Multiple myeloma
M-MSP	Methylated MSP
mRNA	Messenger ribonucleic acid
MSP	Methylation specific PCR
MTS	3-(4,5-dimethylthiazol-2-yl)-5-(3-carboxymethoxyphenyl)-2-(4-sulfophenyl)-2H-tetrazolium]
NCI	National Cancer Institute
ncRNA	Non-coding RNA
NHL	Non-Hodgkin's lymphoma
nt	Nucleotide
NTC	No template control
OG	Oncogene
PAGE	Polyacrylimide gel electrophoresis
PBS	Phosphate buffered saline
PC	Plasma cell
PCA	Principle component analysis
PCL	Plasma cell leukemia
PCR	Polymerase chain reaction
PE	Phycoerythrin
PI	Propidium iodide
PIs	Proteasome inhibitor
Pol II	Polymerase II
Pre-miRNA	Precursor miRNA
Pri-miRNA	Primary miRNA
PSMB5	Proteasome β5 subunit
qRT-PCR	Quantitative real time PCR
R^2	Coefficient of determination
RIN	RNA integrity number
RISC	RNA-induced silencing complex
RNA	Ribonucleic acid
RNAi	RNA interference
RNAse	Ribonuclease
RPMI	Roswell Park Memorial Institute
SC	Subcutaneous
SCID	Severe combined immune-deficient
SCT	Stem cell transplantation
SD	Standard deviation
SDS	Sodium dodecyl sulfate
SEM	Standard error of the mean
SG	Spectrum green
siRNA	Small interfering RNA
SMM	Smoldering multiple myeloma
SO	Spectrum orange

SSC	Standard saline citrate
t	Translocation
TAE	Tris -acetate-EDTA
TRBP	Transactivation-responsive RNA binding protein
TSG	Tumour suppressor gene
U-MSP	Unmethylated MSP
UPR	Unfolded protein response
UTR	Untranslated region
WHO	World Health Organization

Chapter One: Introduction

1.1 Multiple Myeloma

Multiple Myeloma (MM) is an incurable plasma cell (PC) neoplasia characterized by the accumulation of malignant plasma cells, usually within the bone marrow[1-3]. It is estimated that in 2011 there were 2,300 new cases, with 1,350 deaths in Canada[4]; the second most common haematological malignancy, after non-Hodgkin's Lymphoma (NHL)[5]. MM is a malignancy of antibody-secreting terminally differentiated B cells that home to and expand in the bone marrow. The most common symptoms include fatigue, anemia, bone pain and frequent infections[2] and criteria for diagnosis include hypercalcemia, bone lesions and renal failure. In regions adjacent to plasma cell foci, bone lesions develop from the activation of osteoclasts and the inactivation of osteoblasts[6]. Patients will also present with detectable levels of monoclonal plasma cells. Patients with nonsecretory myeloma will have no detectable monoclonal protein, which may be monitored using the serum free light-chain assay[2]. In many cases, MM is preceded by a pre-malignant tumour called monoclonal gammopathy of undetermined significance (MGUS). This type of tumour is the most common lymphoid tumour in humans and occurs in approximately 3% of individuals over the age of 50[7].

1.1.1 Staging

Although multiple myeloma is considered to be a single disease, it consists of several cytogenetic, molecular and biological subtypes. However, survival for MM patients depends on many variables, including disease stage, age and renal function. The

current classification system of MM staging relies on tumour mass, renal function and immune response, the latter being secondary features of host reaction to the disease[8]. There are two methods of staging including the Durie-Salmon Stage (DSS)[9] and the International Staging System (ISS)[10] as summarized in Table 1-1. The ISS for myeloma uses serum-β2-microglobulin and serum albumin as prognosis predictors to classify in three stages[10]. The stages have median survival of 62, 44 and 29 months respectively. While this staging method may be useful in some cases, it does not take into account disease burden and cytogenetic characteristics. For example, a patient with Stage I myeloma and a (4;14) translocation has a significantly shorter expected survival. Treated with standard chemotherapy, the median survival is 26 months, and 33 months with high-dose therapy. A significantly shorter expected survival is also seen in patients with a (14;16) translocation, with a median survival of 16 months, regardless of what ISS stage they have been classified in[11].

Myeloma has also been classified into early and advanced Myeloma regardless of the ISS or Durie-Salmon criteria. Depending on the level of monoclonal Ig (M-Ig), MGUS can progress sporadically to multiple myeloma, expressing the same M-Ig levels[12]. However, as there are no defined genetic or phenotypic markers, it is difficult to distinguish MGUS from MM cells. Smoldering MM (SMM) has stable bone marrow tumour content but has no osteolytic lesions, anemia or other secondary characteristics of MM and has a high probability of progressing to MM[13]. Extramedullary MM is an aggressive tumour, often called secondary or primary plasma cell leukemia (PCL).[7]

Table 1-1. Multiple Myeloma Durie-Salmon and ISS Staging Criteria

Stage	Durie-Salmon Criteria	ISS Criteria
I	A relatively **small** number of myeloma cells are found. All of the following features must be present: - Hemoglobin level only slightly below normal (above 10 g/dL) - normal bone x-rays or only 1 area of bone damage - normal blood calcium levels (less than 12 mg/dL) - small amount of monoclonal immunoglobulin in blood or urine	Serum Beta-2 microglobulin is less than 3.5 mg/L Albumin level is 3.5 g/dL or higher
II	A **moderate** number of myeloma cells are present. Features are between stage I and stage III	Serum Beta-2 microglobulin level is between 3.5 and 5.5, and any albumin level OR Albumin is below 3.5 while the beta-2 microglobulin is less than 2.5
III	A **large** number of myeloma cells are found One or more of the following features must be present: - low hemoglobin level (below 8.5 g/dL) - high blood calcium level (above 12 mg/dL) - 3 or more areas of bone destroyed by cancer - large amount of monoclonal immunoglobulin in blood or urine	Serum Beta-2 microglobulin is greater than 5.5 mg/L

Adapted from Hideshima et al. [14]

1.1.2 Cytogenetic Aberrations

For most hematological disorders, routine cytogenetic analysis has become a part of routine laboratory testing, providing valuable diagnostic and prognostic indicators. The cytogenetic aberrations help to understand the molecular pathogenesis of the disease [15]. Routine metaphase cytogenetics allows for detection of large clonal populations and supports the cytomorphic diagnosis and provides useful prognostic information. Chromosomal abnormalities are not present in all MM cases. In approximately 50% of patients, an abnormal karyotype is seen, although this may be reflected by the low resolution of cytogenetic analysis, approximately 1 to 10 megabases (Mb)[16]. Studies using comparative genomic hybrization arrays have shown that almost 100% of the patients with myeloma have chromosomal abnormalities.[5] While a normal cytogenetic result indicates a more favorable prognosis, there is a large clinical diversity within the normal group.

Using routine metaphase cytogenetics, this group cannot be further differentiated using this criteria alone [15]. Cryptic clonal lesions are not found using this method and are missed in both cytogenetically normal and abnormal patients. Cryptic rearrangements further contribute to clinical heterogeneity and will modify the prognosis from the original karyotype[16]. Common cytogenetic rearrangements have been seen in Myeloma patients and have been commonly associated with certain prognostic outcomes. The presence of hyperdiploidy is generally considered favorable and leads to extended life after high dose chemotherapy treatments. The four most frequently recurring translocations involve regions 4p16 (FGFR3), 11q13 (Cyclin D1), 6p21(cyclin D3) and 16p23 (c-maf) and all have breakpoints that fall within IgH regions and result in IgH

switch recombination[17,18]. Common translocations including t(11;14) and t(6;14) are present in approximately 20% of patients and is associated with neutral prognosis. There are many genetic features of high risk disease including t(4;14), t(14;16) and t(14;20), accounting for 15, 6 and 8 percent of patients respectively. The t(14:16)(q32;q23) and t(14;20)(q32;q11) translocations result in the activation of c-MAF and MAFB proto-oncogenes and t(4;14)(p16;q32) translocation results in hyeractivation of both the FGFR3 and MMSET genes. Cyclin D1 is activated by the t(11;14)(q13;q32) translocation, and CCND3 is activated by the t(6;14)(p21;q32) recurring translocations in MM.

Clonal evolution and secondary events that alter prognosis include inactivation of p53 (17p13), chromosome 13 deletions and amplification of chromosome 1 (10, 50 and 35 percent of patients)[5,19]. The cytogenetic results need to be combined with other diagnostic and prognostic data to select the best treatment option for best chance of survival. Multiple myeloma is not of one disease, but rather one of many. Each of the subtypes of MM is largely defined by the specific genetic and cytogenetic aberrations. The ultimate application of predictive classification and targeted therapies is needed on the basis of primary genetic changes.

1.1.3 Molecular Classification of MM

With the advent of high density oligonucleotide DNA microarray it has been made possible to simultaneously analyze messenger RNA (mRNA) expression patterns of thousands of genes. To better define the molecular bases of MM, gene-expression profiling has also be used to classify patients with adverse prognosis using gene-specific signatures[6,20]. An eight group classification system using knowledge of cytogenetic

results and cyclin D genes determined by gene expression profiling (GEP)[21] has been suggested although the system proposed by Zhan et al for newly diagnosed myeloma patients into seven subgroups based on common gene expression signatures is more widely used[6]. Unsupervised hierarchic clustering of messenger RNA (mRNA) expression of syndecan-1 (CD 138 MM marker) in patients has identified seven disease subtypes that are largely influenced by known genetic lesions, including c-MAF, MAF-B, CCND1/3 and FGFR3/MMSET-activating translocations as well as hyperdiploidy. While favorable prognosis is seen in patients with hyperdiploidy and CCND1 activation[22,23], poor prognosis is associated with MAF, FGFR3/MMSET activation as well as deletion of chromosomes 13 and 17[24-26]. Molecular classification has tremendous clinical implications to identify the main genetic subtypes to the other high-risk subgroups effecting treatment plans and potentially outcomes.

1.1.4 Therapeutic Agents in the Treatment of MM

New therapeutic agents in the treatment of multiple myeloma have led to dramatic improvements in outcomes over the last decade. New agents including bortezomib[27], lenalidomide[28], thalidomide[29] and autologous stem-cell transplantation (ASCT) have increased the three year survival rates to 75-80%, with a median survival of 5 years.

Treatment for newly diagnosed MM depends largely on the eligibility for ASCT, determined by age, performance status and comorbidities. Patients who are eligible for ASCT are typically treated with a regimen that is non-toxic to the hematopoietic stem cells. This typically includes vincristine, doxorubicin and dexamethasone as induction therapy for three to four months before stem-cell harvest. Other therapeutic agents

including melphalan, an alkylating agent, are not typically used for pre-ASCT as it can interfere with adequate stem-cell mobilization[30]. The most frequently used regimens for the treatment of newly diagnosed MM include combinations of lenalidomide, bortezomib, thalidomide and dexamethasone. Patients who are not eligible for transplantation due to factors such as age, physical condition or other co-existing conditions, receive standard therapy with alkylating agents[31]. Although ASCT is not considered a curative therapy, it greatly improves the likelihood of achieving a complete response (CR), prolongs disease-free survival and overall survival and has proven to be a major advantage therapy option in the treatment of MM[32]. Allogeneic SCT (allo-SCT) is also a treatment option for patients, although a smaller percentage of patients are candidates for this type of transplant[33]. The availability of an HLA-matched sibling donor, adequate organ function and age, makes many candidates ineligible. While this type of treatment has a biological advantage as it is not contaminated with any tumor cells, such as in ASCT, there is also a high rate of treatment related death and graft versus host diseases, making it unacceptable for most patients.

Almost all MM patients have a risk of eventual disease relapse. If relapse occurs after six months after conventional chemotherapeutics, an additional round may be used, or for those who had stem cells cryopreserved, can benefit from the use of ASCT as salvage therapy[34]. Additional chemotherapeutics such as thalidomide or bortezomib are also used in the treatment of refractory MM to target alternative biological pathways.

1.2 Proteasome Inhibitors

Degradation of proteins in the ubiquitin-proteasome pathway is a crucial process to regulate translation, signal transduction, cell-cycle control and receptor function[35]. This pathway plays a vital role in cellular events and is responsible for intracellular protein degradation. Targeting this pathway using inhibitors of the proteasome demonstrate a novel approach in the treatment of cancer. Inhibitors of this pathway have been developed for research and clinical use[36]. The FDA approved inhibitor Bortezomib (PS-341, Velcade®) has been in clinical use for the treatment of relapsed multiple myeloma and is in trial for use in many others cancer types[37]. The rapid approval and effectiveness in clinical trials of bortezomib has led the way for discovery for other proteasome inhibitors (PIs) and other inhibitors targeting the ubiquitin-proteasome pathway.

1.2.1 The Proteasome

The proteasome is a multi-subunit protein complex found in the nucleus and cytoplasm of eukaryotic cells. The main function is to degrade intracellular proteins that are tagged with a poly-ubiquitin chain [35,38]. The 26s proteasome is a cylindrical structure, made up of a 20s catalytic core complex and two 19s regulatory subunits that cap the core complex (Figure 1-1). The 20s core is made up of 4 stacked rings including 2 outer α rings and 2 inner β rings, which are each made up with seven similar subunits [39,40].The outer rings interact with the 19s subunit and control entry of tagged proteins into the core complex while the inner rings include enzyme sites that degrade the protein. Proteins that are targeted for degradation are modified with a poly-ubiquitin protein chain through a process called ubiquitination. These tagged molecules are recognized by the 19s subunit

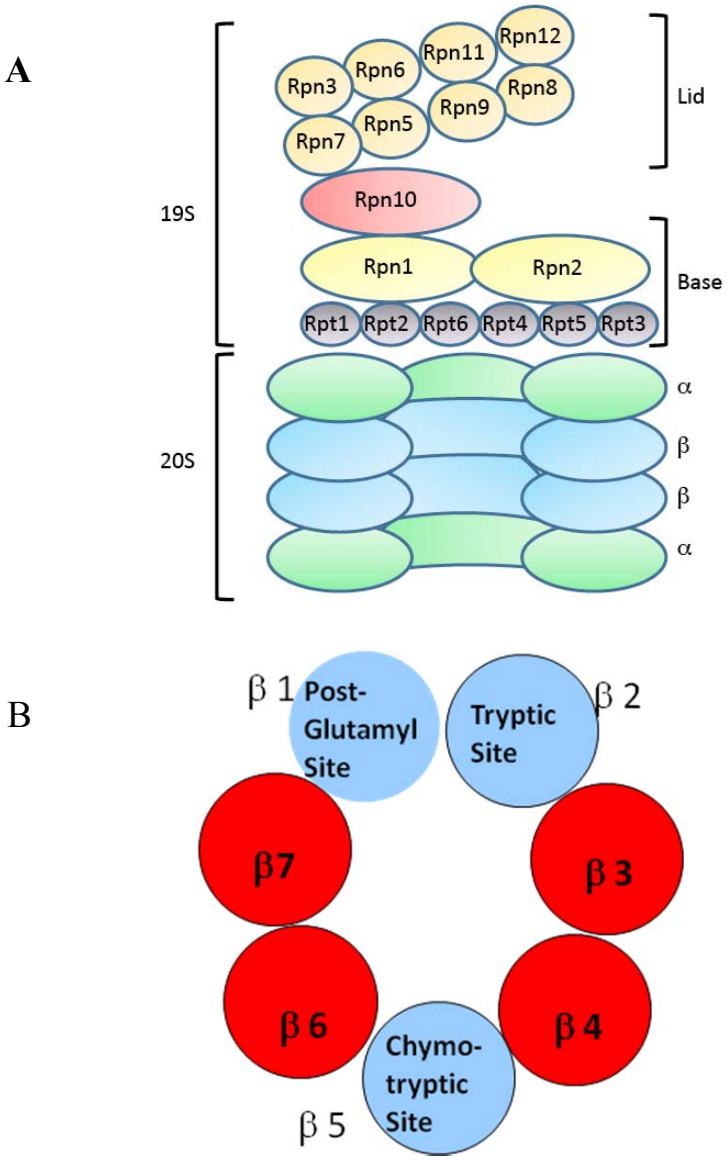

Figure 1-1. Structure of the 26s proteasome complex

A. The 26s proteasome is composed of a core 20s complex capped by 19s regulatory complexes at both ends. **B**. The cross-section of a the β ring of the 20s subunit of the proteasome contain the post-glutamyl, tryptic and chemotryptic sites.

which removes the ubiquitin chain and denatures the protein. The denatured protein is then fed through the center of the 20s complex and is subsequently reduced into short polypeptides[41]. Proteins that enter the 20s complex are hydrolyzed by six active proteolytic sites on the β-subunits including chemotryptic, tryptic, and peptidylglutamyl-like activity sites [42].

1.2.2 Proteasome Inhibition

The proteasome pathway is responsible for degrading several tumour suppressors, regulatory proteins, transcription factors and oncogenes. Inhibition of this pathway induces apoptosis by altering levels of target proteins including proaptotic proteins such as p53 and Bax and results in the inhibition of NF-κB activity. Clinical studies using proteasome inhibitors have shown that transformed malignant cells are more sensitive to proteasome inhibition than normal cells[43]. Numerous studies have shown in preclinical and clinical trials that the use of proteasome inhibitors induces apoptosis in various cancer types although they generally lack specificity. [40,43-46]. These studies have shown that the proteasome is a valid and useful target for anti-Myeloma therapy.

1.2.3 Bortezomib (Velcade ®)

Bortezomib (N-pyrazinecarbonyl-l-phenylalanine-L-leucine boronic acid or PS-341, MLN-341) was approved in the United States in 2003 and in the European Union in 2004 for the treatment of relapsed and refractory multiple myeloma patients [36,39]. Adams et al designed and developed boronic acid-derived compounds that inhibit the proteasome pathway in a specific manner [36]. It is a small, cell-permeable molecule that inhibits the

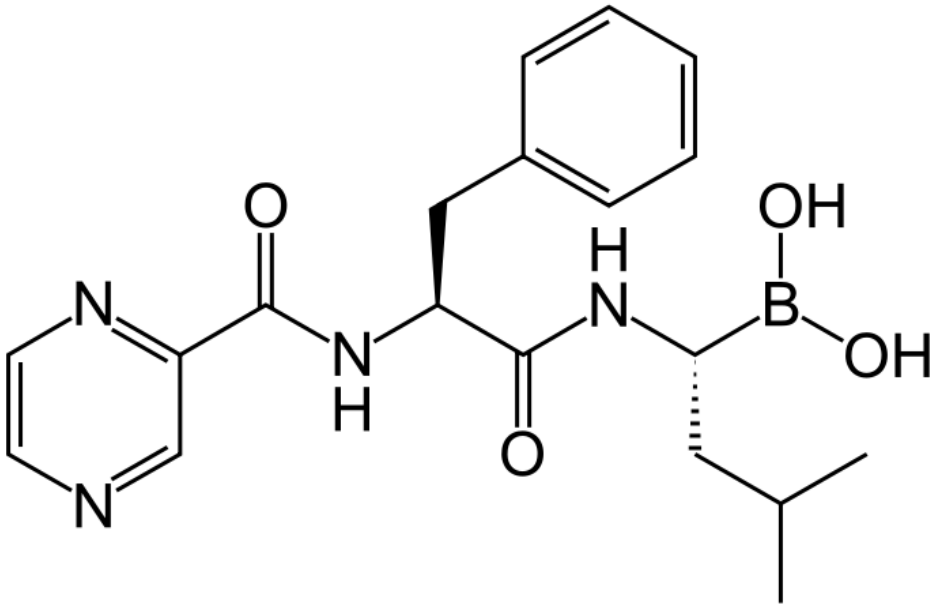

Figure 1-2. Chemical structure of Bortezomib

proteasome in a selective and reversible manner and blocks the β5 chemotryptic site of the 20s subunit of the proteasome [40]. Bortezomib induces apoptosis in malignant cells by stabilizing proapoptotic proteins and through the inhibition of NF-κβ[39]. It inhibits the proteasome pathway in a reversible and rapid manner by binding with the 20s proteasome complex, effectively blocking its enzymatic activity.

Preclinical studies have shown that the apoptotic and cytotoxic effects of bortezomib are correlated with proteasome inhibition, independent of p53 status and do not overlap with other chemotherapeutic agents. It was used against the National Cancer Institute's (NCI) cell line panel and averaged 50% growth inhibition. The same effect was seen when used as a single agent in human xenograft tumor models [47]. The success of the preclinical trials led to the rapid approval of a phase I trial run by Orlowski et al where 27 patients with advanced refractory hematological malignancies were treated with Bortezomib[48]. The success of this trial led to other phase I trials and furthermore phases II and III and ultimately approval into clinical use. In each of the trials, it had been assessed that Bortezomib had a significant activity against MM cells. The most common adverse effects of bortezomib include gastrointestinal symptoms, cytopenia, fatigue and peripheral neuropathy[49] and is generally tolerated well.

Bortezomib inhibited proliferation induced apoptosis and inhibited binding of MM cells to bone marrow stroma[37,48]. Bortezomib also sensitized MM patients and cell lines to other active chemotherapeutic agents, such as doxorubicin and melphalan. In patients with relapsed myeloma following conventional dose therapy or stem cell transplantation, bortezomib is often combined with conventional dose chemotherapy, corticosteroids or thalidomide[50,51]. Clinical trials for the use of bortezomib in other hematological and non-

hematological malignancies are ongoing and have shown promising data particularly in mantle-cell lymphoma and low grade follicular lymphoma[45,52]. More work is needed in this area with bortezomib and other proteasome inhibitor compounds, including multi-agent models.

1.2.4 The Mechanism of Action of Bortezomib

Bortezomib was originally developed as a proteasome inhibitor which blocked the degradation of ubiquitinated Iκβα, a negative regulator of the canonical nuclear factor (NF)-κβ pathway, preventing its translocation into the nucleus[53,54]. However, several groups have proposed additional mechanisms for its anti-tumour activity, focusing on the accumulation of misfolded proteins followed by endoplasmic reticulum (ER) stress associated apoptosis, and the activation of the ATF4 and CHOP pathways[55,56].

1.2.5 Accumulation of Misfolded Proteins

When proteasome function is inhibited by bortezomib, damaged proteins including mis-folded proteins accumulate in the intracellular environment. This results in an ER overload and stress, which induces the unfolded protein response (UPR)[57]. The UPR aims to decrease the synthesis and influx of protein into the ER and increase the synthesis of chaperone proteins in order to promote refolding and elimination of misfolded proteins[58]. However, sustained ER stress resulting from proteasome inhibition activates the apopototic pathway through activation of ATF4 and CHOP, caspase-4 and caspase-12, ultimately leading to cell death. It has been demonstrated that preventing the

accumulation of misfolded proteins, and avoiding ER stress plays an important role in bortezomib resistance in MM cells[59].

1.2.6 Bortezomib resistance

Unfortunately, bortezomib, largely used in the treatment of relapsed and refractory MM is only effective in approximately 40% of treated patients[27] and presently there are no clinical biomarkers available to predict responders to this class of drugs.

In order to understand the mechanism of bortezomib resistance, recent studies have used RNA interference (RNAi) screens to evaluate the genetic determinants that may influence sensitivity to bortezomib. Chen *et al*, performed a genome-wide small interfering RNA (siRNA) screen and identified 100 genes whose knockdown affected the cytotoxicity of bortezomib[60]. They have demonstrated that more than half of their genes interacting with bortezomib cytotoxicity gave similar phenotypes in three different cell types (colon cancer, melanoma, and cervical cancer). While they have identified common themes including translation inhibition and key ubiquitin pathways, detailed work is needed in MM cell lines to further elucidate this resistance mechanism. A similar study was performed by Zhu *et al*, whereby a druggable genome RNAi screen was performed on MM cells to identify modifiers of bortezomib sensitivity[61]. Measuring proliferation in MM cells transfected with siRNAs in the presence and absence of bortezomib, 37 genes were identified which when silenced; potentiate the cytotoxic effect of bortezomib.

Additionally, mutations in the gene encoding for the proteasome β5 subunit (PSMB5), which is the target site of bortezomib, has been shown to increase resistance to bortezomib[59].

There is little known about the biology and genetics of Multiple Myeloma and the advancement in therapy options has been slow. Myeloma cells have antiapoptotic signaling mechanisms which results in resistance to current chemotherapy treatments and ultimately a fatal outcome for most patients. [62] Although high-dose therapy has improved Multiple Myeloma prognosis, individual patient survival is extremely variable. It is difficult to accurately predict prognostic outcomes with current testing. By gaining further understanding of the biology of myeloma cells and identifying potential therapeutic targets, new treatments can be identified to not only improve patient outcome but will also assist in more accurate diagnosis and prognosis to treat patients more effectively. Identification of the mechanisms of drug sensitivity and resistance can also be made to develop more effective therapies and treatment strategies.

1.3 microRNA

One of the most important discoveries in the past decade is that non-coding RNAs (ncRNAs) identified in tumours and are involved in tumour initiation, progression and dissemination of disease. The most studied ncRNA constitute a class of RNAs named microRNAs (miRNA). In recent years, miRNA has been identified as an important new class of regulatory biomolecules. miRNA are small non-coding RNAs of 18-24 nucleotides (nts) that regulate mRNA at the post-transcriptional level and their deregulation contributes to the initiation and progression of several cancers[63]. miRNAs are strongly conserved among organisms including invertebrates, vertebrates and plants and are involved in many biologic processes including cell cycle regulation, proliferation, differentiation, development, and carcinogenesis[63,64]. Since the discovery of the first

small non-coding RNAs, known as in lin-4 and let-7 in *Caenorhabditis elegans*[65,66], over 15,000 unique miRNA sequences have been identified in over 140 species[67-71]. The approximate number of human miRNAs reported so far exceeds 1,900 (Nov, 2011 release of miRBase 18.0, Sanger Institute) and each miRNA has the potential to target a large number of genes. Computational predictions have estimated that approximately 30% of all human genes are targets of miRNA[72]. miRNAs are capable of regulating gene expression by binding to the 3' untranslated region (UTR) of their target mRNAs through partial or complete complementarities. As such, miRNAs are involved in crucial biological processes including apoptosis, differentiation, proliferation and development[63,73]. By targeting the mRNA of protein-coding genes and regulating the transcriptional expression, miRNA plays a pivotal role in biological function.

1.3.1 miRNA Processing

Processing of miRNA begins in the nucleus, where RNA polymerase II (Pol II) transcribes primary miRNA transcripts, (called pri-miRNA), a capped polyadenylated portion of a larger RNA hairpin. The Ribonuclease III (RNAase III) enzyme called Drosha then cleaves the upper part of the hairpin to produce precursor miRNA (pre-miRNA) of ~70 nts[74,75]. The pre-miRNA is then exported to the cytoplasm by the nuclear export factor, exportin 5[76]. It then binds to the RNase II Dicer and the RNA-induced silencing complex (RISC)[77] which is composed of the transactivation-responsive RNA-binding protein (TRBP) and Argonaute 2 (Ago2)[78]. Ago2 cleaves the miRNA at the 3' end and then Dicer cleaves it into the mature 18-24-nt miRNA duplex. This duplex contains the 'guide strand' and the 'passenger strand', which must be separated in order

for the miRNA in RISC to anneal to the target. The strand retained in RISC is the guide strand and the discarded strand is the passenger strand[79] Selection of the guide strand is not random and one is preferred to be the guide strand based on the thermostability of the first 1-4 bases at each end of the miRNA duplex[80]. The strand which has the least stability at the 5' end serves as the guide strand, while the other strand is degraded. The single stranded mature miRNA can direct the RISC to downregulate expression by two posttranscriptional mechanisms: mRNA translational repression or mRNA cleavage. Once bound to RISC, the seed sequence (2-8 nts) at the 5' end of mature miRNA strand recognizes complementary sequences in the 3'UTR of mRNAs, resulting in translation inhibition. The choice of posttranscriptional mechanisms is largely unknown, but has been suggested it is determined by the mRNA target and the level of complementarity.

1.3.2 miRNA and the Role in Cancer

It has been widely known that cancer is caused in part by genetic and/or epigenetic modifications to protein-coding oncogenes and tumour suppressor genes. These modifications result mainly from somatic mutation events that are caused by chromosomal rearrangements, amplifications and deletions. The discovery of miRNAs has introduced a new level of gene regulation and additional understanding of the pathogenesis of many cancers. Among the first clues for the involvement of miRNAs in cancers was an observation that miRNAs are frequently located in cancer associated chromosomal regions. This includes regions of amplifications, deletions, fragile sites, common cancer associated translocation sites and breakpoint regions in or near tumour suppressors (TSG) or oncogenes (OG)[81]. The global miRNA expression (known as

miRNome) has been investigated in many different human tumours. It has been demonstrated through large profiling and functional studies that miRNA can function as OGs (as in the case of miR-155 or the miR-17-92 cluster) or TSGs (as in the case of miR-15a and miR-16-1[82]), when the functional loss of a target mRNA can initiate, enhance or inhibit malignant transformation[83-86]. Interestingly, miRNAs have also been reported to play dual roles, as both tumour suppressors and oncogenes, depending on the distinct pathways it targets[87,88]. This implies that miRNAs may target multiple distinct pathways resulting in different effects on growth, cell survival and proliferation, which may be distinct in varying cell types. The genetic abnormalities found to influence the activity of miRNAs are similar to the alteration of protein-coding genes such as chromosomal translocations or rearrangements, genomic deletions or amplifications or mutations. In tumours, abnormalities are found that influence both the protein-coding genes and miRNA[89].

Since the discovery of miRNA, an increasing number of studies have suggested that miRNA influences tumour development, progression and metastases. The first study demonstrating a role of miRNAs as TSG, was through the investigation of a frequently observed chromosomal abnormality in chronic lymphocytic leukemia (CLL); the hemizygous or homozygous deletion of the 13q14.3 region[82]. A cluster of miRNAs, miR-15a and miR-16-1 was discovered in this chromosomal region mapping to the 30-kb deleted region of the LEU2 gene. Over-expression of miR15a/16-1 reduces the expression levels of the prosurvival molecule Bcl2 inducing apoptosis[88]. Mouse models that lacked the miR-15a/16-1 clustered developed B-cell abnormalities, suggesting the importance of this miRNA cluster in pathogenesis of disease.

One of the first oncogenic miRNAs identified was the miR-17-92 cluster, which contains seven homologous miRNAs (miR-17-3p, miR-17-5p, miR-181a, miR-20a, miR-19a, miR-19b-1 and miR-92a-1). It has been shown that the cluster is frequently overexpressed in many hematopoietic malignancies, particularly in B-cell lymphoma. Alterations of miRNAs have since been detected in nearly all tumour types to date including benign and malignant, solid and liquid tumours, suggesting miRNAs have a large role in tumorigenesis. It has been suggested that alterations and over-expression of miRNA play a large role in most, if not all, human cancers[86].

1.3.3 miRNA and the Role in Multiple Myeloma

Differential miRNA expression associated with distinct genetic subtypes has been reported in numerous hematologic malignancies, such as acute myeloid leukemia (AML)[90,91] and chronic lymphocytic leukemia (CLL)[87,92]. The presence of specific genetic abnormalities including trisomy 12 and 13q14, 11q23 and 17p13 deletions have been associated with specific miRNA signatures. The miRNAs identified in the signature were largely localized to the chromosomal regions specific for the abnormality. The identification of specific miRNA patterns may help to distinguish distinct genetic subgroups as well as provide a better understanding of the miRNA pathogenesis.

In MM, an association between high-risk disease and global elevation of miRNA expression has been reported[93]. Zhou *et al* has shown that total miRNA expression levels in CD138-positive plasma cells from patients with MM are significantly higher than in normal plasma cells. They have also shown that high expression levels of miRNA may be associated with high MM risk score[93]. In addition, miRNA involvement in the clonal

evolution of plasma cells from MGUS to MM stages and correlation with specific MM molecular subgroups has been described[94-96]. Mechanistically, over-expression of selected miRNAs has been also shown to reduce MM cell growth and viability[97]. Pichiorri *et al* has reported a set of miRNA that is associated with progression and neoplastic transformation of MM and Lionetti *et al* has reported differential microRNA patterns that have been associated with the major IGH translocations[95]. Specific signatures were found to be associated in t(4;14) patients, where the over –expression of let-7e, miR-125a-5p and miR-99b was seen, and to a lesser extent in patients with t(11;14). While attempts have been made to use miRNA in classifying and staging MM, little is known about the expression of miRNAs and their effects on response to MM treatments.

1.3.4 miRNA and Bortezomib Resistance in MM

The first mechanism to suggest that microRNA may play a role in MM cell resistance to bortezomib is based on the concept of the activation of the UPR. As discussed previously, it has been shown that high-risk myeloma patients have a global elevation of miRNA[93] . As miRNA target mRNA and inhibit translation, an increase of miRNA would result in decreased levels of protein synthesis. This would then decrease the stress on the ER, resulting in decreased levels of the UPR, providing a crucial role in resistance to bortezomib. This concept is based on the notion that decreased accumulation of mis-folded proteins alleviates ER stress and therefore increases bortezomib resistance has been previously described above where mutations in PSMB5 result in a bortezomib

resistance. This is the first study to correlate increased miRNA levels, UPR stress and bortezomib resistance.

The second mechanism to correlate miRNA levels and bortezomib resistance is based on the concept that valuable genes mediating sensitivity are potentially regulated by miRNA. As discussed previously, RNAi screens have identified several genes known to be sensitizers to bortezomib. These include several cell cycle regulators and kinases that are mRNA targets regulated by miRNA expression. Based on these two possible mechanisms of how microRNAs may modulate bortezomib drug resistance it is has led to the following hypothesis:

We hypothesize that miRNAs regulate MM cells sensitivity to proteasome inhibitors and may represent a valuable predictive biomarker of response to therapy.

1.4 Study Objectives

While reports provide strong evidence for the role of miRNAs in MM, studies investigating their value as predictive biomarkers of response to individual therapies are still needed. Based on our preliminary studies and published literature, we have postulated that ***miRNAs regulate MM cells sensitivity to proteasome inhibitors and may represent a valuable predictive biomarker of response to therapy.***

This hypothesis was tested under the following specific aims:

1. *Identify differential miRNA expression signatures in resistant versus sensitive primary multiple myeloma cell lines.*
2. *Determine in vitro, the function of selected differentially expressed miRNA in resistant and sensitive cell lines.*
3. *Examine in vitro and in vivo, the effect of silencing or over-expressing selected miRNA on MM cell growth and sensitivity to bortezomib.*

By gaining further understanding of the influence of miRNA on myeloma cells and the mechanisms of drug resistance, it will be possible to identify potential therapeutic targets and further understand the biology of this disease.

Chapter Two: Materials and Methods

2.1 Cell Line and Cell Culturing

The human MM cell lines NCI-H929, RPMI-8226 and U266 were purchased from the ATCC, Manassas, USA; KMS11, MM1s, and OPM2 cells were kindly provided by Dr Lawrence Boise (Emory University, Atlanta, GA) and INA-6 cells were provided by Dr. Renate Burger (University of Erlangen-Nuernberg, Erlangen, Germany). MM cell lines were maintained in RPMI-1640 media, with L-glutamine and $NAHCO_3$, supplemented with 10% fetal bovine serum and 1% penicillin and streptomycin (100 U/ml penicillin, and 100 μg/ml streptomycin) (Sigma-Aldrich, Oakville, ON), in a humidified incubator at 37°C with 5% CO_2. INA-6 cells were maintained in culture media supplemented with 2.5 ng/ml of human interleukin-6 receptor (IL-6) (Sigma-Aldrich).

2.2 Viability Assays

IC_{50} was determined by calculating the concentration of Bortezomib or 5'Azacytidine that caused a 50% loss of viability measured by [3-(4,5-dimethylthiazol-2-yl)-5-(3-carboxymethoxyphenyl)-2-(4-sulfophenyl)-2H-tetrazolium] (MTS) according to the manufacturer's directions(Promega, Madison, WI).

2.2.1 Bortezomib

Bortezomib was obtained from the Tom Baker Cancer Center (Calgary, AB) and reconstituted in water and stored at 4°C. Bortezomib was freshly diluted in free RPMI

Media before use. MM cell lines were treated with various concentrations of Bortezomib ranging from 0.625 nM to 5.0 nM for 24 and 48 hours.

2.2.2 5'Azacytidine

5' Azacytidine (5'AZA) was obtained from Sigma Aldrich (Cat # A2385). 5'AZA was freshly made by dissolving 5'AZA powder in complete 10% RPMI to a final concentration of 1.0uM. MM cell lines were treated with 12.5 – 100 nM for 12-48 hours.

2.2.3 MTS Assay

Proliferation was measured by [3-(4,5-dimethylthiazol-2-yl)-5-(3-carboxymethoxyphenyl)-2-(4-sulfophenyl)-2H-tetrazolium] (MTS) according to the manufacturer's directions (Promega, Madison, WI). MM cells with appropriate drug concentration were plated in a 96 well plate, in a total of 200ul volume. After appropriate timing, 40ul of Cell Titer 96 Aqueous One Solution was added to each well and incubated for three hours in a humidified 5% C02 chamber. After 3 hours, the plate was read on a 96 well plate reader at a wavelength of 490nm.

2.3 Cell Cycle Analysis

Cells were synchronized at the G1/S phase using a double-thymidine block. MM cells were seeded in standard growth medium (RPMI – 10% FBS) the night before synchronization. 100 mM Thymidine stock was made up in PBS and was filter sterilized. Thymidine was added to a final concentration of 2mM in the media, and cells were incubated for 16 hours under normal conditions. To remove the thymidine-containing

media, the cells were spun down and rinsed once with fresh media. Cells were re-fed with fresh standard media and incubated for 8 hours. The second thymidine was again added to a final concentration of 2mM in the media and incubated for an additional 16 hours. The thymidine-containing media was then removed, washed once and fed with fresh media. The cells were then collected at various time points, (Time 0, 4, 8, 16, 24 and 48 hours), spun down and washed twice with cold PBS. Cells were re-suspended in 500ul cold PBS and fixed by adding 500ul of cold 95% ethanol dropwise while vortexing. Cells were fixed for a minimum of 24 hours, stored at -20°C before proceeding with flow cytometric analysis of nucleic content.

2.4 DNA Extraction

MM cells were collected and harvested and DNA was extracted using Qiagen Dneasy kit according to manufacturer's instructions. DNA was stored in DNase-free water at -20°C until use. Quantity and purity of DNA was measured on a NanoDrop spectrophotometer (ThermoScientific). Purity of DNA was gauged used the A260/A280 ratio where a ratio of 1.7-1.9 was considered acceptable.

2.5 RNA Extraction

MM cells were collected and harvested and RNA was extracted using Qiagen miRNeasy kit according to manufacturer's instructions. RNA was stored in RNase-free water at -80°C until use. Quantity and purity of RNA was measured on a NanoDrop spectrophotometer

(ThermoScientific). Purity of RNA was gauged used the A260/A280 ratio where a ratio of 1.9-2.1 was considered acceptable.

.

2.6 Preparation of cDNA

200 ng of total RNA were reverse transcribed to cDNA with SuperScript II Reverse Transcriptase (Invitrogen, Carlsbad, CA, USA) using random primers according to manufacturer's instructions.

cDNA intended for use with TaqMan q-RT-PCR was made using TaqMan microRNA Reverse Transcription Kit starting with 10ng of RNA according to manufacturer's instructions. 1ul of the specific Reverse Transcriptase Primer (miR-34a and U6) was used to make cDNA for each sample.

cDNA intended for use with Stratagene qPCR miRNA kit, was made using 200 ng and Stratagene's miRNA 1st-Strand cDNA synthesis kit and performed according to manufacturer's instructions.

2.7 Quantitative Real-Time PCR (qRT-PCR)

Quantitative Real-Time PCR was performed using a light cycler (BioRad) and analyzed using the CFX manager (BioRad). All assays were performed in triplicate, including no-template controls (NTC) and miRNA expression was normalized the RNU6, calculated using the $2^{-\Delta\Delta Ct}$ method.[98] miRNA reference RNA from a pool of placental tissue, fetal brain tissue, adult liver, brain, heart, breast, colon and testis tissue cells was used as a reference sample(Stratagene cat # 750700).

2.7.1 Stratagene High-Specificity miRNA qRT-pCR

Using the cDNA created from the 1st strand cDNA synthesis kit (Stratagene), qRT-PCR was performed according to Manufacturer's instructions. 1.0µl of the cDNA sample was added to each reaction and the specific forward primer for the miRNA was used (mature miRNA sequence). A universal reverse primer (Stratagene) was used for all reactions (Figure 2-1A).

2.7.2 TaqMan Gene Expression Assay

Stem-loop quantitative reverse transcription-PCR (q-RT-PCR) for mature miRNA-34a was performed in triplicate using Taqman ® microRNA assays (Applied Biosystems, Foster City, CA) as per the manufacturer's directions on an Applied Biosystems ABI7900 Real Time PCR system. qRT-PCR assays were performed using primers and probes from Applied Biosystems for miR-34a and RNU6. All PCR reactions were run in triplicate and miRNA expression relative to RNU6 was calculated using the $2^{-\Delta\Delta Ct}$ method.[98] Applied Biosystems TaqMan Gene Expression Assays were used (Figure 2-1B).

2.8 Polymerase Chain Reaction (PCR)

An optimization of PCR conditions was conducted with respect to concentration of genomic DNA, 10X PCR buffer, Mgcl2, dNTPs, primer and Taq DNA polymerase. Template DNA, *Taq* DNA polymerase and Mgcl2 with different concentrations were used to standardize the PCR conditions in order to obtain bright and reproducible bands on agarose gels.

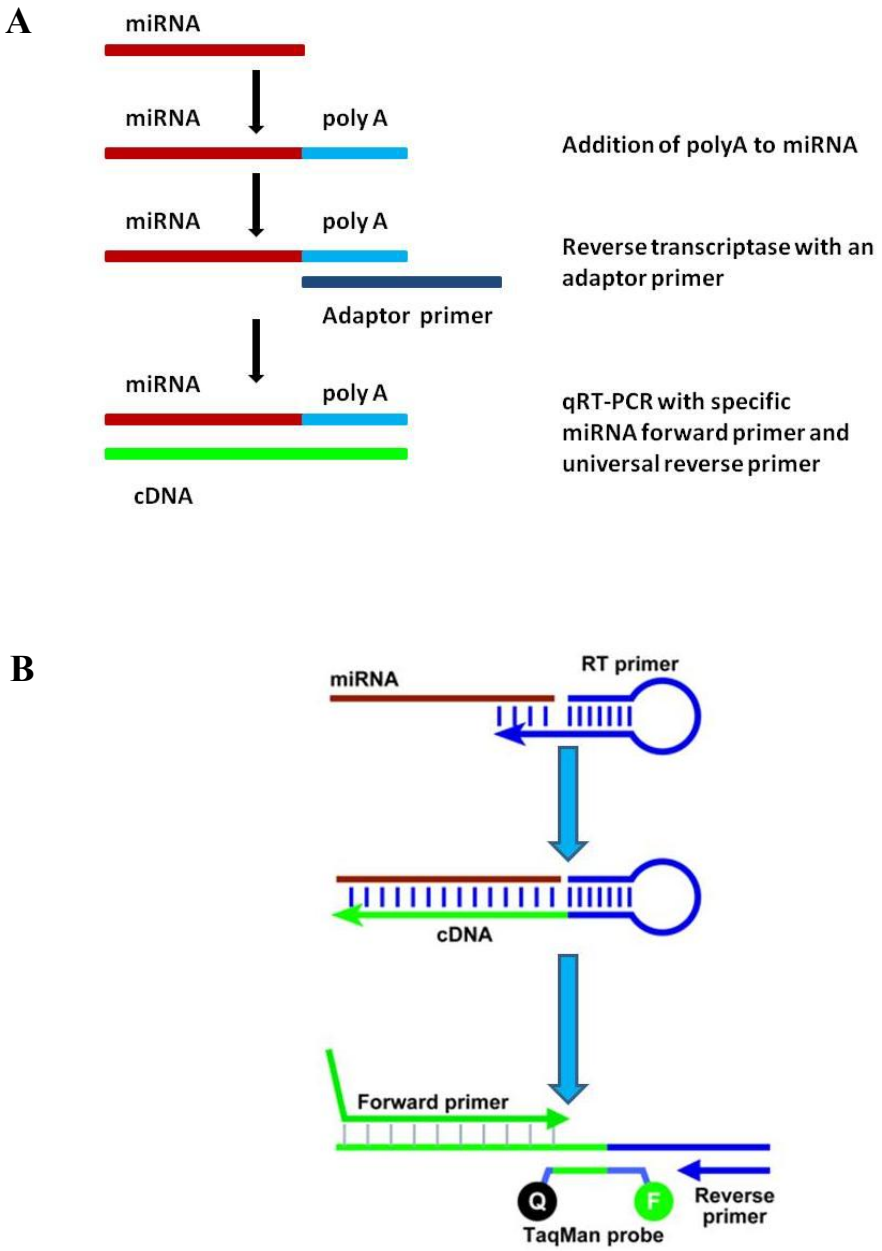

Figure 2-1. Schematic of qRT-PCR design.

(A) Stratagene cDNA is made by adding a poly A tail followed by reverse transcriptase with an adaptor primer. qRT-PCR is performed using miRNA-specific forward primer and a universal reverse primer. (B) TaqMan cDNA is made with the addition of a miRNA-specific RT primer. qRT-PCR is performed using miRNA-specific primers and probes. Fluorescent signal (F) is quenched (Q) until polymerase acts on sequence.

2.8.1 Methylation Specific PCR – miR-34a

2.8.1.1 Bisulfite conversion

DNA was collected using the Qiagen DNeasy kit and treatment of 500ng of DNA with bisulphite for conversion of unmethylated cytosine to uracil was performed with a commercially available kit (EpiTect Bisulphite Kit, QIAGEN, Hilden, Germany).

2.8.1.2 Methylation specific PCR (MSP)

Methylation-specific polymerase chain reaction (MSP) for promoter methylation was performed as described previously[99]. Primers used for the methylation-specific polymerase chain reaction (M-MSP) and unmethylated-specific polymerase chain reaction (U-MSP) were used as previously described[99].

Unmethylated control DNA was obtained from QIAGEN and was used as a control in all the experiments. Fifteen microliters of PCR products were loaded onto 1% agarose gels, electrophoresed and visualized under ultraviolet light after staining with ethidium bromide.

2.8.2 Detection of TP53 mutations

PCR conditions for amplifying p53 were performed as previously described. Methodological details are shared publicly at the World Health Organization's (WHO) International Agency for Research on Cancer (IARC) TP53 database available at:

http://www-p53.iarc.fr/download/tp53_directsequencing_iarc.pdf

2.8.3 Agarose Gel Electrophoresis

1% agarose gels were made in 50 ml of 1 x TAE in a 8 x 10 cm mini-gel casting tray. 10-15 ul of PCR product was loading with 2 ul of Orange G loading dye and run in 1 x TAE buffer at 90-130V. Gels were visualized by ethidium bromide staining on a GelDoc 1000 (Bio-Rad, Hemel Hempstead, UK).

2.8.4 Sequencing

All sequencing was run on the Applied Biosystems (ABI) 3730XL genetic analyzer at the University of Calgary Core DNA Services Lab. Chromatograms were analyzed manually by a visual inspection of sequences imported in a sequence analysis software using the reference sequence, NC_000017.9 (SeqScape, ABI). Variations were checked with the mutation validation tool available in the IARC TP53 database available at http://www-p53.iarc.fr/mutationvalidationcriteria.asp. This tool enabled us to check whether the variation is a known polymorphism or a mutation.

2.9 Western Blot Analysis

Equal amounts of total cellular protein (40ug) from each sample were electrophoresed on sodium dodecyl sulfate-polyacrylamide gel electrophoresis (SDS-PAGE) gels and transferred to nitrocellulose membranes (Invitrogen NuPAGE® Bis-Tris Mini Gel). The membranes were blocked with 5% nonfat milk in a Tris-buffered saline solution containing 0.1% Tween 20 for thirty minutes, probed overnight with relevant antibodies, washed, and probed with species-specific secondary antibodies coupled to horseradish peroxidise (Santa Cruz Biotechnology, Santa Cruz, CA). A Hi-Mark pre-

stained high molecular weight protein standard was used to estimate the approximate size of proteins (Invitrogen). Immunoreactive material was detected by enhanced chemiluminescence (PerkinElmer, Waltham, MA). The antibodies used were: Anti - CDK6 (Cell Signaling, Beverly, MA);Anti – YY1, Bcl-2, CDK4, E2F-3, C/EBP α (Santa Cruz Biotechnology. Santa Cruz, CA); Anti - SIRT1 (abcam).

2.10 Flow Cytometry

All flow cytometric analysis was performed using a LSRII flow cytometer (Becton Dickinson, San Jose, CA) and analyzed using Cellquest software at the University of Calgary Flow Cytometry Core Facility.

2.10.1 Annexin V – PE

Apoptotic cell death was measured by immunofluorescence flow cytometric analysis using Annexin V Phycoerythrin stain (V-PE) (Biovision), according to manufacturer's instructions. Specifically, cells were resuspended in 500 ul of 1X Annexin V binding buffer and 1 ul of Annexin V-PE. The percentage of apoptosis indicated was corrected for background levels found in the corresponding untreated controls. The percentage of apoptotic cells was expressed as the mean ± SD of three experiments, relative to the untreated empty vector.

2.10.2 Cell Cycle Analysis

Fixed and permeabilized cells stored at -20° C were spun down and washed twice with cold PBS. A 0.5 ml of a solution was added to each samples containing 50 ug/ml of

Propidium Iodide (PI), 0.1% TritonX100, and 200ug/ml of RNAse in PBS and incubated in the dark for 30 minutes.

2.11 Microarray analysis

Quality control of RNA was performed on an Agilent 2100 Bioanalyzer, using the RNA 6000 assay. All samples had a RNA integrity number (RIN) greater than 9.0, on an integrity scale from 1.0 to 10.0, a value of 9.0 showing high quality without degradation. cDNA was hybridized to the miRNA Affymetrix gene-chip (847 hsa-miRNA probes) and raw miRNA expression values were extracted from scanned gene-chips, $\log_2$ transformed and normalized (miRNA-QC tool, Affymetrix). mRNA profiling was performed using the Affymetrix Human Genome U133 Plus 2.0 Array. miRNA and mRNA expression data was analyzed using the Partek Genomic suite software.

2.12 Lentivirus constructs

Lentivirus particles were created in the producing cell line HEK 293TN cells (human embryonic kidney, ATCC) by combining the miR-181a plasmid and packaging plasmid according to manufacturer's instructions (System Biosciences, Cat # LV100A-1). After 48 hours post transfection, the supernatant containing the virus particles were collected and stored in 0.5 ml aliquots at -80°C. Transduction into the parental MM cell lines were performed by adding Polybrene at a final concentration of 5ug/ml with the prepared virus to 0.5 x 10^5 cells in complete media with antibiotics. Several 24 wells were used with varying amounts of virus particles (0.5 ul, 1.0, 2 ul, 5.0 ul and 10 ul). After 24 hours, the culture medium was replaced with complete medium (without Polybrene or

virus) The miRZIP lentivector containing the antagomir (miR-zip-181a) with perfect complementarity to the mature miRNA was transfected into MM cells and stable cell lines were created by the use of antibiotic selection with 2 ug/ml of puromycin. The creation of the empty vector control was made in the same fashion, according to manufacturer's directions.

Lentiviral transduction particles (ThermoScientific) were used to deliver miRNA expressed from shMIMIC™ pSMART microRNAs for over-expression of mature mir-34a into KMS11, OPM2 and INA-6 MM cells. miRIDIAN Mimic hsa-miR-34a and miRIDIAN microRNA empty vector mimic were used. [Thermoscientific, Cat # VSH5842-101207452 (miR-34a) and HMR5888 (empty vector)] The virus particles were added at various MOIs (0.5, 1, 2, 5 and 10) and then individually added into MM-cell suspensions in the presence of 6 μg/mL polybrene and transduced for 24 hours followed by selection in puromycin (2 μg/mL; Invitrogen) to obtain stable expression of miR-34a. Transfected cells were maintained in media supplemented with 2 ug/ul Puromycin.

Vector maps used for miR-181a antagonism (miRZIP, System Biosciences) and miR-34a over expression (shMIMIC-pSMART, Thermoscientific) are shown in (Figure 2-2A and B respectively).

A

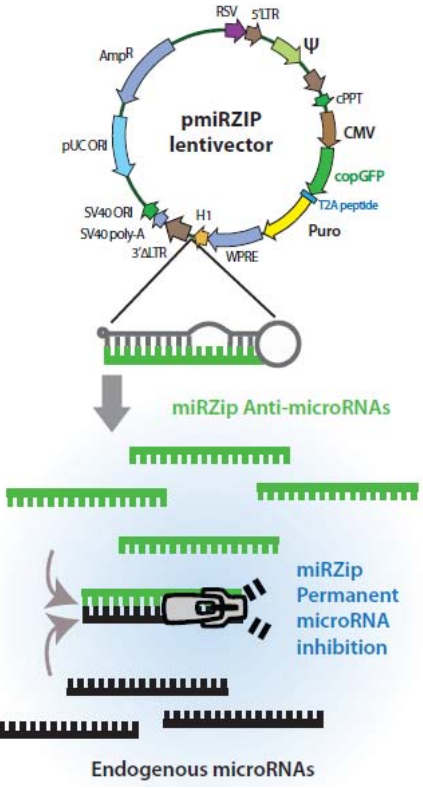

B

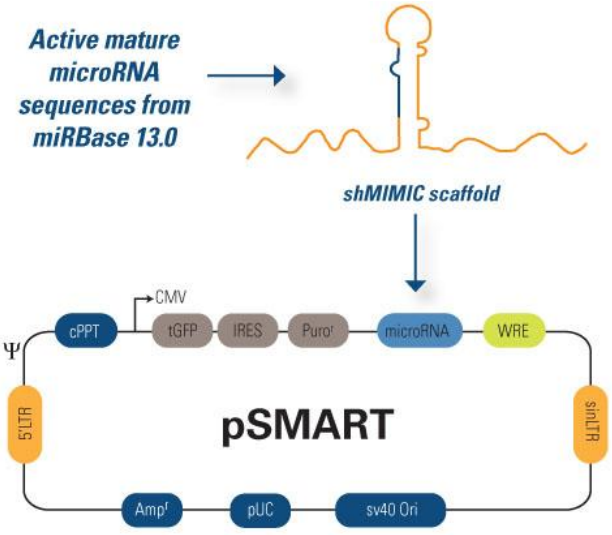

Figure 2-2.Vector maps of lentivirus constructs.

(A) miRZIP (miR-181a antagonism, System Biosciences) (B) pSMART shMIMIC (miR-34a over-expression, Thermoscientific).

2.13 Fluorescent in situ Hybridization (FISH)

TP53 gene deletion in MM cells was determined by fluorescent in situ hybridization (FISH) analysis of the chromosome 17p deletion. Harvesting at 24 hours was accomplished using colchicine incubation for 20 minutes. The metaphase preparations were fixed with methanol and acetic acid in a ratio of 3 to 1. Hypotonic cell suspensions were dropped onto air-dried clean slides. The slides were aged in a hybridization oven at 60°C and denatured in 2× standard saline citrate (SSC; pH 7.0) at 73 ± 1°C for 5 minutes, and dehydration in 70% and 85% ethanol for 1 minute each, and then transferred into 100% ethanol and air-dried before hybridization.

The TP53/CEP 17 FISH probe kit was used to determine loss of these genetic regions within interphase and metaphase nuclei (Vysis - Abbott Laboratories, Illinois, U.S.A). The probes were used in accordance with the manufacturer's specifications. Each probed region on each slide was covered with a cover slip, sealed with rubber cement, co-denatured at 73° for 5 minutes and incubated overnight at 37°C. After incubation, the rubber cement and coverslips were removed from the slides and were then washed with 0.4× SSC / 0.3% NP-40 at 73 ± 1°C for 2 minutes and 2× SSC / 0.1% NP-40 at ambient temperature for 1 minute and air-dried in darkness. Ten microliters of 4′,6-diamidino-2-phenylindole (DAPI II) counterstain was applied to the target area of the slide and the coverslip was reapplied. Slides were stored at −20°C in the dark before being examined and imaged in the Calgary Laboratory Services - Cancer Cytogenetics Laboratory.

2.14 *In vivo* Studies

All animal studies were conducted according to protocols and standard procedures approved by the University of Calgary Animal Care Committee. CB-17 SCID-mice (Charles River Laboratories, Wilmington, MA) were irradiated with 150 cGy and 24 hours later subcutaneously (SC) inoculated in the interscapular area with 2 x 10^6 miR-*34a or EV KMS11* cells[100]. Following the detection of measurable tumors, animal cohorts were treated with bortezomib (0.4 mg/kg SC every Monday and Thursday). Tumor sizes were measured every 3 days in 2 dimensions using calipers, and the tumor volume was calculated using the following formula: $V = 0.5\ a \times b^2$, where a and b are the long and short diameter of the tumor, respectively. Animals were sacrificed when their tumors reached 2 cm in largest diameter or when exhibiting any distress symptoms.

2.15 Statistical Analysis

Each assay was performed at least 3 times, with the exception of the microarray analysis which was performed in triplicate in one assay. The data of qRT-PCR are expressed as the mean of the 3 experiment triplicates ±SEM and the Student's t-test was used to determine the significance of the differences. All tests were two-sides and associations were considered statistically significant at a level of $\rho < 0.05$ was (*).

Chapter Three: Results

3.1 MM cell lines express variable sensitivity to bortezomib.

Using a panel of 7 MM cell lines, the relative resistance to bortezomib was determined. Each cell line was treated with varying doses of bortezomib, measuring viability by annexin-V staining followed by flow cytometry and the IC50 was identified for each cell line. The percentage of cell viability was determined by comparing the number of viable cells (annexin V negative) by the total number of cells (annexin V positive and negative), relative to the untreated sample. Each cell line was treated with the proteasome inhibitor bortezomib for 24 hours and set up in triplicate with doses ranging from 1.25nM to 5 nM. After the 24 hour incubation, each sample was collected and flow cytometric analysis was performed, using the Annexin-V-PE apoptotic stain. As expected, a decrease in cell viability was seen as the concentration of Bortezomib was increased (Figure 3-1). As shown in Table 3-1, the concentration at which 50% inhibition of cell viability was induced (compared to the untreated control), is noted as the IC50 for each cell line. The cell lines were then classified into 2 relative groups, cells with IC50<2.5nM to be sensitive (S) to bortezomib and those with an IC50~5.0nM to be resistant (R) to bortezomib. NCI-H929, MM1s, RPMI-8226 and U266 can be considered relatively sensitive cells lines while KMS11, OPM2 and INA-6 are relatively resistant cell lines.

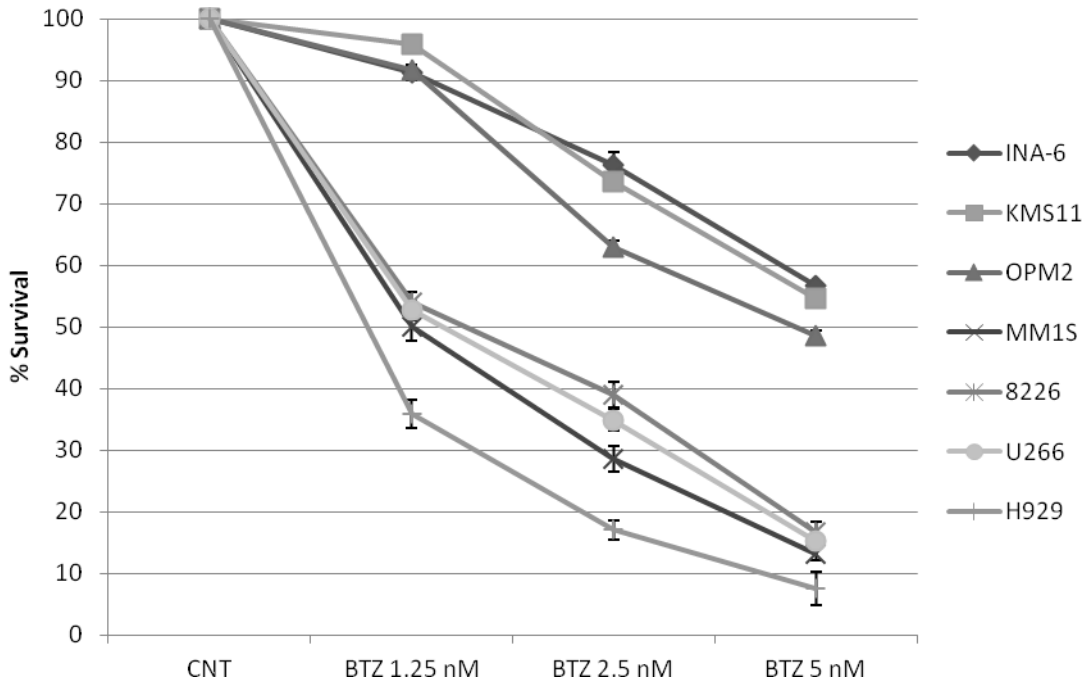

Figure 3-1. MM Cell Sensitivity to Bortezomib.

The cytotoxic effect of bortezomib on cell viability in MM cells was evaluated following treatment with bortezomib for 24 hours. Cells were treated with 1.25nM, 2.5nM and 5 nM of Bortezomib for 24 hours and survival was measured by flow cytometry. Percent survival is shown as the percentage of Annexin V negative cells ±SD of 2 independent experiments.

Table 3-1. Classification and IC50 of MM cell lines.

The relative IC50 groupings and relative response to bortezomib as plotted in Figure 1. The category of relative resistance or sensitivity is defined herein and the approximate IC50 is used in all further data.

Cell Line	IC50 Grouping	Relative Resistant Or Relative Sensitive
INA-6	~5.0 nM	Resistant
KMS11	~5.0 nM	Resistant
OPM2	~5.0 nM	Resistant
H929	<2.5 nM	Sensitive
MM1S	<2.5 nM	Sensitive
8226	<2.5 nM	Sensitive
U266	<2.5 nM	Sensitive

3.2 miRNA microarray profiling reveals unique signature between relative sensitive and resistant MM cell lines.

To identify a distinctive miRNA signature mediating MM cells sensitivity to bortezomib, microarray profiling was performed on extracted RNA from "R" and "S" MM cell lines using the Affymetrix miRNA Genechip. Prior to array hybridization, RNA quality and RNA Integrity Number (RIN) was determined by analyzing samples on the Agilent 2100 Bioanalyzer and samples were chosen with an RIN greater than 9.0. (Figure 3-2).

Raw miRNAs expression values were extracted from scanned gene-chips, log2 transformed and normalized (miRNA-QC tool, Affymetrix). As shown in Figure 3-3, comparison of normalized miRNAs expression in "S" versus "R" patients (Anova testing) identified 24 differentially expressed miRNAs (Fold change < -2 or > 2 with False discovery rate [FDR] <0.05) and clustered "S" and "R" MM cells into 2 distinct groups.

In order to establish a "Bortezomib risk score" based on the expression of these 24 mirRNAs, the data was summarized into a univariate score by calculating the difference between the mean $\log_2$-scale expression of the 16 up-regulated and the mean of the 8 down-regulated miRNAs. This difference is interpreted as the geometric mean ratio (GMR), or the up/down-regulated mean ratio, on the $\log_2$ scale.

$[\text{Log}_2\ \text{GMR}] = \text{Log}_2\ [(2^{\wedge\sum\text{up-regulated miRNA}/n_i}) / (2^{\wedge\sum\text{down-regulated miRNA}/n_{ii}})$, where n_i and n_{ii} represent the number of up-regulated and down-regulated miRNA respectively. This univariate score (GMR) of the 24-miRNA expression profiles enabled the accurate prediction of "S" versus "R" phenotype for each cell. (Figure 3-4A)

A

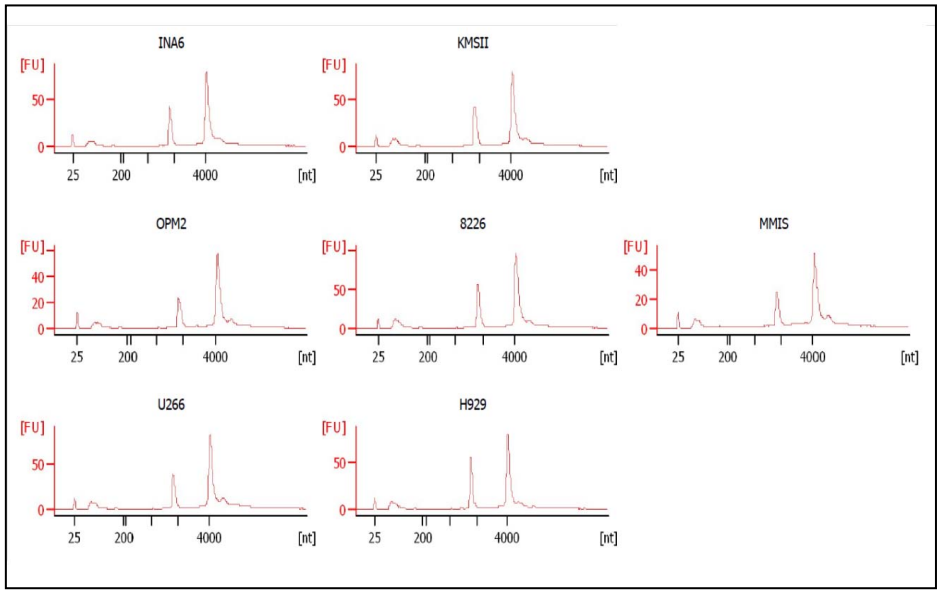

B

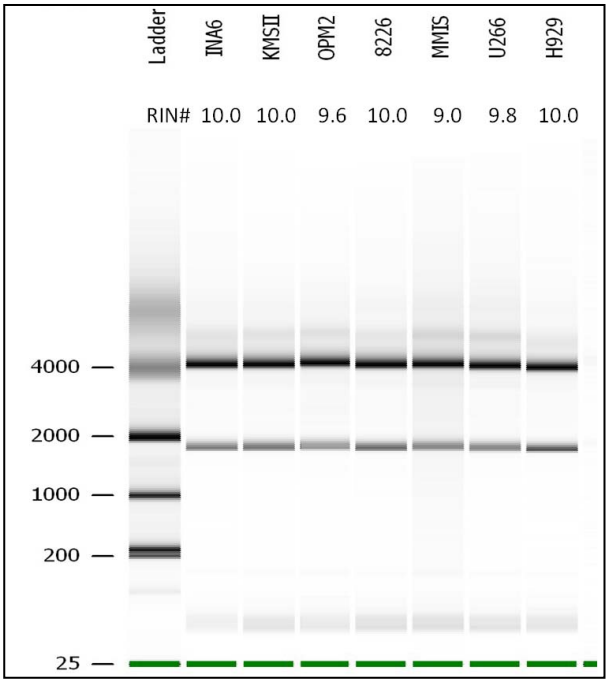

Figure 3-2. Quality control for MM cell lines for preparation of microarray

(A) Fluidics based electropherogram analysis for 18s and 28s subunit of each sample is represented. Distinct peaks for each subunit are seen without contaminating products, as well as presence of small nucleotides representing miRNA. (B) Gel-like image demonstrating distinct peaks and corresponding RIN value for each sample.

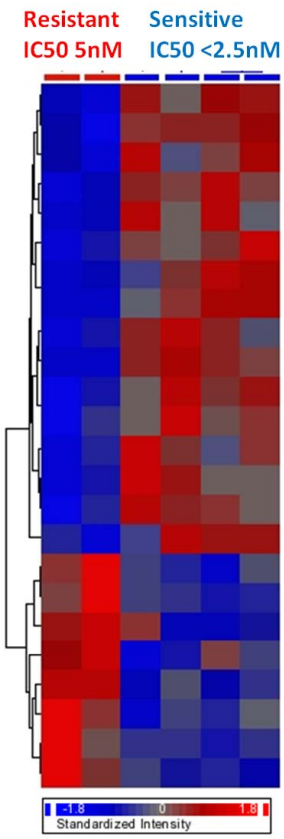

Probeset ID	Fold-Change (S vs. R)	Fold-Change Description	p-value	False Discovery Rate (FDR)
hsa-miR-1202_st	2.78174	S up vs R	0.033304	0.027249
hsa-miR-1228-star_st	2.58876	S up vs R	0.024619	0.027746
hsa-miR-125a-5p_st	2.35413	S up vs R	0.003494	0.023069
hsa-miR-1270_st	2.31027	S up vs R	0.030791	0.045683
hsa-miR-130b_st	-2.16296	S down vs R	0.003395	0.023114
hsa-miR-142-5p_st	-3.29919	S down vs R	0.032335	0.002691
hsa-miR-181a_st	-4.7721	S down vs R	0.043127	0.037869
hsa-miR-181d_st	3.62704	S up vs R	0.011825	0.045963
hsa-miR-185_st	-2.66805	S down vs R	0.021969	0.034588
hsa-miR-193a-5p_st	3.24114	S up vs R	0.046175	0.045621
hsa-miR-23b_st	2.90039	S up vs R	0.044804	0.023540
hsa-miR-28-5p_st	-4.14928	S down vs R	0.049694	0.025478
hsa-miR-330-3p_st	9.73349	S up vs R	0.001954	0.004936
hsa-miR-342-3p_st	-4.65178	S down vs R	0.045621	0.030944
hsa-miR-34a_st	12.6751	S up vs R	0.024649	0.028037
hsa-miR-486-5p_st	-3.34991	S down vs R	0.042808	0.049310
hsa-miR-557_st	2.01355	S up vs R	0.032325	0.046110
hsa-miR-663_st	2.83521	S up vs R	0.027830	0.034488
hsa-miR-708_st	-6.47568	S down vs R	0.032703	0.044769
hsa-miR-744-star_st	2.20764	S up vs R	0.031757	0.012625
hsa-miR-886-3p_st	11.064	S up vs R	0.006692	0.044078
hsa-miR-886-5p_st	27.9824	S up vs R	0.003664	0.043109
hsa-miR-92b_st	3.18297	S up vs R	0.001171	0.026037
hsa-miR-93_st	2.02306	S up vs R	0.043895	0.025273

Figure 3-3. Microarray miRNA heatmap demonstrates unique signature between relative resistant and sensitive MM cell lines.

Heatmap showing the 2 clusters of Bortezomib sensitive IC50 <2.5nM (MM1S, 8226, U266 and H929) versus Resistant IC50 5nM (INA6 and KMS11) MM cell lines and the list of differentially expressed miRNA. Heatmap was generated after supervised hierarchical clustering using the ANOVA test. Expression of miRNA patterns is shown by up-regulation (red) versus down-regulation (blue).

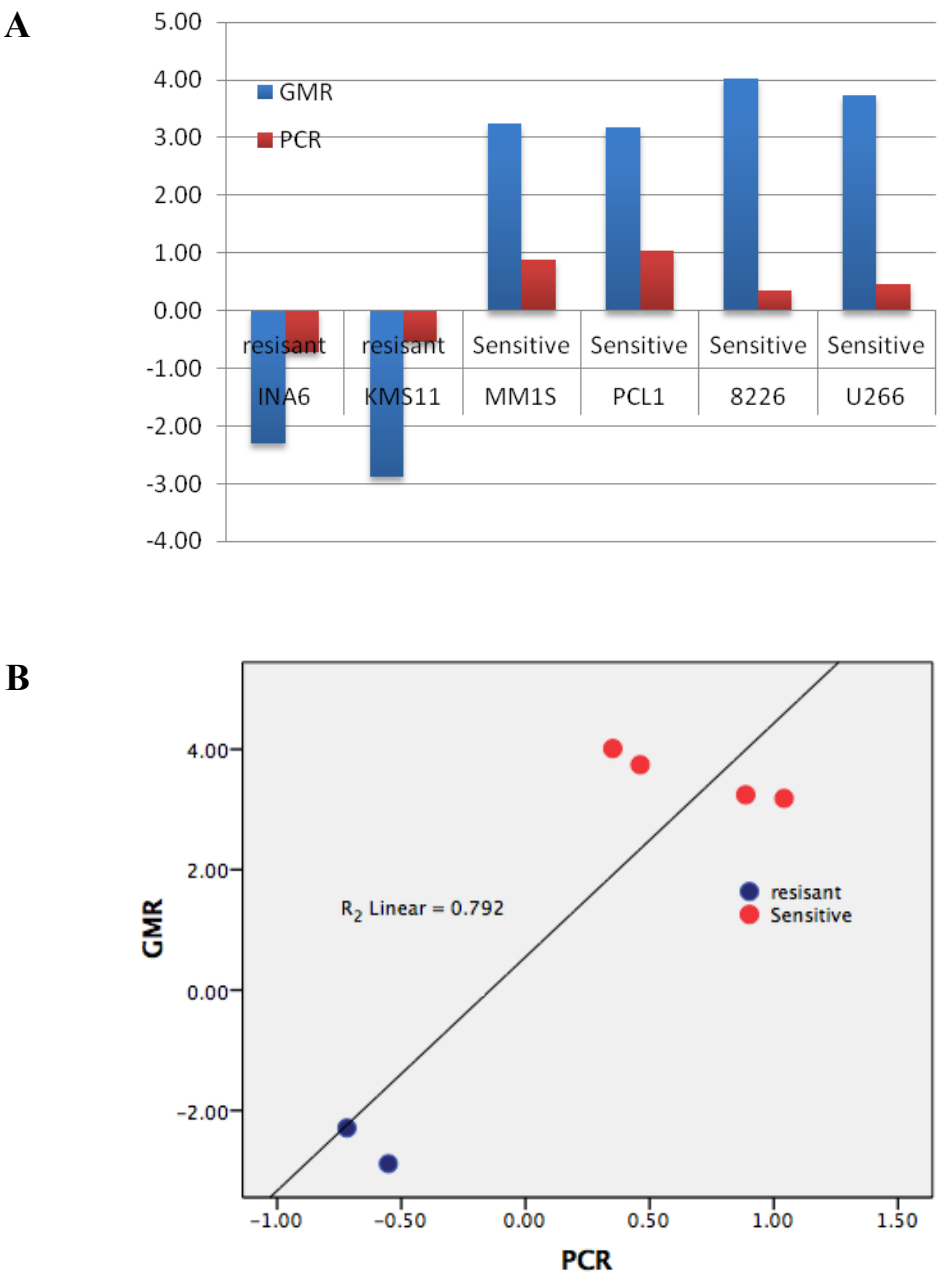

Figure 3-4. Correlation between the microarray (GMR) and PCR generated "Bortezomib risk" scores.

(A) The geometric mean ratio (GMR) was calculated using expression values from microarray analysis and qRT-PCR (PCR). (B) Linear regression analysis comparing the GMR and PCR analysis.

3.3 Quantitative real time PCR (qRT-PCR) validates miRNA expression from microarray analysis.

To validate the expression of miRNAs from the microarray results, quantitative real time PCR (qRT-PCR) was performed for miR-181a/b/c, miR-28-5p, miR-34a, miR-886-3p/5p, miR-330-3p, miR-92b and miR-708 in the MM cell lines. Consistent with the microarray data, confirmation of up-regulation of miR-181a/b/c, miR-28-5p, and miR-708 and down-regulation of miR-34a, miR-886-3p/5p, miR-330-3p and miR-92b was seen in the resistant MM cell lines and the GMR predicted the same groupings of resistant and sensitive samples as shown in Figure 3-4A (PCR). Expression of individual miRNAs was calculated relative to endogenous gene RNU6, calculated using the $2^{-\Delta\Delta Ct}$. Furthermore, this group of miRNA validated by qRT-PCR to calculate the GMR for each sample demonstrated a strong correlation between microarray and qRT-PCR results, with a coefficient of determination (R^2) value of 0.792. (Figure 3-4B) Taken together, it is suggested that qRT-PCR is a valid method for measuring miRNA expression levels and support the microarray data. Recognizing that analysis was performed on a relatively small number of MM cell lines, it has provided a framework for investigation of the influence of miRNA in multiple myeloma.

3.4 Expression of microRNA-181a in MM cell lines

To determine the effect miRNAs have on MM sensitivity to the proteasome inhibitor bortezomib, we performed miRNA gain and loss of function analysis in MM cell lines. Specifically, miR-181a was found to be up-regulated in resistant MM cell lines by a fold increase of 4.77 compared to the sensitive MM cell lines. The up-regulation of

miR-181a in resistant MM cell lines was also confirmed using qRT-PCR validation as shown in Figure 3-5. To determine whether resistance to bortezomib is influenced by miR-181a expression, stable cells were created whereby the resistant cell lines had miR-181a expression antagonized. Using a lentivirus mediated system, stable cell lines with a miR-181a antagonist were created using the parental resistant cell lines. (named herein as KMS11-181a, OPM2-181a and INA6-181a). A control empty vector was used as a negative control in all cell lines (KMS11-000, OPM2-000, INA6-000) along with a reagent-only control to ensure the vector and transduction reagents had no effect on the normal functioning of cells. Specifically, the resistant MM cell lines, which express relatively high levels of miR-181a, were virally-transduced with the pmiRZIP-181a and pmiRZIP-000 lentivector which contained the antagomir (miR-zip-181a) with perfect complementarity to the mature miRNA and the empty control vector respectively. Cells were left for 48 hours post transduction before stable cell lines with miR-181a antagonism were created by the use of antibiotic selection with puromycin. Successful transductions were confirmed by the high percentage of cells expressing the green fluorescent protein (GFP) as viewed under a fluorescent microscope and by flow cytometric analysis.

3.4.1 qRT-PCR confirmation of miR-181 antagonism.

While detection of GFP confirmed successful transduction, it was also necessary to confirm that the miR-181a antagomir was in fact present and inhibiting miR-181a expression. Cells were collected from the stable cell lines containing both the miR-181a antagomir and miRZIP-000 empty vector. To determine the expression level of

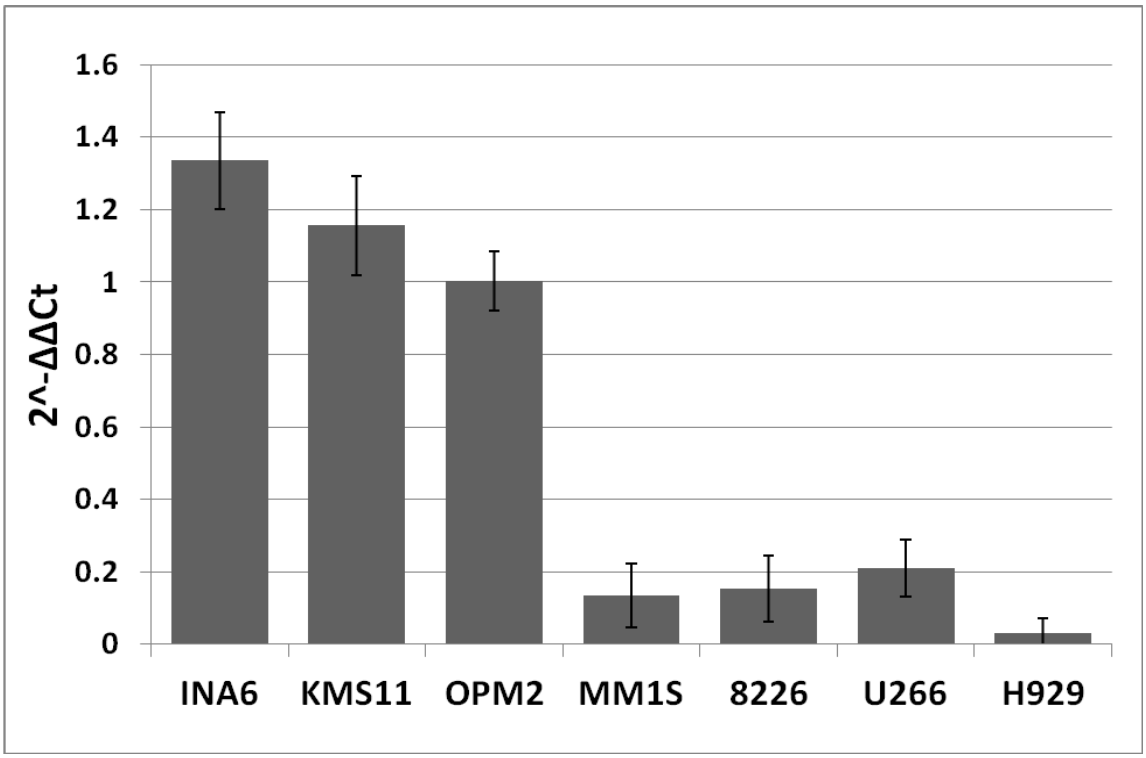

Figure 3-5. Quantitative Real time-PCR (qRT-PCR) validation of miR-181a expression.

The results of miR-181a expression are expressed as a fold change of miR-181a expression relative to a pooled miR references sample. The expression of miR-181a has been normalized to the housekeeping gene RNU6 and calculated using the $2^{-\Delta\Delta Ct}$ method.

miR-181a, RNA was extracted from collected cells, cDNA was created and qRT-PCR was performed. Expression of miR-181a was normalized to the endogenous gene RNU6, and relative to the empty vector control, calculated using the $2^{-\Delta\Delta Ct}$ method. [98] Using the Stratagene miRNA expression system, cDNA was first created using a universal reverse primer and adaptor primer (Figure 2-1A in methods). The qRT-PCR was then performed using a forward primer that was identical to mature miR-181a sequence (complementary to the cDNA) and a universal reverse primer that bound to the adaptor primer used in cDNA production. Figure 3-6 demonstrates that the expression levels of miR-181a in KMS11-181a appear to increase relative to the empty vector, rather than the expected decrease in this cell line. This can be explained by the fact that the cDNA sequence is now in fact identical to the miR-181a antagomir sequence in miRZIP vector.This then leads to the over-estimation of miR-181a copy number making KMS11-181a appear to have higher expression than the expected antagonism. This is further explained by the concept that the miRZIP lentivector based anti-microRNA creates very small, stable complexes, which do not degrade easily as in typical use of lentivector based siRNA systems[101]. miR-181a expression levels appear to increase despite the antagonism, due to the mIRZIP antagomir sharing the same sequence as the cDNA, resulting in falsely detected increased expression. Additional methods are required in order to confirm the effective antagonism of miR-181a.

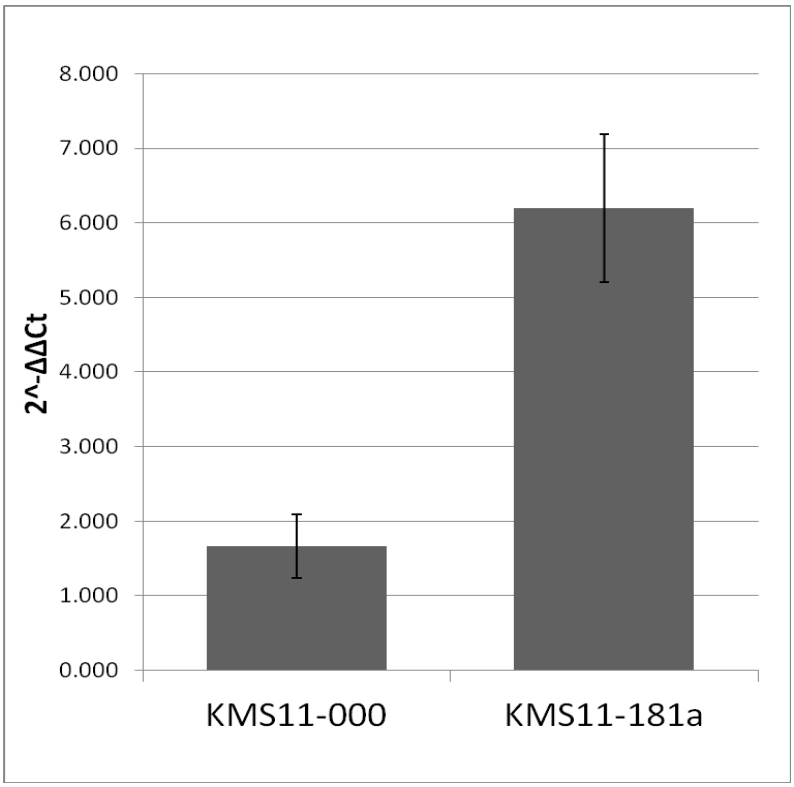

Figure 3-6. miR-181a expression following transduction in KMS11 cells.

qRT-PCR validation of miR-181a expression in KMS11-EV versus KMS11-000. The results are expressed as a fold change of miR-181a expression relative to the empty vector. The expression of miR-181a has been normalized to the housekeeping gene RNU6 and calculated using the $2^{-\Delta\Delta Ct}$ method.

3.4.2 Cell Cycle Analysis of KMS11-181a versus KMS11-000

To evaluate whether the antagonism of miR-181a in resistant KMS11 cell lines resulted in the alteration of proliferation and cell cycle progression, proliferation rate and cell cycle analysis was performed in the empty vector control cell compared to the miR-181a antagomir. Using the MTS enzymatic assay to measure the proliferation rate, a uniform number of unsynchronized cells were plated and assessed every 24 hours. As seen in Figure 3-7, cells treated with the miR-181a antagomir showed significantly increased growth rate estimated by the MTS assay as compared to the empty vector control cells. In order to analyze cell cycle distribution in mir-181a antagonized cells, cells were first treated with a double thymidine block in order to synchronize cells in G1. Cells were then "released" from the block, by replacing the thymidine with fresh complete media and cells were collected and fixed at 4, 8 and 24 hours after the release. Cell cycle analysis was performed by measuring DNA content by prodipidium iodide (PI) staining of fixed cells by flow cytometry after cell synchronization. As demonstrated in Figure 3-8, after double thymidine synchronization and release, an increase in the G1 population in the KMS11-181a cells was seen after 24 hours, consistent with the observation of increased proliferation in vitro. A similar result was seen in INA6-181a and OPM2-181a (data not shown). These results suggest that antagonism of miR-181a causes an increased cell proliferation in MM cells.

3.4.3 Inhibition of miR-181a levels increases sensitivity to bortezomib.

To elucidate the influence of mir-181a antagonism on sensitivity to bortezomib, in vitro cytotoxic assays were conducted. KMS11-181and OPM2-181a (and the respective

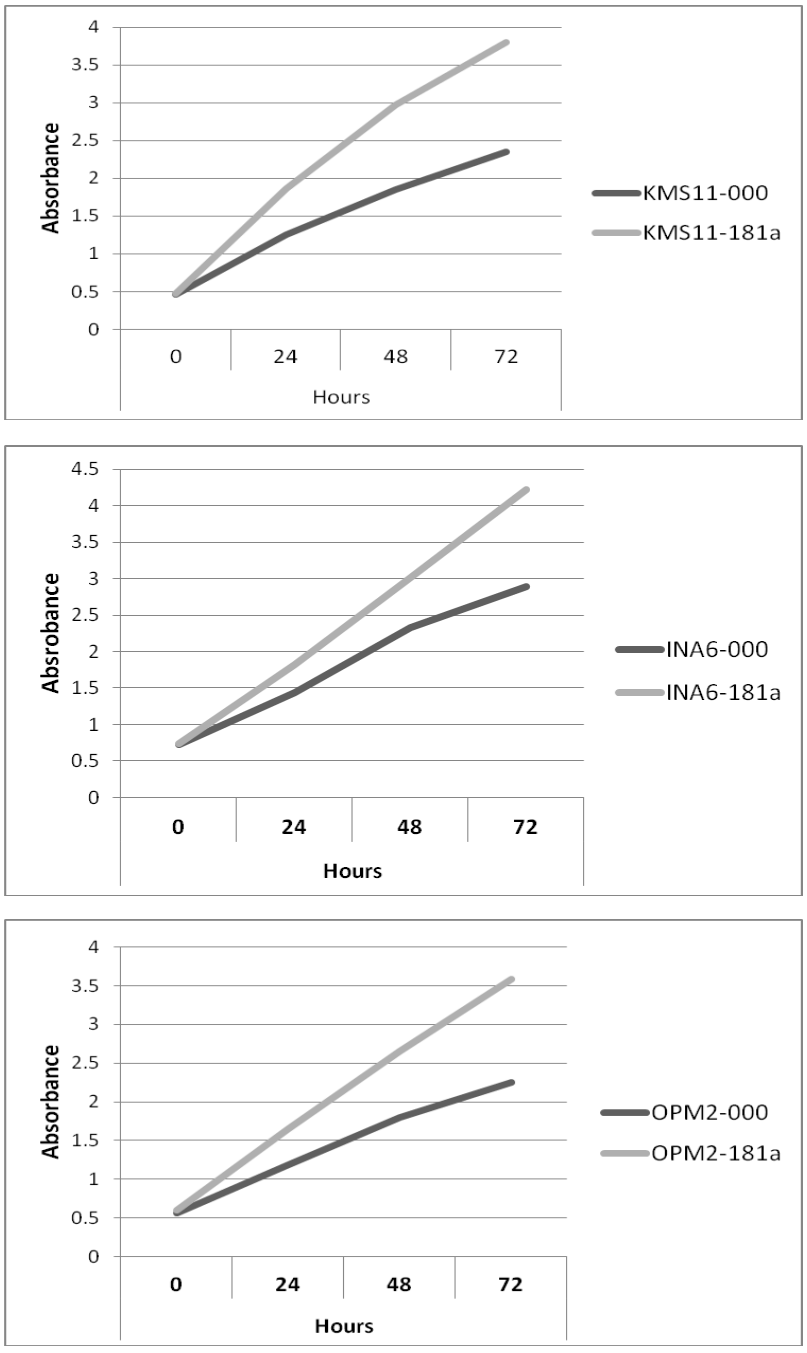

Figure 3-7. Proliferation rates of miR-181a transduced cells versus empty vector control.

The cells were harvested 7 days post transduction and assessed for proliferation by MTS assay, every 24 hours for 3 days. The results demonstrate that miR-181a increases cell proliferation relative to the empty vector.

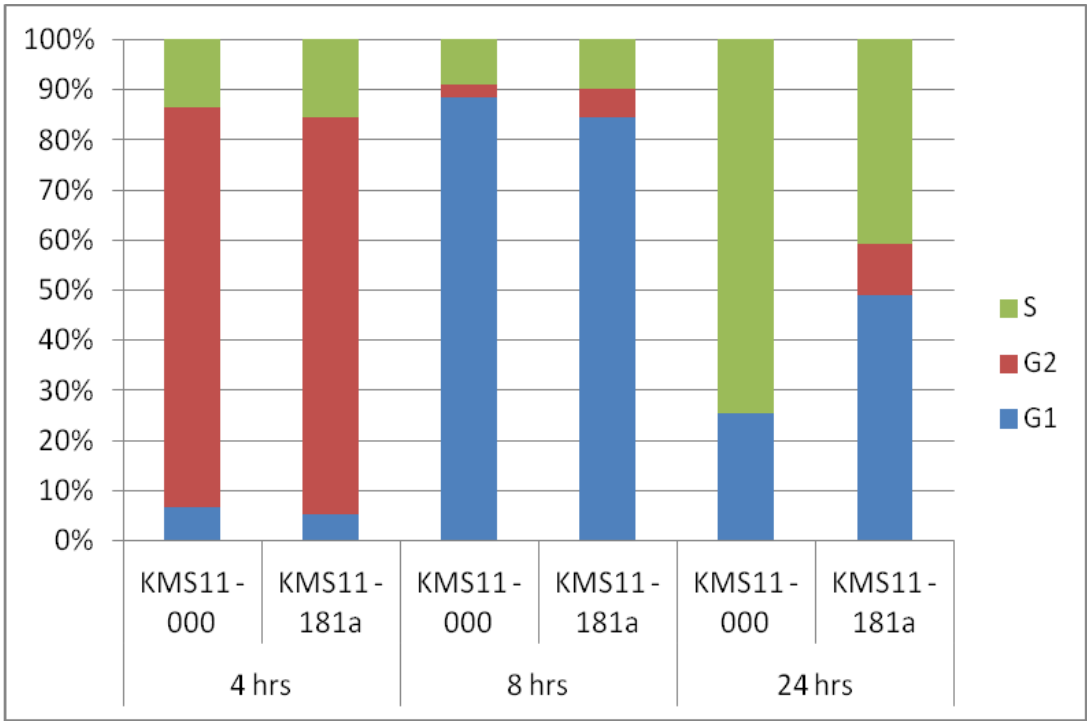

Figure 3-8. miR-181a antagomir influences cell cycle progression

KMS11-000 and KMS 11-181a cells were harvested 7 days post transduction and assessed for cell cycle by propidium iodide flow cytometry following double thymidine synchronization. The results demonstrate that miR-181a increase progression into G1 phase of the cell cycle.

empty vectors) were seeded in triplicate in 24 well plates and treated with 2.5 nM and 5.0 nM of bortezomib; an untreated well serving as the control. After 24 hours, cells were harvested and washed with PBS. Cells were stained with Annexin-V-PE and flow cytometric analysis was performed to measure apoptosis. As shown in Figure 3-9, KMS11 and OPM2 cells transfected with the miR-181a antagomir, demonstrated an increase of sensitivity to bortezomib, relative to the miR-000 empty control vector. This sensitivity is best demonstrated in KM11-181a treated with 2.5 and 5nM of bortezomib with an approximate 20% increase in Annexin V staining, treatment of OPM2-181a demonstrates a 15% increase. This provides a rationale that decreased levels of miR-181a in MM cells, may influence sensitivity to bortezomib.

While miR-181a antagonized cells appear to have biological importance in modulating resistance to bortezomib, an increase in proliferation rate in MM cells is also seen. While this provides an interesting mechanistic question as to miR-181a's modulation to bortezomib sensitivity, it is not as clinically relevant. Clinically, while it may increase sensitivity to bortezomib treatment, it would not be a suitable microRNA to target due the prospect of also increasing tumour growth.

3.5 Expression of microRNA-34a in MM cell lines

Another interesting miRNA identified in the miRNA microarray screen was miR-34a. miR-34a has been previously shown to be a direct target of the tumour suppressor p53[102,103], which has interesting implications in the context of cancer. In particular, it was noted that mir-34a had high expression in sensitive MM cell lines in comparison to relatively resistant cells with a fold change of 12.68 (S up vs. R). To determine the effect

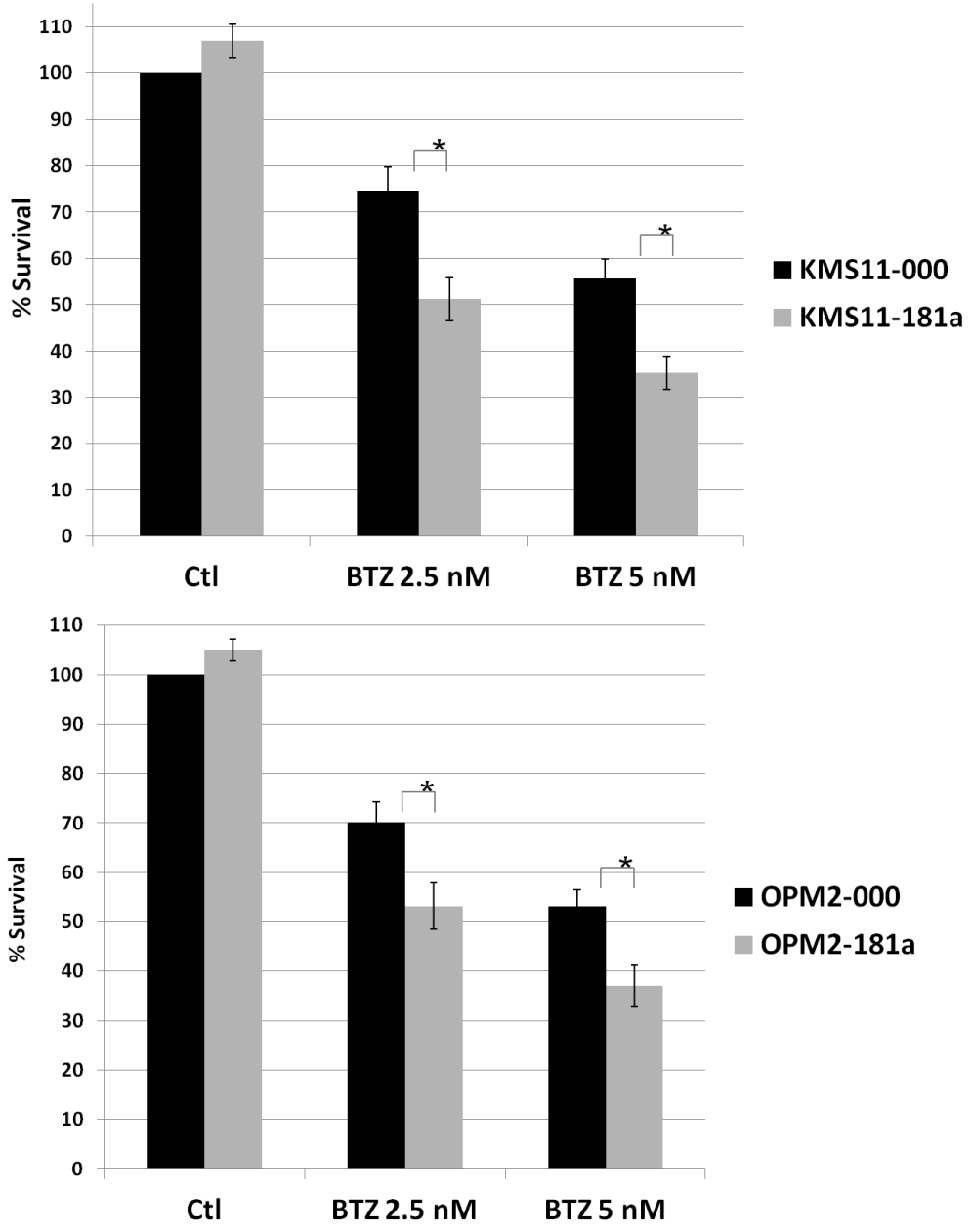

Figure 3-9. Cytotoxic Effect of Bortezomib on miR-181a antagomir versus control

Sensitivity to bortezomib after being cultured for 24 hours in the absence and presence of Bortezomib (2.5nm a nd 5 nM). Flow c ytometric a nalysis was used to e valuate the cytotoxic effects of Bortezomib. KMS11-181a and OPM2-181a demonstrate an increase of sensitivity relative to the empty vector controls. Student t-test was used to check for significance and interaction between all the variables. Bonferroni posttest was then used to check for significance with significance se t a t $p<0.05$.

of miR-34a on MM sensitivity to bortezomib, miRNA gain of function analysis was performed in the relative resistant MM cell lines. To validate the expression levels of miR-34a in MM cell lines, qRT-PCR was performed to detect the levels of miR-34a. Taqman-qRT-PCR was performed on all MM cells and as expected from the microarray data, cell lines with relative resistance to bortezomib have low expression of miR-34a, compared to the sensitive MM cell lines (Figure 3-10). Expression of miR-34a relative to endogenous gene RNU6, was calculated using the $2^{-\Delta\Delta Ct}$ method. [98]

To further elucidate the potential therapeutic role of miR-34a in MM we performed gain of function analysis for miR-34a using the shMIMIC™ microRNAs with a lentivirus delivery system (Thermoscientific). Lentiviral transduction particles with validated miR-34a shMIMIC™ microRNA or control (empty vector) were transduced into three relative resistant MM cell lines (herein named as KMS11-34a, OPM2-34a and INA6-34a). A control empty vector and a reagent-only control were used as negative controls in all cell lines (KMS11-EV, OPM2-EV, INA6-EV) to ensure the vector and transduction reagents had no effect on the normal functioning of cells. Cells were left for 48 hours post transduction before stable cell lines with miR-34a over-expression were created by the use of antibiotic selection with puromycin. Successful transductions were confirmed by the high percentage of cells expressing the green fluorescent protein (GFP), viewed under a fluorescent microscope and by flow cytometric analysis. As shown in Figure 3-11, following transduction with lentivirus particles, significantly increased levels of miR-34a were confirmed by qRT-PCR in all three cell-lines when compared to the empty vector. It is important to note that while the expression level of miR-34a in INA6-34a cells appears to be approximately 275 times higher than INA6-34a, this is largely due to the fact the

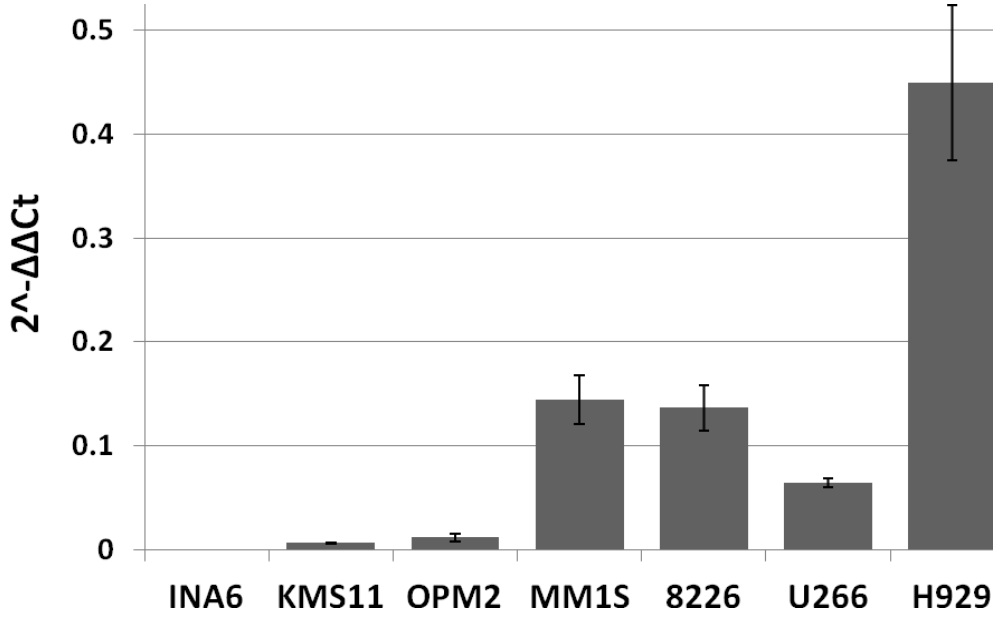

Figure 3-10. Quantitative Real time -PCR (qRT-PCR) validation of miR-34a expression.

qRT-PCR validation of miR-34a expression. The results are expressed as a fold change of miR-34a expression relative to a pooled miR references sample. The expression of miR-34a has been normalized to the housekeeping gene RNU6 and calculated using the $2^{-\Delta\Delta Ct}$ method.

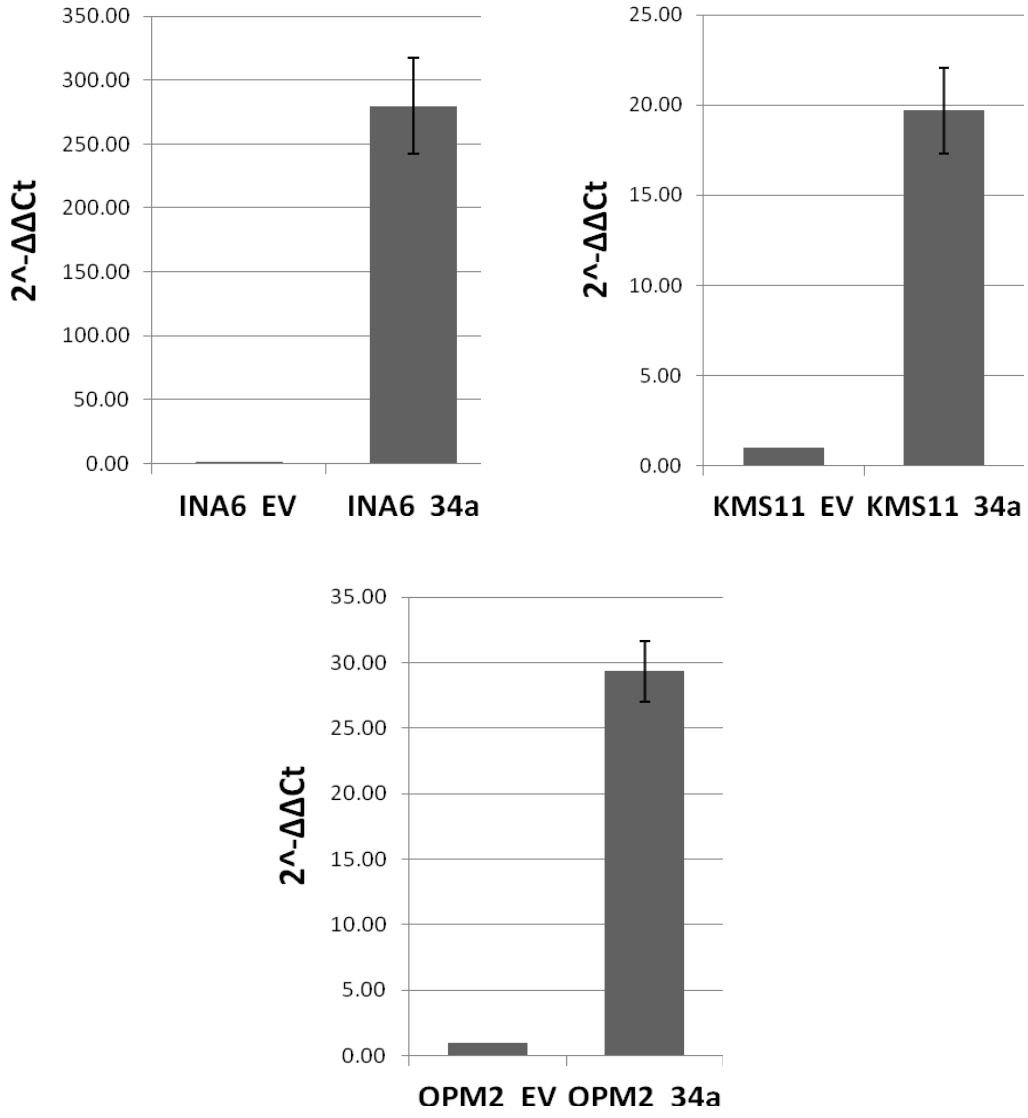

Figure 3-11. miR-34a expression following transduction in resistant MM cell lines. MM cell lines KMS11, OPM2 and INA6 were transduced with miR-34a and miR-EV, harvested 7 days post-transduction in selection. The results are expressed as a fold change of miR-34a expression relative to the empty vector control. The expression of miR-34a has been normalized to the housekeeping gene RNU6 and calculated using the $2^{-\Delta\Delta Ct}$ method. A dramatic increase of expression is observed following transfection.

expression of miR-34a in INA6-EV was essentially zero. The final raw expression values, before normalization to the empty vector were comparable in all three transfected cell lines. Lentivirus-mediated stable expression of miR-34a as demonstrated in KMS11 and OPM2 cells had a minimal effect on MM cell proliferation and cell viability (~ 5% increase in Annexin V staining compared to infection with mock lentiviral control).

3.5.1 Over-expression of microRNA-34a in MM cell lines increases sensitivity to the proteasome inhibitor bortezomib.

To elucidate the influence of miR-34a expression on MM cell sensitivity to bortezomib, assays were conducted to test the cytotoxic effect of bortezomib on miR-34a transduced cells relative to the empty vector control. KMS11-34a and OPM2-34a (and respective empty vectors) were seeded in triplicate in 24 well plates and treated with 2.5 nM and 5.0 nM of bortezomib; an untreated well serving as the control. After 24 hours, cells were harvested, washed with PBS, and stained with Annexin-V-PE for flow cytometric analysis to measure apoptosis. As shown in Figure 3-12, KMS11-34a and OPM2-34a cells, with over-expression of miR-34a, demonstrated an increase of sensitivity (~20% increase in Annexin V staining) to the cytotoxic effect bortezomib, relative to KMS11-EV and OPM2-EV. Not only does miR-34a expression induce a slight cytotoxic effect on the cells, but this effect is enhanced when treated with bortezomib. This provides a strong rationale for studying the influence of miR-34a expression *in vitro* to uncover a mechanism of modulation of sensitivity.

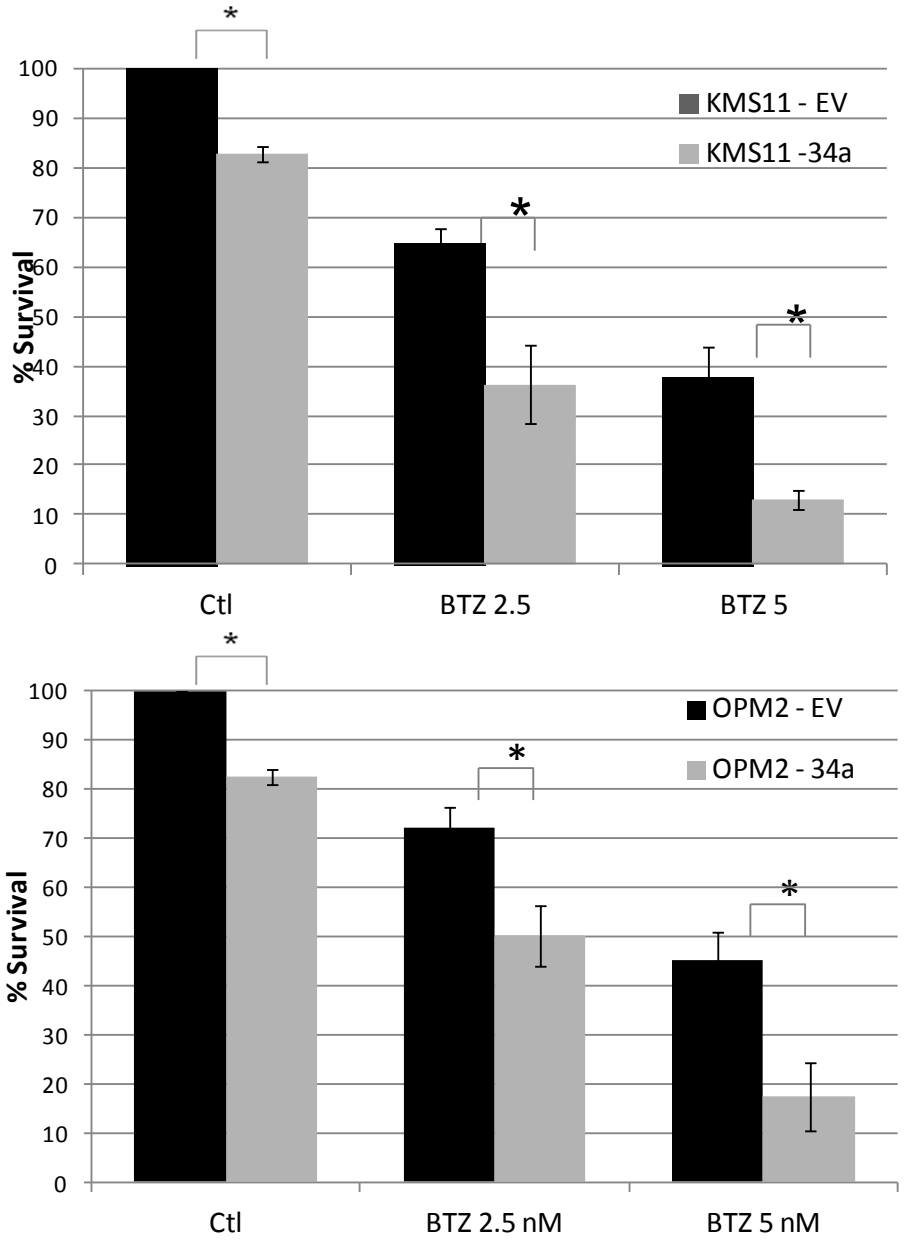

Figure 3-12. m iR-34a in fluences MM c ell sensitivity to the c ytotoxic effect of bortezomib.

Sensitivity to bortezomib after being cultured for 24 hours in the absence and presence of Bortezomib (2.5nm a nd 5 nM). Annexin V -PE flow cytometric analysis was used to evaluate th e c ytotoxic effects of B ortezomib. KMS11-34A a nd OPM2-34a de monstrate an increase of sensitivity relative to the empty vector controls. Student t-test was used to check for significance a nd interaction between all the variables. Bonferroni posttest was then used to check for significance with significance set at $p<0.05$.

3.5.2 Epigenetic modification of the promoter region of mir-34a correlates with low expression of miR-34a

Epigenetic inactivation of miR-34a has been shown to be present in hematological malignancies[99] as well as solid tumors including breast, colon and lung[104]. In order to examine the epigenetic modifications associated with miR-34a expression in the MM cell line panel, bisulfate conversion based PCR was performed on DNA extracted from all seven MM cell lines. Treatment of DNA with sodium bisulfite (EpiTect, Qiagen) results in the conversion of all cytosine residues to uracil, but leaves the 5-methylcytosine residues unaffected[99]. After washing off any residual sodium bisulfite, methylation specific PCR was performed. Specific primers were used to detect methylated and unmethylated products in the miR-34a promoter region, followed by bisulfite specific sequencing. As shown in Figure 3-13, all MM cell lines with low miR-34a expression (KMS11, OPM2, INA6) are shown to have methylation sites present in the miR-34a promoter region. KMS11 is shown to have has allelic differences of methylation sites as there is presence of both methylated and un-methylated sequences. Interestingly, none of the relative sensitive cell lines (MM1S, 8226, U266 and H929) have methylation present in this region. The presence of methylation sites on the promoter region of miR-34a in the resistant MM cell lines can partly explain the low expression of miR-34a and provides a rationale for epigenetic silencing of miR-34a through promoter methylation. Further sequencing of the methylation specific PCR products confirmed the expected nucleotide changes indicating methyl group conversions.

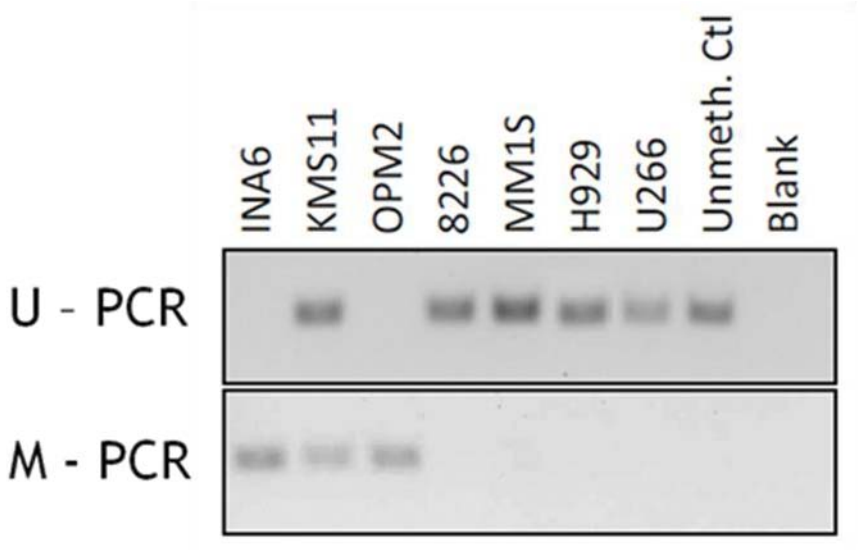

Figure 3-13. Bisulfite conversion and methylation specific PCR (MSP)

Bisulfite conversion was performed on DNA from each of the MM cell lines followed by methylated (M) and umeth ylated (U) specific PCR for pr omoter region of mi R-34a. Methylation of the pr omoter r egion exists in only the r elative resistant s amples (INA6, KMS11, OPM 2), c ompared to no meth ylation present in the sensitive samples (8226, MM1S, H929, U266).

3.5.3 Epigenetic silencing of miR-34a is reversible with the treatment of 5'Azacytidine

To determine whether promoter methylation found in the resistant cell lines is responsible for epigenetic silencing of miR-34a, cells were treated with the demethylating agent 5'-Azacytidine (5'AZA). Treatment with 5'AZA for 24 hours, followed by bisulfite conversion and methylation-specific PCR demonstrated the removal of methyl groups on the miR-34a promoter region (Figure 3-14A). Furthermore, treatment with 5'AZA led to an up-regulation of miR34a expression, as demonstrated by qRT-PCR analysis, suggesting that miR-34a is under epigenetic control (Figure 3-14B). Taken together, these findings confirm that hypermethylation of the promoter region of miR-34a is associated with gene silencing and this phenomenon can be moderately reversed with treatments with a demethylating agent. This provides a possible rationale for combining 5'AZA with bortezomib to achieve similar results with increased expression of miR-34a.

3.5.4 Genetic modification of p53correlates with low expression of miR-34a

Furthermore, and since p53 is reported to activate miR-34a expression (ref) , miR-34a levels were correlated with the TP53 mutational status and del17p.13 in MM cells. Cytogenetic fluorescent *in situ* hybridization (FISH) was performed on each MM cell line using a TP53 specific probe. Cells were treated with the metaphase arresting agent colchicine, which functions to inhibit spindle formation and arresting at metaphase. Treatment with a hypotonic solution, followed by fixation, then made it possible to prepare metaphase spreads on slides. The prepared slides were then incubated with a specific locus specific indicator (LSI) FISH probe for TP53 (orange), and a control probe, specifically a centromeric enumeration probe (CEP) for chromosome 17 (green).

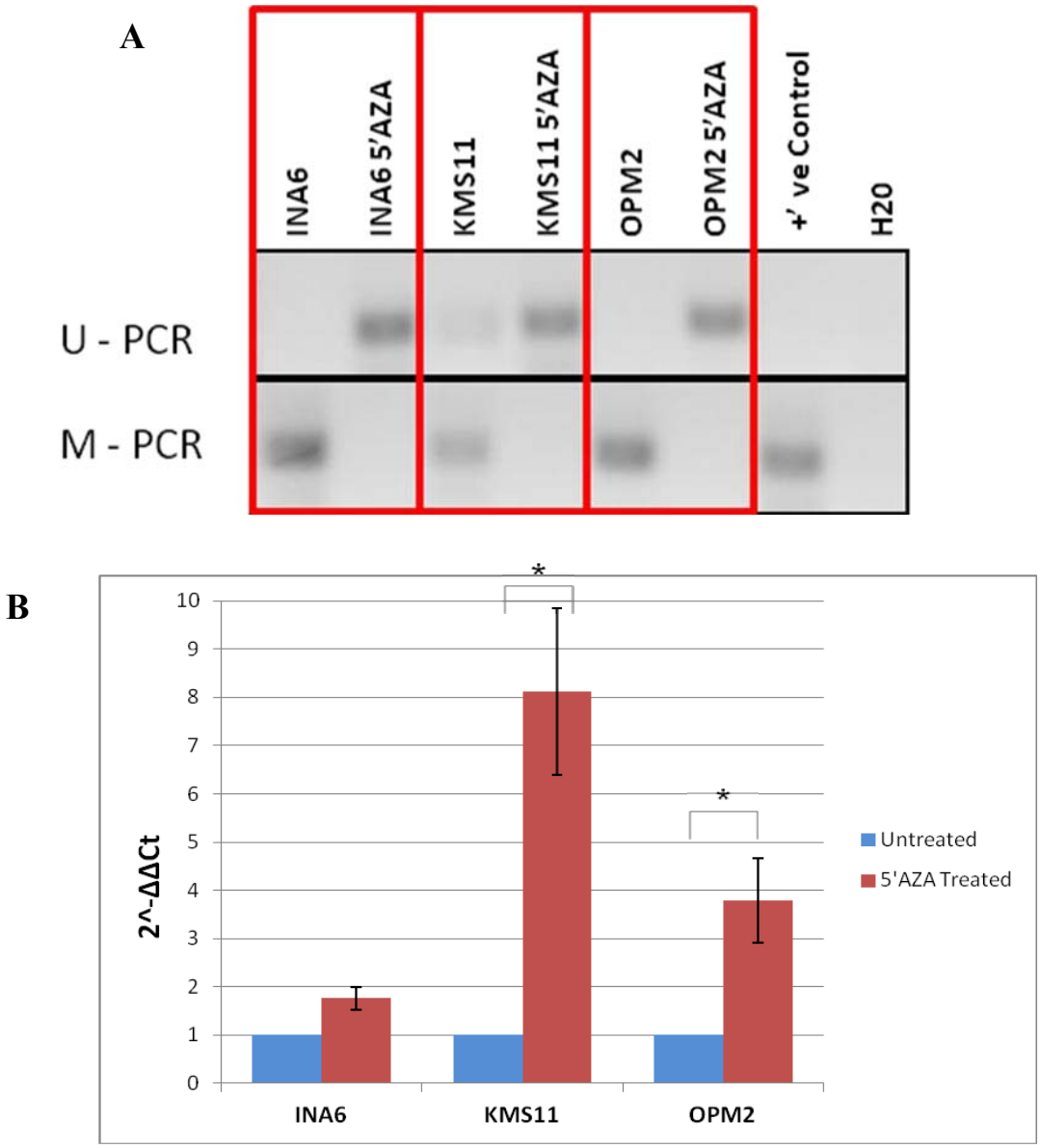

Figure 3-14. Epigenetic silencing is reversible with treatment of 5'AZA

Resistant cell lines (INA6, KMS11, OPM2) were treated with 0.3uM 5'Azacytidine (5'AZA) for 6 hours. Bisulfite conversion followed by methylation specific PCR following treatment result in (A) a reversal of methylation on the promoter region of miR-34a and (B) an increase of miR-34a expression as measured by qRT-PCR. Student t-test was used to check for significance and interaction between all the variables. Bonferroni post test was then used to check for significance with significance set at $p<0.05$.

The TP53/CEP 17 FISH probe was used to determine loss of the genetic region of 17p13.1. As shown in Figure 3-15, an allelic loss of chromosome region 17p13.1 was detected by FISH in KMS11 cells. All other cell lines had a minimum of 2 signals present for the 17p13 region (orange loci), although multiple copies of chromosome 17 were present (green loci), with the exception of INA6 and H929, each with the normal complement of chromosome 17(Figure 3-15). Western blot analysis of p53 has confirmed the complete loss of p53 expression in KMS11 cells due to the deletion of TP53 at locus 17p13.1.

In addition, exonic sequencing of TP53 was performed in the MM cell lines. Mutations were identified in 5 of the 7 cell lines, as shown in Table 3-3, present in KMS11, INA6, OPM2, 8226, and U226. Notably, no mutations were found in MM1S and H929, the two cell lines with the highest miR-34a expression levels as previously shown in Figure 3-10. Mutations were found in all other cell lines in exons 5, 7 and 8, correlating with lower miR-34a expression levels. Furthermore, with respect to the resistant MM cell lines, these genetic modifications of TP53 together with the epigenetic modifications observed on the promoter region of miR-34a provide an additional explanation for the low miR-34a expression observed in our resistant MM cell lines. A summary of miR-34a expression, epigenetic and genetic alteration of all MM cell lines is summarized in Table 3-4. It is of particular interest that while p53 mutations were found in most MM cell lines, methylation of the miR-34a promoter was seen only in the resistant cell lines.

Figure 3-15. Fluorescent in situ hybridization reveals p53 status in MM cell lines

p53 Fluorescent *in situ* hybridization (FISH) on interphase and colcemid induced metaphase cells. The Vysis TP53/CEP 17 probe was used with the probe map shown inset. The green loci (Spectrum green) indicate the centromeric region of chromosome 17 and the orange loci (Spectrum orange) indicate the 17p13.1 region, the p53 locus.

INA6 - (2 x CEP 17, 2 x p53), KMS11 - (4 x CEP 17, 1 x p53), OPM2 - (4 x CEP 17, 2 x p53), MM1S - (2 x CEP 17, 2 x p53), 8226 - (4 x CEP 17, 2 x p53), U266 - (4 x CEP 17, 2 x p53), H929 - (4 x CEP 17, 2 x p53)

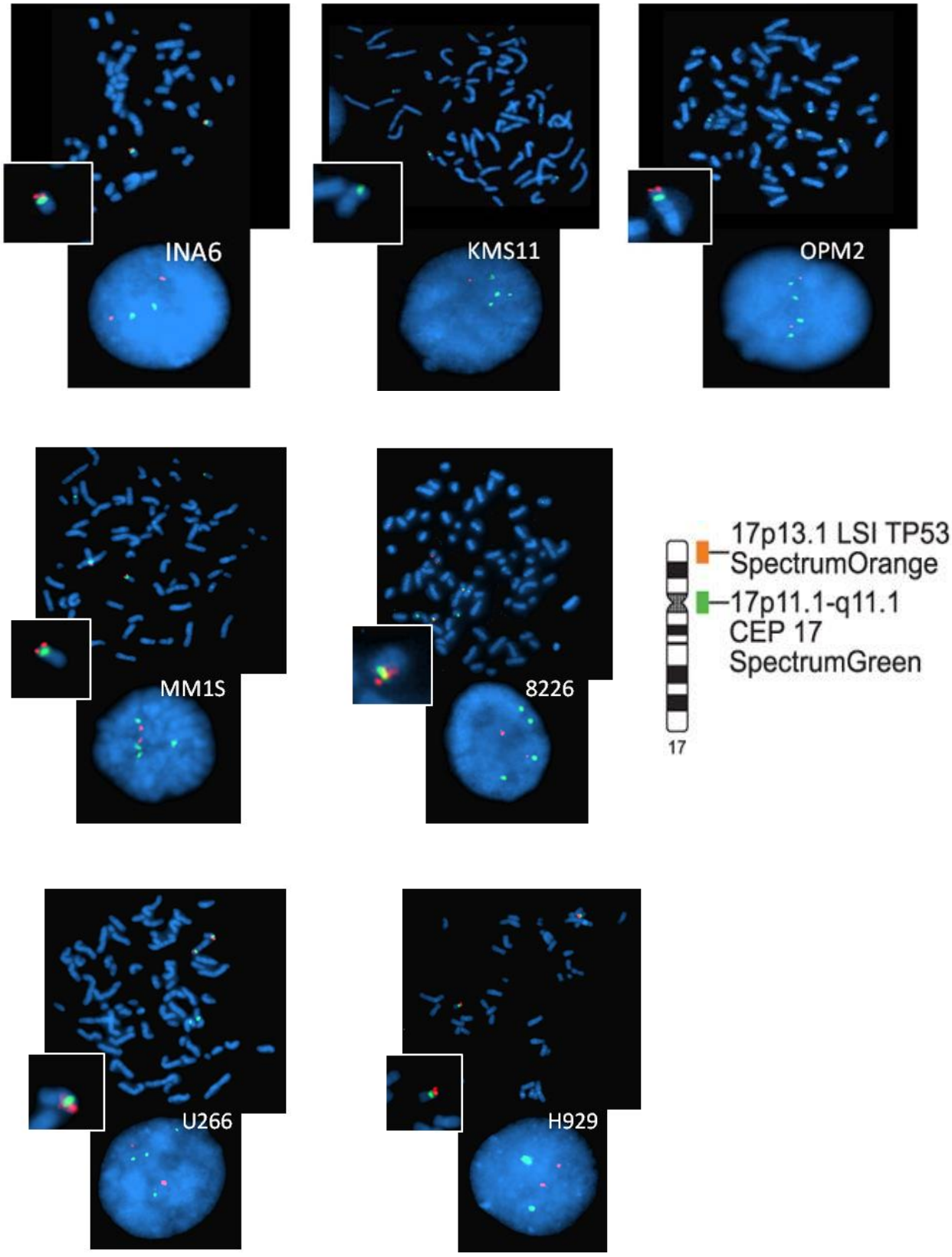
INA6
KMS11
OPM2
MM1S
8226
17p13.1 LSI TP53
SpectrumOrange
17p11.1-q11.1
CEP 17
SpectrumGreen
17
U266
H929

Table 3-2. Summary of p53 FISH status in MM cell lines.

The number of fluorescent loci visualized in MM cell lines for chromosome 17 centromeric region and 17p13.1 as seen in a minimum of 50 interphase cells of each cell line.

Cell Line	# of Signals CEP 17	# of Signals 17p13.1
INA6	2	2
KMS11	4	1
OPM2	4	2
MM1S	2	2
8226	4	2
U266	4	2
H929	4	2

Table 3-3. Mutational Analysis of p53 in MM cell lines.

Full exonic sanger sequencing of p53 was performed on all cell lines and run on a ABI 3330 sequencer. A mutation was present in INA6, KMS11, OPM2, 8226 and U266 as indicated by the codon and protein mutational change. A single nucleotide polymorphism (SNP) was present in all MM cell lines with the exception of MM1s and 8226.

Cell Line	Exon of Mutation	Mutation (codon)	Mutation (protein)	SNP
INA6	**Exon 7**	**c.14069G>A**	**p.Arg248Trp**	**Exon 4 c.12139C>G**
KMS11	**Exon 7**	**c.14069G>A**	**p.Arg248Trp**	**Exon 4 c.12139C>G**
OPM2	**Exon 5**	**c.13203G>A**	**p.Arg175His**	**Exon 4 c.12139C>G**
H929	**N/A**	**N/A**	**N/A**	**Exon 4 c.12139C>G**
MM1S	**N/A**	**N/A**	**N/A**	**N/A**
8226	**Exon 8**	**c.14522G>A**	**p.Glu285Lys**	**N/A**
U266	**Exon 5**	**c.13160G>A**	**p.Ala161Thr**	**Exon 4 c.12139C>G**

Table 3-4. Summary of epigenetic and genetic modifications in MM cell lines.

Cell Line	mir-34a expression	17p FISH		P53 mutation	Methylation
KMS11	↓	4-17	1-p	Exon 7	+/-
INA6	↓	2	2	Exon 7	+
OPM2	↓	4	2	Exon 5	+
H929	↑	2	2	None	-
MM1S	↑	4	2	None	-
8226	↑	4	2	Exon 8	-
U266	↑	4	2	Exon 5	-

3.5.5 Mechanism of miR-34a modulation to bortezomib

In order to define the mechanisms mediating miR-34a effect on sensitivity to bortezomib in MM, the transcriptome of KMS11 transfected cell lines expressing miR-34a and the empty control vector (KMS11-34a and KMS11-EV) were analyzed by performing gene expression profiling (GEP) analysis. Total RNA was isolated from three samples of each KMS11-EV and KMS11-34a, and quality control analysis was performed to determine the RIN. RNA was hybridized onto the U133 Plus 2.0 gene chip (Affymetrix) and raw mRNAs expression values were extracted from scanned gene-chips, $\log_2$ transformed and normalized. As shown in Figure 3-16, comparison of normalized miRNA expression in the three empty vector samples versus the three miR-34a samples identified differentially expressed miRNAs (Fold change < -1.2 or > 1.2 with False discovery rate [FDR] <0.05) and clustered the empty vector and miR-34a samples into 2 distinct groups. Principle component analysis (PCA) mapping correlation was 67.7 %.

Gene ontology (GO) analysis was also performed between the empty vector and miR-34a expressing KMS11 cells. GO analysis identified several molecular functions and biological processes that are modified by the increased expression of miR-34a (Figure 3-17). Processes of interest that may be involved in the modulation to bortezomib sensitivity include transcriptional regulator activity, biological adhesion and regulation and cell growth. Of the differentially expressed mRNAs identified between KMS11-EV and KMS11-34a, three classes of genes have been identified as shown in Table 3-5.

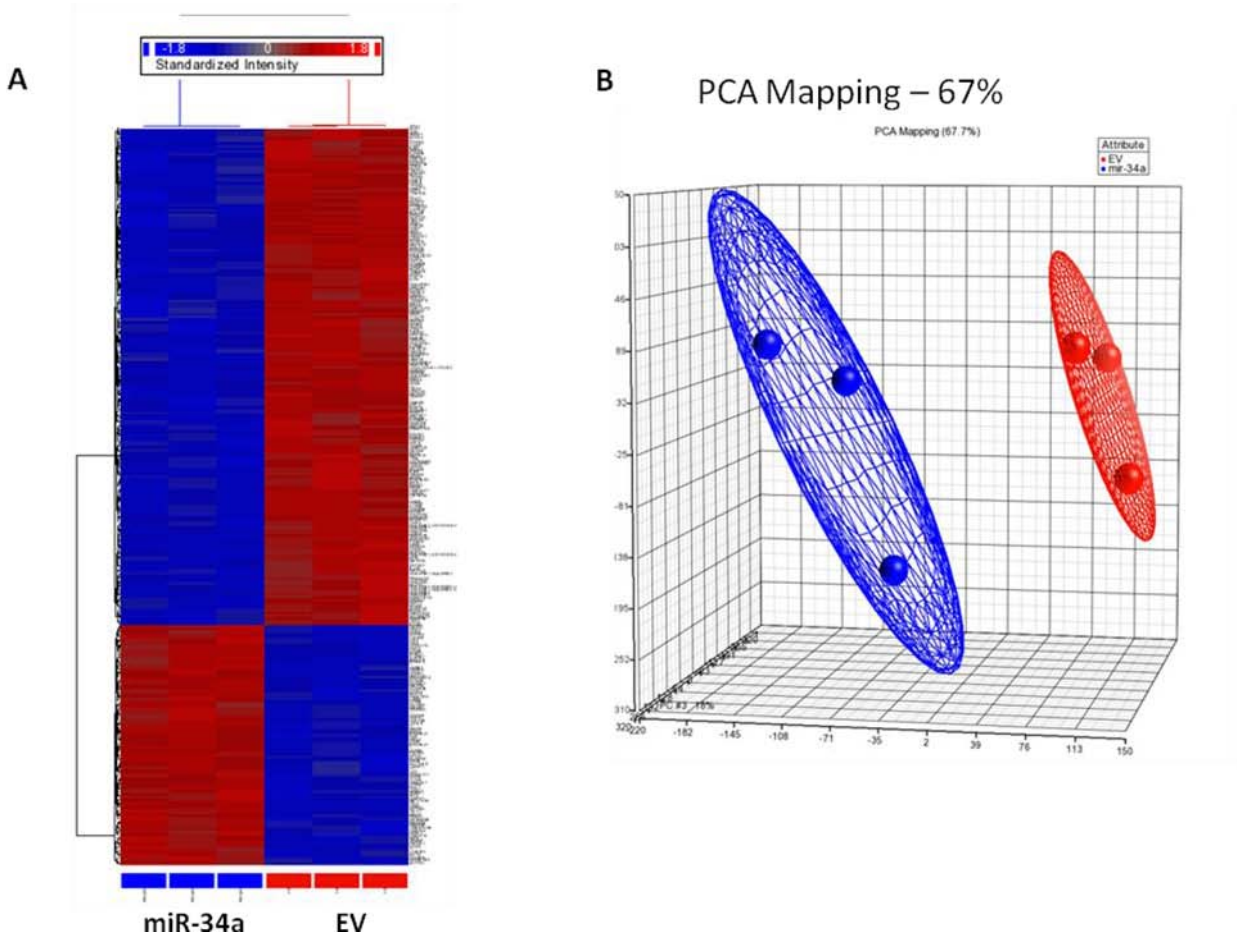

Figure 3-16. Microarray analysis of KMS11-EV versus KMS11-34a.

(A) Heatmap showing the 2 clusters of KMS11-34a and KMS11-EV cells. Heatmap was generated after supervised hierarchical clustering using the ANOVA test. Expression of miRNA patterns is shown by up-regulation (red) versus down-regulation (blue) (B) PCA mapping of the expression data is 67%.

Figure 3-17. Gene Ontology Enrichment Score

Gene Ontology (GO) analysis performed on microarray results from KMS11-EV versus KMS11-34a, performed using Partek software. GO analysis identified several molecular functions and biological processes that are modified by the increased expression of miR-34a. (A) Molecular function enrichment score. (B) Biological processes enrichment score.

A

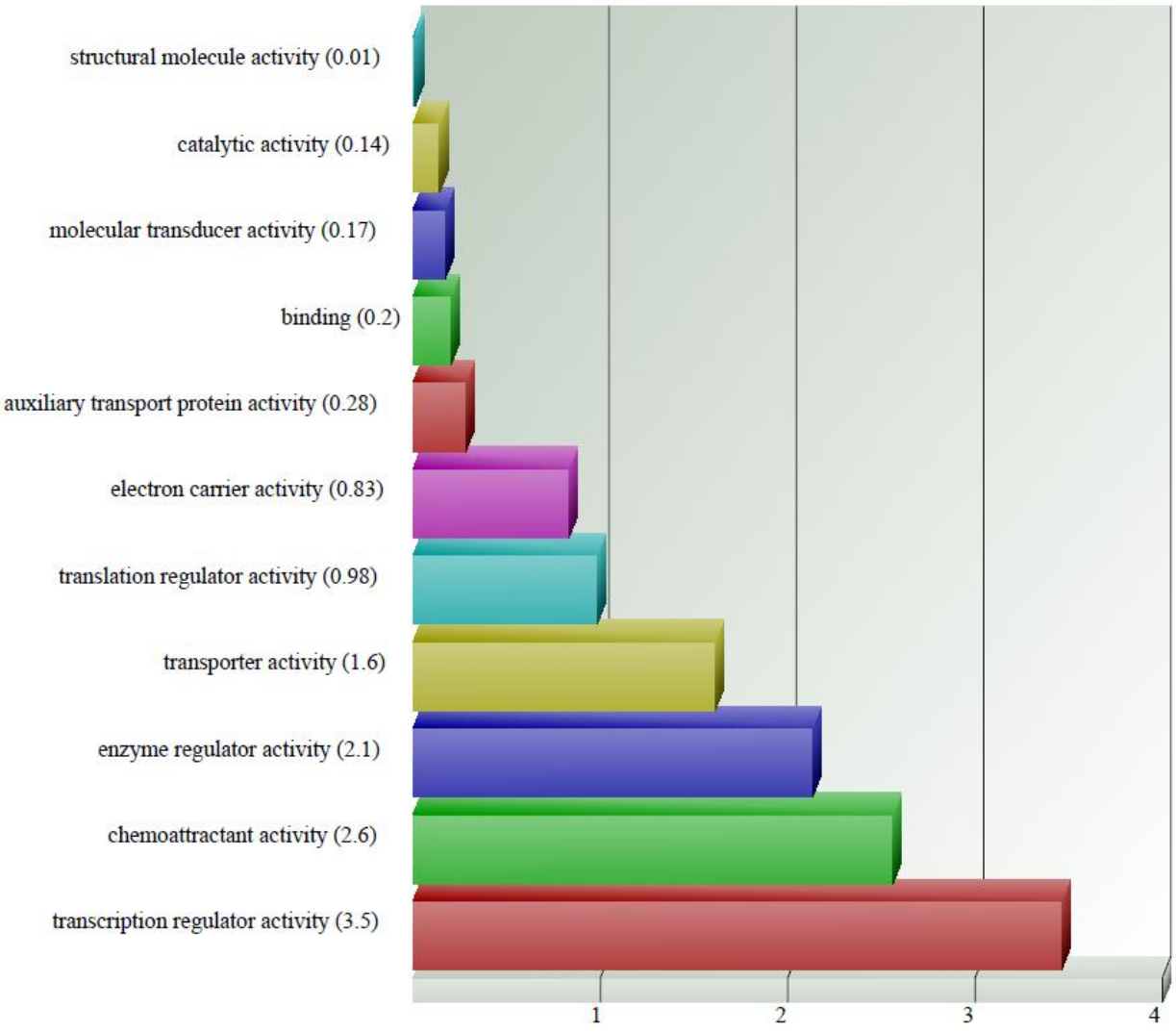
structural molecule activity (0.01)
catalytic activity (0.14)
molecular transducer activity (0.17)
binding (0.2)
auxiliary transport protein activity (0.28)
electron carrier activity (0.83)
translation regulator activity (0.98)
transporter activity (1.6)
enzyme regulator activity (2.1)
chemoattractant activity (2.6)
transcription regulator activity (3.5)
1
2
3
4

B

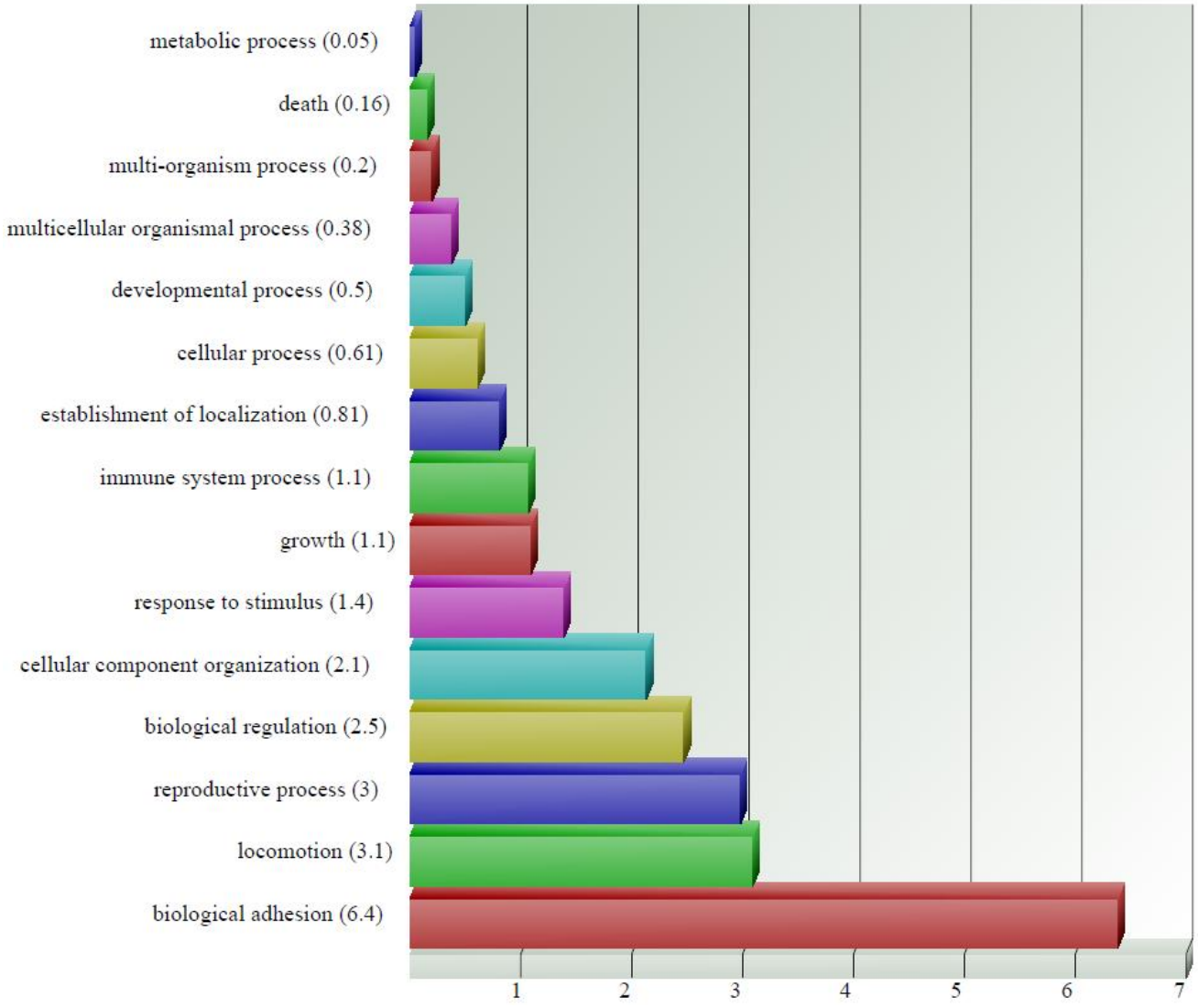
metabolic process (0.05)
death (0.16)
multi-organism process (0.2)
multicellular organismal process (0.38)
developmental process (0.5)
cellular process (0.61)
establishment of localization (0.81)
immune system process (1.1)
growth (1.1)
response to stimulus (1.4)
cellular component organization (2.1)
biological regulation (2.5)
reproductive process (3)
locomotion (3.1)
biological adhesion (6.4)
1
2
3
4
5
6
7

Table 3-5. Targets identified in microarray analysis of KMS11-EV vs. KMS11-34a. (A) Representative target genes of mir-34a that have been previously shown to be important in MM biology and pathogenesis. (B) Target genes previously shown to be sensitizers to bortezomib. (C) Novel target genes of miR-34a.

GENE	FOLD CHANGE	
CXCL10	-1.80289	miR34a down vs EV
CXCR4	-1.46477	miR34a down vs EV
BCL2	-1.23956	miR34a down vs EV
IL6R	-1.21764	miR34a down vs EV

GENE	FOLD CHANGE	
E2F3	-1.35528	miR34a down vs EV
CDK6	-1.32004	miR34a down vs EV
CDK4	-1.28884	miR34a down vs EV

GENE	FOLD CHANGE	
OGFOD1	-58.2608	miR34a down vs EV

While these samples so not represent all of the highest differentially expressed genes in this screen, they have been identified as probable candidates to explain miR-34a modulation of sensitivity to bortezomib.

Firstly, the screen identified several gene targets that have been previously shown to be in important in the biology of multiple myeloma, including IL6r, CXCL10, CXCR4 and BCL2. Second, targets were identified that when down regulated, have been previously shown to be sensitizers to Bortezomib, including E2F3, CDK4 and CDK6[61]. These were previously identified by Zhu et al[61] in a high throughput shRNA screen which identified sensitizers to bortezomib. More importantly, novel targets have been identified that may provide insight into the role of modulation of miR-34a and the mechanism of resistance, including the most highly differentiated gene, OGFOD1.

Many of the genes identified in the microarray screen are directly regulated by miR-34a, shown using predictive microRNA match analysis tools and by analysis of the 3'UTR to the seed match sequences to miR-34a. Figure 3-18 demonstrates that a number of target genes indentified have strong seed match complementarity in the 3'UTR with miR-34a. Genes identified in the microarray screen were also validated at the protein level by western blot analysis. As shown in Figure 3-19, expression of mir-34a in KMS11-34a and OPM2-34a results in a dramatic reduction of many of the targets compared to KMS11-EV and OPM2-34a. Proteins involved in apoptosis and cell cycle regulation including Bcl-2, CDK4, CDK6, CEBPα, SIRT-1 and YY1, all predicted targets of miR-34a, have reduced expression levels when compared to the empty vector control.

Figure 3-18. Seed matches of miR-34a and target genes.

Images demonstrating the sequence match of miR-34a and the 3'UTR of the target genes. Seed match at the 3'UTR end in: CXCL10 (7 bp match), BCL2 (6 bp match), IL6R (7 bp match), E2F3 (8 bp match), CDK6 (8 bp match), OGFPD1 (7 bp match)

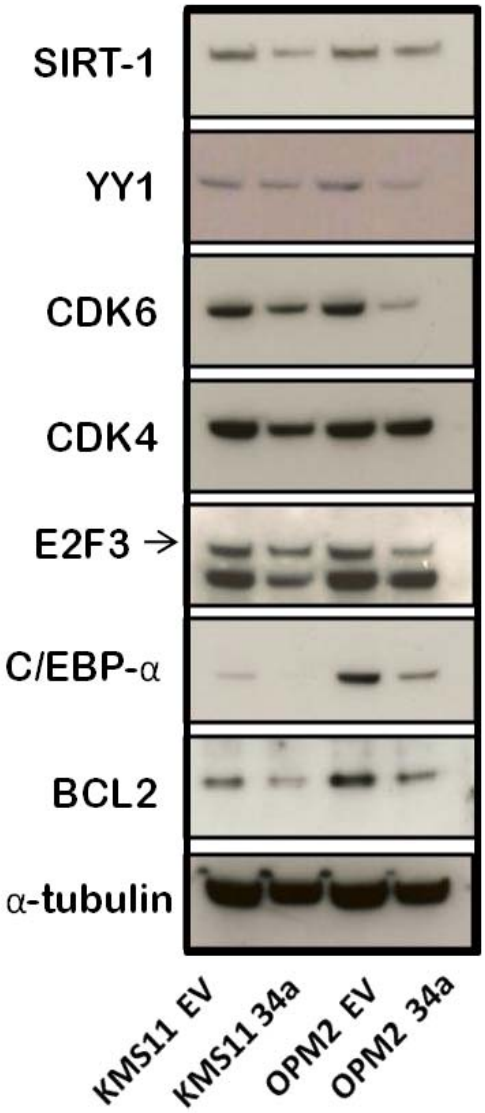

Figure 3-19. Immunoblot analysis of miR-34a targets

Protein levels of SIRT-1, YY1, CDK4/6, E2F3, CEBPα, BCL2 in KMS11-EV, KMS11-34a, OPM2-EV, OPM2-34a. Representative blot of 2 independent experiments compared to the housekeeping gene α-tubulin.

3.5.5.1 Investigation of novel target OGFOD1.

As previously mentioned, OGFOD1 is the target gene that is most differentially expressed between KMS11-EV and KMS11-34a, a 58 fold change higher in KMS11-EV versus KMS11-34a. Although little is known of the function of OGFOD1 [2-oxoglutarate and Fe(II) dioxygenase1], a recent study has shown that it interacts directly with eIF2α (eukaryotic translation initiation factor 2 alpha)[105]. In the response to stress, eIF2α is phosphorylated (p-eIF2α), resulting in down-regulation of cellular translation[106]. Given the implication of translation levels and UPR stress on the sensitivity to bortezomib, the influence of p-eIF2α and OGFOD1 was examined in the response to bortezomib. KMS11-EV and KMS11-34a cells were treated with the IC50 dose of bortezomib (1.25 nM) and cells were collected at varying time points (O, 3, 6, 12, 18, 24 and 36 hours), protein lysate was collected and immunoblotting was performed. It was hypothesized that in KMS11-34a cells, which have significantly lower OGFOD1 levels, p-eIF2α levels would be lower, therefore leading to higher cellular translation, load and stress on the UPR. While basal levels of p-eIF2α appear to be slighter lower in the KMS11-34a cells compared to the KMS11-EV, as shown in Figure 3-20, there is no significant change in the p-eIF2α levels in response to bortezomib. Further work investigating the role of novel targets in the response to bortezomib is required.

3.5.6 miR-34a expression increases sensitivity to Bortezomib in MM xenograft model

Based on *in vitro* data where miR-34a over-expression has shown to increase sensitivity to bortezomib in MM cells, the role of miR-34a on tumor growth and response to Bortezomib treatment was then investigated *in vivo*. A murine xenograft human MM

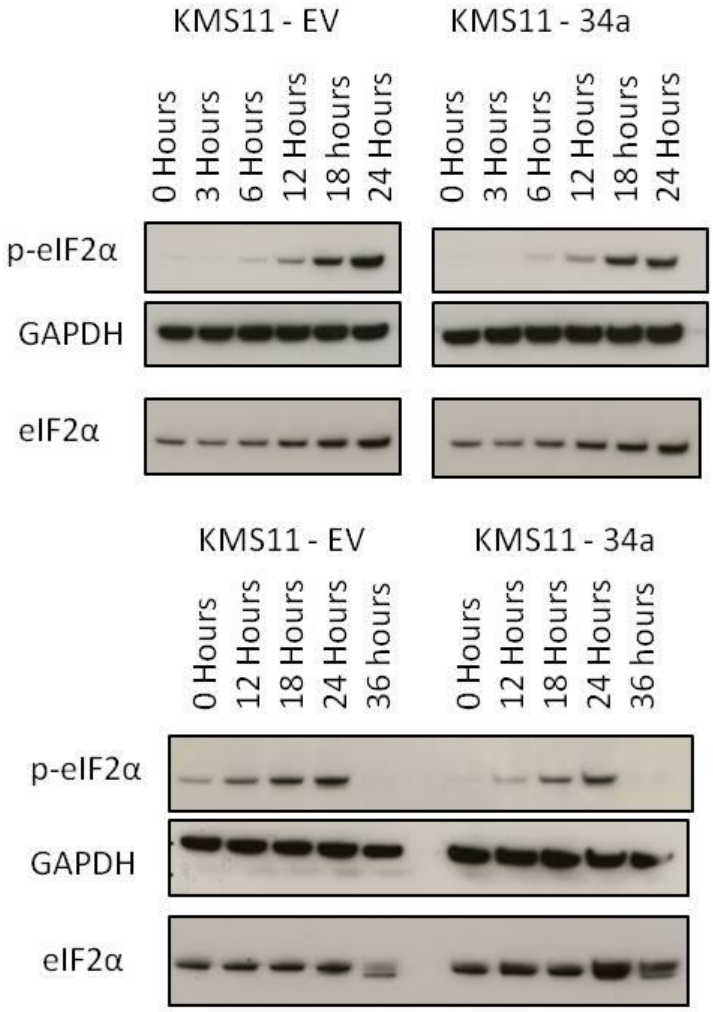

Figure 3-20. Immunoblot analysis of ρ-eIF2α and eIF2α.

Protein levels of total eIF2α and ρ-eIF2α in KMS11-EV and KMS11-34a in response to 1.25nM of bortezomib, collected at various time points following treatment. Representative blot of 2 independent experiments compared to the housekeeping gene GAPDH.

model with severe combined immuno-deficient (SCID) mice was used to investigate the effect of miR-34a on tumour growth and response to bortezomib. Cohorts of SCID mice were injected subcutaneously with KMS11-34a or KMS11-EVand the effect on tumour growth was monitored. Human xenografts were treated with bortezomib or vehicle alone for 3 weeks. As seen in Figure 3-21, the growth kinetics of KMS11-34a xenografts were significantly slower compared to that of KMS11-EV. The tumor volumes were 1000 mm^3 versus 2000 mm^3 respectively on day 10. Following treatment with bortezomib, this effect was even more evident in treated mice where the tumor volume on day 14 was 3000 mm3 in KMS11-EV versus 1200 mm3 in KMS11-34a. While this is a small cohort of mice, without statistical significance, it provides a framework for future in vivo studies to examine the role of miR-34a in tumour kinetics and bortezomib sensitivity.

Overall, these results demonstrate that miR-34a expression has a significant influence on MM cell sensitivity to bortezomib and may support a potential therapeutic role for miRNA manipulation, in particular miR-34a in MM. Figure 3-22 schematically illustrates the summary of the postulated mechanisms mediating miR-34a effects in MM.

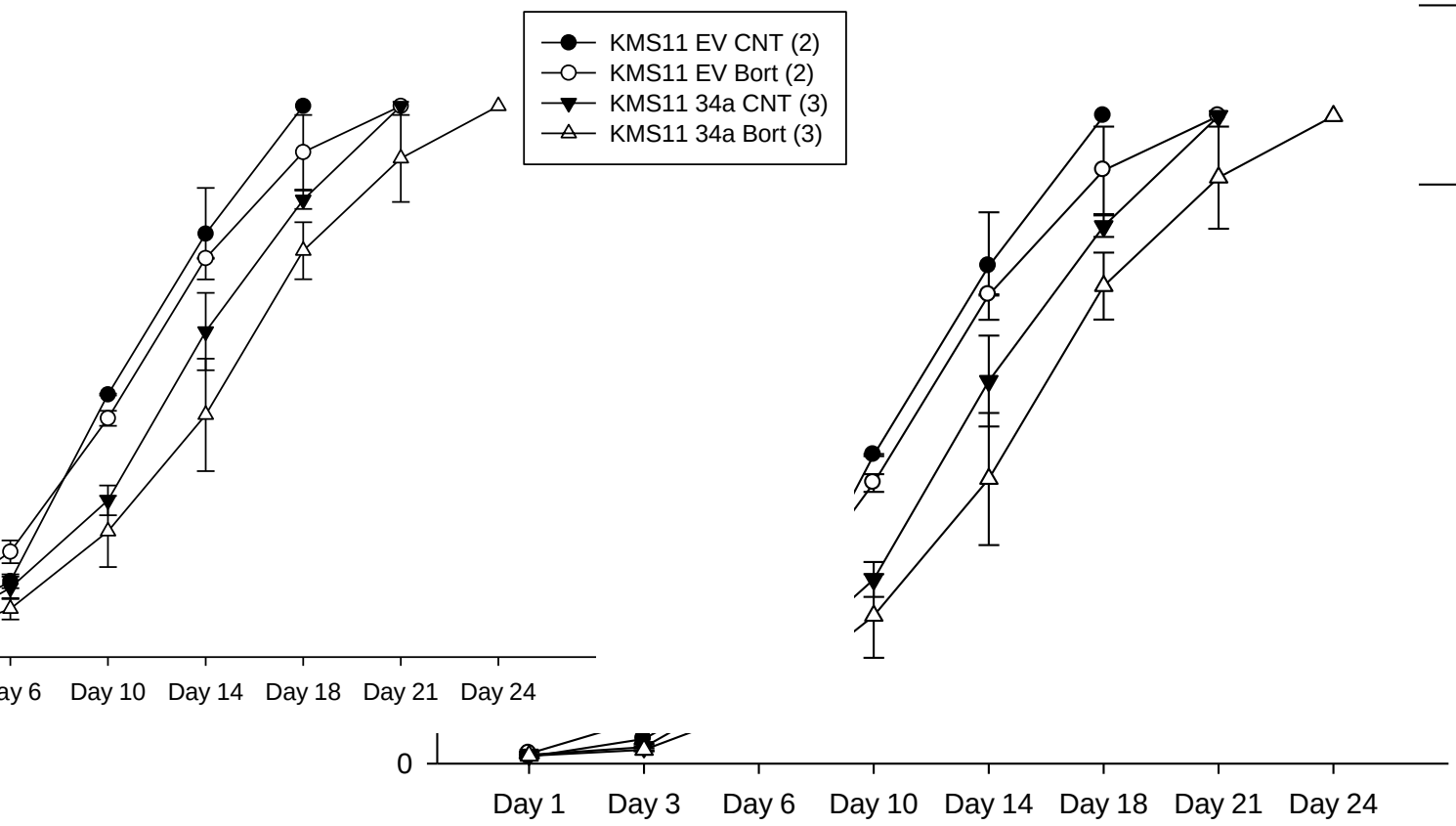

Figure 3-21. *in vivo* analysis of miR-34a in SCID-xenograft model.

CB-17 SCID mice were injected SC with 2 X 10^6 KMS11-EV and KMS11-34a cells. After the detection of a measureable tumour, animals were treated with vehicle alone or bortezomib (0.4mg/kg SC twice weekly). Tumour volume was accessed in 2 dimensions twice weekly until the day of sacrifice. n= 2 in KMS11-EV mice, and n=3 in KMS11-34a mice. Two-way ANOVA was used to check for significance and interaction between all the variables.

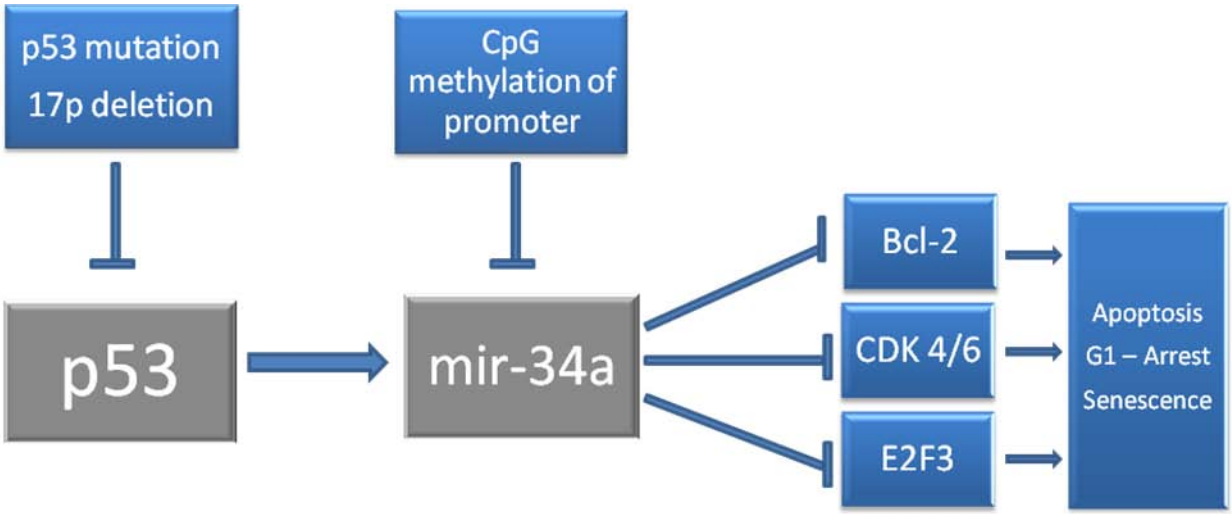

Figure 3-22. Schematic of miR-34a regulation, expression and targets.

Chapter Four: Discussion and Conclusion

While improvements have been made to improve overall survival of MM, response of individual MM patients is highly variable, despite the availability of new agents, including immulomodulatory drugs (thalidomide, lenalidomide), proteasome inhibitors (Bortezomib) and stem cell transplantation (SCT). In particular, the agent studied in this study bortezomib, used in the treatment of relapsed MM is effective in approximately 50% of patients. However, currently adopted clinical biomarkers have not been able to predict response to this class of drugs. While survival in MM has improved significantly in the past ten years, the treatment of MM still remains challenging and further classification and treatment strategies are needed. miRNA involvement in the clonal evolution of plasma cells from MGUS to MM stages and correlation with specific MM molecular subgroups have been described previously[94-96]. In addition, an association between high-risk disease and global elevation of miRNA expression has been reported .[93] miRNA are small (~ 22 nucleotides) non-coding RNAs that regulate mRNAs translation and degradation and alterations and over-expression of miRNA expression are reported to play a large role in most cancers. While attempts have been made to use miRNA in classifying and staging MM, little is known about the expression of miRNA and the effect on response to treatment of proteasome inhibitors in MM.

4.1 Microarray profiling identifies differential expressed miRNAs

Using a high throughput microarray screen in human MM cell lines, we have identified a subset of miRNAs that may potentiate or hinder the cytotoxic effect of bortezomib. A set of deregulated miRNAs in MM cell lines have been identified that are differentiated between relative sensitivity and resistance to Bortezomib. In particular, miR-181a was found to be highly expressed in resistant cell lines, while mir-34a, a target of tumor suppressor p53, has been found to have high expression in sensitive MM cells.

4.1.1 Limitations

In interpreting this screen, we have accepted the limitations of extrapolating data from a small number of MM cell lines in each the sensitive and resistant group. Functional analysis was performed to offset this limitation to verify the significance of our results. We acknowledge that this study may not be comprehensive for all MM classifications to find a unique miRNA signature, however the intention was to simply identify miRNAs that may play a role in bortezomib sensitivity. Additionally, stringent statistical conditions were used when analyzing the microarray data, with false discovery rate (FDR) less than 0.05 and only microRNAs that had differential gene expression fold changes that were greater than 2, or less than -2. We recognize that these stringent conditions may have excluded miRNA that may be important in the role in bortezomib sensitivity. However, these conditions were used to create a small manageable group of miRNA in which to study. Furthermore, calculating the GMR using the results of the microarray and qRT-PCR expression successfully classified both the sensitive and resistant groups. This suggests that despite using a small group of microRNA from

stringent conditions, they may be of significance in the role of bortezomib sensitivity. Should further investigation be required, different statistical conditions may be used to expand the group of microRNAs. An additional limitation of this study is the mechanism by which relative "resistance or sensitivity" to bortezomib has been defined. In MM cell lines *in vitro*, it is relatively easy to define as simply evaluating the IC50 value. However, in MM patients, it is more difficult to determine resistance to one particular therapeutic agent as there are many confounding factors, including combination therapeutic strategies. This may have an influence on how these data are interpreted in patient samples. Further investigations are required to determine the influence of this study on patient samples and the response to bortezomib. However, recognizing that analysis was performed on a small number of MM cell lines, this study has provided a framework for investigation of the influence of miRNA in multiple myeloma and the role in sensitivity to bortezomib.

4.1.2 The influence of miR-181a on bortezomib resistance in MM

Our study has identified miR-181a to be highly expressed in resistant cell lines, with a fold increase of 4.77 compared to the sensitive MM cell lines. It is well known that the miR-181 family, one of the most studied miRNAs, is deregulated in many tumours. The physiological and pathological function of miR-181a has been studied in many tumour types. Shi *et al* have identified miR-181a as a tumour suppressor in human glioma cells, and when down-regulated were involved in oncogenesis of glioma[107]. Additionally, miR-181a has shown to correlate with specific sub-classes of acute myeloid leukemia and the expression of its target genes[108]. Of particular interest to us was the

investigation that identified miR-181a as a microRNA involved in haematopoietic differentiation and a positive regulator of B-cell differentiation[109]. The involvement in haematopoiesis and the role as a tumour suppressor led us to investigate the role of miR-181a in sensitizing MM cells to the cytotoxic effect of bortezomib. When miR-181a expression was antagonized in resistant MM cell lines, a greater cytotoxic response was seen with the treatment of bortezomib. However, while miR-181a antagonized MM cells appear to have biological importance in modulating resistance to bortezomib, an increase in proliferation rate in MM cells is also seen. While this provides an interesting mechanistic question as to how miR-181a modulates to sensitivity to bortezomib, this investigation may not be as clinically relevant. Clinically, while miR-181a antagonism may increase sensitivity to bortezomib treatment, it would not be a suitable microRNA to target due the prospect of also increasing tumour growth. Functional investigation of the role of miR-181a on modulating sensitivity to bortezomib is still required. Additionally, miR-181a antagonism was difficult to study, due to the difficulties in validating miR-181a expression. Due to the nature of the cDNA production, which created the same sequence as the miRZIP vector, overestimation of the miR-181a copy number was seen. With this method, it was difficult to prove that in fact miR-181a expression had been antagonized and was causing the functional changes. Further investigation of miR-181a in MM cell lines may elucidate some of the functional changes, which may provide insight on the mechanism of modulation of sensitivity to bortezomib.

4.1.3 The influence of miR-34a on bortezomib resistance in MM

In the present study we have characterized the influence of miR-34a expression level on the sensitivity to bortezomib; demonstrating that increased levels of miR-34a increases sensitivity to bortezomib. While miR-34a has been implicated in progression of many cancer types and results in alterations in cell cycle and proliferation[102,110,111], a correlation of expression and response to therapeutics is largely unknown. We have demonstrated that TP53 loss or mutation or epigenetic silencing through promoter methylation reduces miR-34a expression in MM cells. Conversely, restored miR-34a expression down-regulates BCL2, CDK4/6, E2F3 and YY1and sensitizes MM cells to bortezomib. Taken together these results may provide insight into prediction of a patient's response to proteasome inhibitors and may support a potential therapeutic role for miR-34a in MM.

miR-34a has been a large focus of cancer research in the last five years. It was originally identified as a possible tumour suppressor in neuroblastoma, where it was down-regulated and induced apoptosis[112]. miR-34a has since been identified to be down-regulated in many tumour cell types such as leukemia, colon cancer, non-small cell lung cancer and hepatocellular carcinoma[103,113,114]. The deregulated function of miR-34a has been studied and has been demonstrated to affect apoptosis, senescence and proliferation[112,114-116]. Furthermore, it became an interesting miRNA to study as it had been identified as a transcriptional target of p53, the most commonly mutated gene in cancer[111,117-119]. The tumor suppressor p53 is the most frequently mutated gene in all human tumors and although it is rarely detected at diagnosis in MM, it is typically associated with advanced disease. Deletion of the chromosomal region 17p13, which

includes the TP53 gene, in MM is associated with a poor outcome[120,121]. Recent studies have revealed the relationship between p53 and miRNAs, particularly miR-34a and has been shown that p53 directly targets and regulates miR-34a[115] and miR-34a has previously been reported to induce cell cycle arrest, apoptosis and senescence[119,122,123]. However, its role in the response to therapeutics was largely unknown. This report demonstrates the influence of miR-34a expression and its interactions with p53 to sensitivity to the proteasome inhibitor bortezomib.

4.1.4 Epigenetic and genetic influences on miR-34a expression

We have demonstrated in MM cell lines that mutations in the p53 gene are correlated with low miR-34a expression. Additionally, chromosomal loss of 17p13, where p53 is located, has also been implicated in low miR-34a expression levels. As demonstrated in previous studies[99,104]. Specifically, methylation was found to be present only on the promoter of miR-34a in the three 'resistant' MM cell lines, correlating with low miR-34a expression. Interestingly, no methylation is present on any of the 'sensitive' MM cell lines. Genetic alterations of p53 and epigenetic control of miR-34a expression suggests an important role of p53 signaling in bortezomib cytotoxicity. Mutations of p53 taken together with the methylation on the promoter region provide an additional rational for low miR-34a expression in resistant MM cell lines. It may also provide insight that inactivation of miR-34a via p53 deletions or epigenetic modifications on the promoter of miR-34a may be common event during tumorigenesis and may serve as a useful screening tool in patients.

4.1.5 Novel therapeutic combinations

Furthermore, treatment with the methylation inhibititing agent 5'-Azacytidine, inhibited the methyl groups on the miR-34a promoter and up-regulated miR34a expression. This finding confirms that hyper-methylation of the promoter region of miR-34a is associated with gene silencing and can be moderately reversed with treatments of a methylation inhibitor. DNA methylation inhibitors have been well characterized, tested in clinical trials and have been FDA approved for various cancer types[124]. 5'-Azacytidine is approved to treat patients with high risk myelodysplatic syndromes[125] and is currently in clinical trials for other haematological malignancies[126,127]. This study provides a rationale and novel concept of combining the two agents, 5'AZA and bortezomib; the first to increase miR-34a levels, and the second to further induce apoptosis. Preliminary work not shown in this study has indicated that there is a synergistic effect with this drug combination. Furthermore, use of DNA methylation inhibitors to reverse the silencing of miR-34 may restore sensitivity to other chemotherapeutic agents. Conventional chemotherapeutic agents depend on the activation of pro-apoptotic genes that will respond to the cytotoxic agents, resulting in cell death. Reactivation of epigenetically silenced pro-apoptotic gene and tumour suppressor miR-34a should increase the efficacy of bortezomib and other chemotherapeutic agents. Analysis of promoter methylation may be useful in classifying sub-types of MM patients, and may be useful in predicting therapy response as well as creating new combination studies.

4.1.6 Targets and functional effects of miR-34a in MM

Mir-34a has been previously shown to target miRNAs involved in cell cycle control, apoptosis, and senescence.[102,116,123] Using various miRNA target prediction tools, hundreds of theoretical mRNA targets have been identified. However, it is difficult to accurately predict due to variances between each predictor tool and the varying levels of the miRNAs complementarity to the target sequence. To investigate the mechanism in which miR-34a sensitizes MM cells to bortezomib and the effect mir-34a has on global mRNA expression changes we have performed microarray profiling on the KMS11-34a expressing cells relative to KMS11-EV. We have identified important targets, all of which provide a logical rationale as to the increased levels of apoptosis, identifying important kinases involved in cell cycle control, genes involved in proliferation or involved in apoptotic pathways. Gene expression profiling performed after the introduction of miR-34a revealed many down regulated miR-34a targets, many of which contain seed-matching mir-34a sequences in their 3'UTR, including CDK4/6, E2F3 and YY1. One of the targets of miR-34a, the transcriptional factor YY1 has been previously shown when it is over-expressed, to be involved in resistance to apoptotic signals and resistance to chemotherapeutics[128,129]. YY1 was also identified in the shRNA screens that identified sensitizers to bortezomib and previously discussed[60,61]. This again provides a logical rationale as to why miR-34a over-expression results in increased sensitivity to bortezomib.

Furthermore, miR-34a expression targets the cyclin-dependant kinases 4 and 6 (CDK4 and CDK6), which play important roles in cell cycle control. Inhibition of CDK4/6 in MM cells has previously been shown to decrease tumour growth and

proliferation[130]. Further, in combination with a chemotherapeutic such as dexamethasone, the killing of MM cells is markedly increased. Many of the genes identified as targets of miR-34a have been identified as sensitizers to bortezomib. This includes cell cycle regulators and kinases including CDK4, CDK6, YY1, CDK5, CEPBα and E2F3. As miRNAs regulate the expression of the genes, they represent potential druggable targets through the use of miRNAs. While the role of miR-34a in modulating sensitivity to bortezomib is unknown and the pathway is largely unmapped, targets identified such as YY1, BCL2, and CDK4/6 may provide insight into the mechanism miR-34a plays. Further investigation into the specific role of miR-34a targets in modulating bortezomib sensitivity are required to elucidate this mechanism.

4.1.7 Investigation of novel miR-34a targets and function in MM

An important aspect of this study that requires further investigation, are the novel targets that were identified in the KMS11-EV versus KMS11-34a microarray screen. Investigation of these novel targets may provide insight into the role of modulation of miR-34a and the mechanism of resistance to bortezomib. The most highly differentiated gene between the EV and miR-34a was the target gene OGFOD1 [2-oxoglutarate and Fe(II) dioxygenase1], with a 58 fold expression higher in the EV. Although little is known of the function of OGFOD1, a recent study has shown that it interacts directly with eIF2α (eukaryotic translation initiation factor 2 alpha)[105]. In the response to stress, eIF2α is phosphorylated (p-eIF2α), resulting in down-regulation of cellular translation[106]. As discussed previously, the response to bortezomib is highly dependent on translation levels and UPR stress in the ER. When proteasome function is inhibited by bortezomib,

damaged proteins including misfolded proteins accumulate in the intracellular environment, resulting in ER overload and stress and induction of the UPR. It has been shown that increased levels of phosphorylated eIF2α results in lower levels of translation. We rationalized that if translation levels were lower, there would in turn be less load and stress on the ER and UPR, therefore increased survival following the treatment of bortezomib. In this study, the influence of p-eIF2α and OGFOD1 was examined in the response to bortezomib. It was hypothesized that in cells expressing miR-34a, which would have significantly lower OGFOD1 levels, phosphorylation levels of eIF2α would also be lower. This would then result in increased levels of cellular translation, resulting in more load and stress on the ER, resulting in the UPR. While basal levels of p-eIF2α were demonstrated to be slighter lower in the KMS11-34a cells compared to the KMS11-EV, there is no significant change in the p-eIF2α levels in response to bortezomib. The role of interaction of miR-34a on OGFOD1 and p-eIF2α requires further investigation to determine the influence on sensitivity to bortezomib. Additionally, other novel targets were identified in this study which requires further work to investigate their role in the response to bortezomib.

4.1.8 In vivo investigation of miR-34a in MM

Our findings have demonstrated that over-expression of miR-34a sensitizes MM cells *in vitro* to bortezomib and further supports investigating the role of miR-34a in an *in vivo* model. We addressed this possibility, examining *in vivo* using a SCID murine xenograft human multiple myeloma model. Our preliminary study, although small in numbers, suggest that the expression of miR-34a reduces the tumour burden and

sensitizes the tumour to the treatment of bortezomib. While larger cohort studies are needed, together with the *in vitro* data, these results demonstrate the influence miR-34a has on sensitivity to bortezomib in MM cells. This xenograft MM model has widely been used to study MM *in vivo*, despite it not being highly representative of the MM disease features, which in humans involves bone marrow involvement, bone lesion and renal failure. To investigate the influence of miR-34a on MM pathogenesis and disease progression additional studies are required. Although not allowed for study in Canada, an additional SCID myeloma murine model exists in which primary myeloma cells grow *in vivo* in a human bone marrow micro environment and would serve an excellent model to investigate the role of miR-34a on MM pathogenesis[131]. In this model, myeloma cells are directly injected into an implanted human fetal bone in a SCID mouse. The human bone marrow microenvironment interacts with the myeloma cells and causes myeloma manifestations in the mouse which are typically seen in humans. This often includes bone lesions from osteolysis in the human bone, and appearance of M protein in the serum. Should additional *in vivo* experiments be performed to investigate the role of miR-34a, this model should be used to better represent the MM human model.

4.2 miRNA as therapeutic targets

The potential for using miRNAs as targeted therapeutics in cancer treatment is currently being explored. Targeting of miRNA is based on either selective over-expression or inhibition of miRNA expression. However, the difficulty with targeting miRNA expression is the lack of tissue specificity and the possibility of many off-target effects. There are many different approaches being used to target miRNA in tissues such

as the development of modified miRNA molecules. Anti-miRNA oligonucleotides (antagomiRs)[132], and the locked nucleic acid (LNA) modified oligonucleotide[133] have provided a miRNA oligonucleotide that has a longer half life and efficiency, making it more sustainable for therapeutic use. The antisense oligonucleotides work as a competitive inhibitor of miRNA, by annealing to the guide strand inducing either degradation or the formation of a stable miRNA duplex. AntagomiRs are single stranded molecules that are most often modified with a cholesterol conjugated 2'-O-methyl to maintain stability and minimize degradation[134]. The LNA oligonucleotides have the ribose ring 'locked' by a methylene bridge connecting the 2'-O atom with the 4'-C atom. When the molecule is locked by the methylene bridge, an increased stability and affinity to complementary single stranded RNA is seen[135]. Another approach includes the use of 'miRNA sponges' which contain complementary sites for a specific miRNA, competitively binding to the miRNA, thus interfering with normal targeting[136,137]. Systemic delivery of an unconjugated LNA modified oligonucleotide has been shown to effectively antagonize miR-122 in the liver of non-human primates[138]. Depletion of miR-122 was observed without any evidence of any toxicities from the LNA oligonucleotides or pathological changes in the primates. Additionally, the use of nanoparticles offers an interesting approach for the delivery of miRNAs. They have primarily been used to deliver siRNA, but a recent study has used nanoparticles to deliver miRNA. Specifically, a liposome polycation-Haluronic acid (LPH) particles were used to deliver miR-34a to lung metastasis in a syngeneic mouse model. Growth inhibition of the tumour metastasis, down-regulation of expected targets and apoptosis were seen in this model. The results of

these studies provide rationale for additional therapeutic studies to investigate over-expression of miR-34a in MM.

4.2.1 Limitations

As described above, there are many new advances in order to utilize miRNAs as therapeutic tools, although there will certainly be some limitations. One major limitation with targeting miRNAs is the issue of specificity, as a single miRNA has the potential to target many genes, and not all targets being investigated in preclinical studies. A second limitation is the concern of partial complementarity which may lead to significant off-target up-regulation or gene-silencing. The delivery mechanism of miRNAs to tissue specific sites also requires further investigation. As discussed previously, there has been work done to create stable, long lasting oligonucleotides for delivery or through the use of nano-particle technology. This provides an interesting approach to deliver miRNAs in a tissue specific manner, using targeted antibodies on the nano-particles. Promising miRNA delivery methods require further studies in animal models. miRNA therapeutics may be applicable to multiple malignancies and autoimmune and inflammatory disorders and have the potential to increase patient survival.

4.3 Conclusions

The biological significance of the miRNA gene signature identified in this study is not yet fully understood. However, additional miRNA identified in the microarray screen may also have important function in the pathogenesis of MM. As previously discussed, miRNAs are frequently located at fragile sites and genomic regions involved in cancer[81].

Many of the miRNA identified in the screen are at common translocation breakpoints common in MM. Specifically, miR-708 is located at11q14.1, adjacent to the translation site in the t(11;14) and miR-342-3p is located at 14q32.2 is is the site of rearrangement in the t(11;14) and t(4;14). Additionally, 1q21and 19p13 amplifications and 19q13 deletions are found in MM patients, which is the region where miR-92b, miR-181c/d, and miR-330-3p are located. Future study of these key miRNAs may provide additional insight into the pathogenesis of this disease. The miRNA gene signature identified may also provide insight on the use of 'bortezomib risk' signature as a predictor of treatment outcomes in patients. Additional work is needed to validate this signature in primary patient samples.

As the number of miRNAs investigated in the human genome increase each year, it has become increasingly clear that the regulation of specific target genes by miRNA and the influence on disease is highly complex. While most approaches have studied single miRNAs and single target effects, tumour initiation and progression is likely dependant on multiple miRNAs and target gene networks. It is therefore crucial for integration of target gene patterns with multiple miRNAs in order to investigate the role miRNAs may have as a diagnostic marker or therapeutic target. Although the work presented here on individual miRNA and targets have contributed to the understanding of bortezomib resistance in MM, it is important to investigate the links they may have with other miRNA networks and how this can be utilized for therapeutic targeting.

Overall, these results demonstrate that miR-34a and miR-181a expression has a significant influence on MM cell sensitivity to bortezomib and may support a potential therapeutic role for miRNA manipulation, in particular miR-34a in MM. Understanding the co-operating mechanisms of sensitivity to bortezomib will make it possible to design synergistic drug combinations and predict patient response to therapy as well as allow for a more targeted use of proteasome inhibitors. Understanding the biological basis of this signature will aid in the selection of novel therapies for patients. The study involving epigenetic and genetic alterations in MM cells has enhanced our understanding of the pathogenesis and mechanism of drug resistance. Much work is still needed to be done to fully elucidate this mechanism. Our data opens the possibility that the combination of bortezomib with altered miRNA expression may induce a synergistic effect in cell death in MM.

By uncovering the mechanisms of drug resistance and the influence of miRNA on myeloma cells, we have added to our understanding of the biology of this fatal disease and it may be possible to identify potential therapeutic targets, ultimately improving MM patient survival. While multiple myeloma patients present with many similar histological features, MM displays enormous genomic complexity including variation in clinical characteristics and patient survival. Based on the systems described previously, including concordant gene expression signatures, MM patients may be classified into more distinct groups for better treatments, therapies and increased survival rates. Subsequently, with further exploration of the results of this project, it may be possible to identify novel therapeutic targets for this incurable disease. The results of this project may have implications to cancer therapy beyond the disease investigated in this project.

References

1. Fonseca R, Bergsagel PL, Drach J, et al. International Myeloma Working Group molecular classification of multiple myeloma: spotlight review. *Leukemia.* Dec 2009;23(12):2210-2221.

2. Kyle RA, Rajkumar SV. Multiple myeloma. *N Engl J Med.* Oct 28 2004;351(18):1860-1873.

3. Sirohi B, Powles R. Multiple myeloma. *Lancet.* Mar 13 2004;363(9412):875-887.

4. Canadian Electronic Library (Firm), Public Health Agency of Canada., Canadian Cancer Society., Statistics Canada. Canadian cancer statistics 2011 featuring colorectal cancer. *Canadian cancer statistics,*. Toronto, Ont.: Canadian Cancer Society; 2011: http://ra.ocls.ca/ra/login.aspx?url=http://site.ebrary.com/lib/ocls/Doc?id=10471043.

5. Avet-Loiseau H. Role of genetics in prognostication in myeloma. *Best Pract Res Clin Haematol.* Dec 2007;20(4):625-635.

6. Zhan F, Huang Y, Colla S, et al. The molecular classification of multiple myeloma. *Blood.* Sep 15 2006;108(6):2020-2028.

7. Chng WJ, Glebov O, Bergsagel PL, Kuehl WM. Genetic events in the pathogenesis of multiple myeloma. *Best Pract Res Clin Haematol.* Dec 2007;20(4):571-596.

8. Kyle RA, Rajkumar SV. Criteria for diagnosis, staging, risk stratification and response assessment of multiple myeloma. *Leukemia.* Jan 2009;23(1):3-9.

9. Durie BG, Salmon SE. A clinical staging system for multiple myeloma. Correlation of measured myeloma cell mass with presenting clinical features, response to treatment, and survival. *Cancer.* Sep 1975;36(3):842-854.

10. Greipp PR, San Miguel J, Durie BG, et al. International staging system for multiple myeloma. *J Clin Oncol.* May 20 2005;23(15):3412-3420.

11. Kumar SK, Mikhael JR, Buadi FK, et al. Management of newly diagnosed symptomatic multiple myeloma: updated Mayo Stratification of Myeloma and Risk-Adapted Therapy (mSMART) consensus guidelines. *Mayo Clin Proc.* Dec 2009;84(12):1095-1110.

12. Kyle RA, Therneau TM, Rajkumar SV, et al. A long-term study of prognosis in monoclonal gammopathy of undetermined significance. *N Engl J Med.* Feb 21 2002;346(8):564-569.

13. Kyle RA, Remstein ED, Therneau TM, et al. Clinical course and prognosis of smoldering (asymptomatic) multiple myeloma. *N Engl J Med.* Jun 21 2007;356(25):2582-2590.

14. Hideshima T, Anderson KC. Molecular mechanisms of novel therapeutic approaches for multiple myeloma. *Nat Rev Cancer.* Dec 2002;2(12):927-937.

15. Maciejewski JP, Mufti GJ. Whole genome scanning as a cytogenetic tool in hematologic malignancies. *Blood.* Aug 15 2008;112(4):965-974.

16. Kuehl WM, Bergsagel PL. Multiple myeloma: evolving genetic events and host interactions. *Nat Rev Cancer.* Mar 2002;2(3):175-187.

17. Bergsagel PL, Chesi M, Nardini E, Brents LA, Kirby SL, Kuehl WM. Promiscuous translocations into immunoglobulin heavy chain switch regions in multiple myeloma. *Proc Natl Acad Sci U S A.* Nov 26 1996;93(24):13931-13936.

18. Shaughnessy J, Jr., Gabrea A, Qi Y, et al. Cyclin D3 at 6p21 is dysregulated by recurrent chromosomal translocations to immunoglobulin loci in multiple myeloma. *Blood.* Jul 1 2001;98(1):217-223.

19. Stewart AK, Bergsagel PL, Greipp PR, et al. A practical guide to defining high-risk myeloma for clinical trials, patient counseling and choice of therapy. *Leukemia.* Mar 2007;21(3):529-534.

20. Zhou Y, Barlogie B, Shaughnessy JD, Jr. The molecular characterization and clinical management of multiple myeloma in the post-genome era. *Leukemia.* Nov 2009;23(11):1941-1956.

21. Mahtouk K, Hose D, De Vos J, et al. Input of DNA microarrays to identify novel mechanisms in multiple myeloma biology and therapeutic applications. *Clin Cancer Res.* Dec 15 2007;13(24):7289-7295.

22. Bergsagel PL, Kuehl WM, Zhan F, Sawyer J, Barlogie B, Shaughnessy J, Jr. Cyclin D dysregulation: an early and unifying pathogenic event in multiple myeloma. *Blood.* Jul 1 2005;106(1):296-303.

23. Smadja NV, Bastard C, Brigaudeau C, Leroux D, Fruchart C. Hypodiploidy is a major prognostic factor in multiple myeloma. *Blood.* Oct 1 2001;98(7):2229-2238.

24. Bergsagel PL, Kuehl WM. Chromosome translocations in multiple myeloma. *Oncogene.* Sep 10 2001;20(40):5611-5622.

25. Fonseca R, Blood E, Rue M, et al. Clinical and biologic implications of recurrent genomic aberrations in myeloma. *Blood.* Jun 1 2003;101(11):4569-4575.

26. Shaughnessy J, Jacobson J, Sawyer J, et al. Continuous absence of metaphase-defined cytogenetic abnormalities, especially of chromosome 13 and hypodiploidy, ensures long-term survival in multiple myeloma treated with Total Therapy I: interpretation in the context of global gene expression. *Blood.* May 15 2003;101(10):3849-3856.

27. Richardson PG, Sonneveld P, Schuster MW, et al. Bortezomib or high-dose dexamethasone for relapsed multiple myeloma. *N Engl J Med.* Jun 16 2005;352(24):2487-2498.

28. Rajkumar SV, Hayman SR, Lacy MQ, et al. Combination therapy with lenalidomide plus dexamethasone (Rev/Dex) for newly diagnosed myeloma. *Blood.* Dec 15 2005;106(13):4050-4053.

29. Singhal S, Mehta J, Desikan R, et al. Antitumor activity of thalidomide in refractory multiple myeloma. *N Engl J Med.* Nov 18 1999;341(21):1565-1571.

30. Goldschmidt H, Hegenbart U, Wallmeier M, Hohaus S, Haas R. Factors influencing collection of peripheral blood progenitor cells following high-dose cyclophosphamide and granulocyte colony-stimulating factor in patients with multiple myeloma. *Br J Haematol.* Sep 1997;98(3):736-744.

31. Rajkumar SV, Gertz MA, Kyle RA, Greipp PR. Current therapy for multiple myeloma. *Mayo Clin Proc.* Aug 2002;77(8):813-822.

32. Gertz M. Transplantation for multiple myeloma. Pertinent Questions. *Blood.* Nov 15 2003;102(10):3472-3475.

33. Stockerl-Goldstein KE, Blume KG. A decade of progress in allogeneic hematopoietic cell transplantation: 1990-2000. *Adv Cancer Res.* 2001;81:1-59.

34. Gertz MA, Lacy MQ, Inwards DJ, et al. Early harvest and late transplantation as an effective therapeutic strategy in multiple myeloma. *Bone Marrow Transplant.* Feb 1999;23(3):221-226.

35. Wolf DH, Hilt W. The proteasome: a proteolytic nanomachine of cell regulation and waste disposal. *Biochim Biophys Acta.* Nov 29 2004;1695(1-3):19-31.

36. Adams J, Palombella VJ, Sausville EA, et al. Proteasome inhibitors: a novel class of potent and effective antitumor agents. *Cancer Res.* Jun 1 1999;59(11):2615-2622.

37. Hideshima T, Richardson P, Chauhan D, et al. The proteasome inhibitor PS-341 inhibits growth, induces apoptosis, and overcomes drug resistance in human multiple myeloma cells. *Cancer Res.* Apr 1 2001;61(7):3071-3076.

38. Glickman MH, Ciechanover A. The ubiquitin-proteasome proteolytic pathway: destruction for the sake of construction. *Physiol Rev.* Apr 2002;82(2):373-428.

39. Blade J, Cibeira MT, Rosinol L. Bortezomib: a valuable new antineoplastic strategy in multiple myeloma. *Acta Oncol.* 2005;44(5):440-448.

40. Tsukamoto S, Yokosawa H. Targeting the proteasome pathway. *Expert Opin Ther Targets.* May 2009;13(5):605-621.

41. Adams J. Proteasome inhibition: a novel approach to cancer therapy. *Trends Mol Med.* 2002;8(4 Suppl):S49-54.

42. Rajkumar SV, Richardson PG, Hideshima T, Anderson KC. Proteasome inhibition as a novel therapeutic target in human cancer. *J Clin Oncol.* Jan 20 2005;23(3):630-639.

43. Adams J. Development of the proteasome inhibitor PS-341. *Oncologist.* 2002;7(1):9-16.

44. Bross PF, Kane R, Farrell AT, et al. Approval summary for bortezomib for injection in the treatment of multiple myeloma. *Clin Cancer Res.* Jun 15 2004;10(12 Pt 1):3954-3964.

45. Johnston PB, Yuan R, Cavalli F, Witzig TE. Targeted therapy in lymphoma. *J Hematol Oncol.* 2010;3:45.

46. Chauhan D, Singh AV, Ciccarelli B, Richardson PG, Palladino MA, Anderson KC. Combination of novel proteasome inhibitor NPI-0052 and lenalidomide trigger in vitro and in vivo synergistic cytotoxicity in multiple myeloma. *Blood.* Jan 28 2010;115(4):834-845.

47. Teicher BA, Ara G, Herbst R, Palombella VJ, Adams J. The proteasome inhibitor PS-341 in cancer therapy. *Clin Cancer Res.* Sep 1999;5(9):2638-2645.

48. Orlowski RZ, Stinchcombe TE, Mitchell BS, et al. Phase I trial of the proteasome inhibitor PS-341 in patients with refractory hematologic malignancies. *J Clin Oncol.* Nov 15 2002;20(22):4420-4427.

49. Richardson PG, Barlogie B, Berenson J, et al. A phase 2 study of bortezomib in relapsed, refractory myeloma. *N Engl J Med.* Jun 26 2003;348(26):2609-2617.

50. Laubach J, Richardson P, Anderson K. Multiple myeloma. *Annu Rev Med.* Feb 18 2011;62:249-264.

51. Shah JJ, Orlowski RZ. Proteasome inhibitors in the treatment of multiple myeloma. *Leukemia.* Nov 2009;23(11):1964-1979.

52. Eldridge AG, O'Brien T. Therapeutic strategies within the ubiquitin proteasome system. *Cell Death Differ.* Jan 2010;17(1):4-13.

53. Karin M, Greten FR. NF-kappaB: linking inflammation and immunity to cancer development and progression. *Nat Rev Immunol.* Oct 2005;5(10):749-759.

54. Gilmore TD. Introduction to NF-kappaB: players, pathways, perspectives. *Oncogene.* Oct 30 2006;25(51):6680-6684.

55. Obeng EA, Carlson LM, Gutman DM, Harrington WJ, Jr., Lee KP, Boise LH. Proteasome inhibitors induce a terminal unfolded protein response in multiple myeloma cells. *Blood.* Jun 15 2006;107(12):4907-4916.

56. Nawrocki ST, Carew JS, Pino MS, et al. Bortezomib sensitizes pancreatic cancer cells to endoplasmic reticulum stress-mediated apoptosis. *Cancer Res.* Dec 15 2005;65(24):11658-11666.

57. Schroder M, Kaufman RJ. The mammalian unfolded protein response. *Annu Rev Biochem.* 2005;74:739-789.

58. Schroder M, Kaufman RJ. ER stress and the unfolded protein response. *Mutat Res.* Jan 6 2005;569(1-2):29-63.

59. Ri M, Iida S, Nakashima T, et al. Bortezomib-resistant myeloma cell lines: a role for mutated PSMB5 in preventing the accumulation of unfolded proteins and fatal ER stress. *Leukemia.* Aug 2010;24(8):1506-1512.

60. Chen S, Blank JL, Peters T, et al. Genome-wide siRNA screen for modulators of cell death induced by proteasome inhibitor bortezomib. *Cancer Res.* Jun 1 2010;70(11):4318-4326.

61. Zhu YX, Tiedemann R, Shi CX, et al. RNAi screen of the druggable genome identifies modulators of proteasome inhibitor sensitivity in myeloma including CDK5. *Blood.* Apr 7 2011;117(14):3847-3857.

62. Zhan F, Hardin J, Kordsmeier B, et al. Global gene expression profiling of multiple myeloma, monoclonal gammopathy of undetermined significance, and normal bone marrow plasma cells. *Blood.* Mar 1 2002;99(5):1745-1757.

63. Bartel DP. MicroRNAs: genomics, biogenesis, mechanism, and function. *Cell.* Jan 23 2004;116(2):281-297.

64. Babashah S, Soleimani M. The oncogenic and tumour suppressive roles of microRNAs in cancer and apoptosis. *Eur J Cancer.* May 2011;47(8):1127-1137.

65. Lee RC, Feinbaum RL, Ambros V. The C. elegans heterochronic gene lin-4 encodes small RNAs with antisense complementarity to lin-14. *Cell.* Dec 3 1993;75(5):843-854.

66. Reinhart BJ, Slack FJ, Basson M, et al. The 21-nucleotide let-7 RNA regulates developmental timing in Caenorhabditis elegans. *Nature.* Feb 24 2000;403(6772):901-906.

67. Kozomara A, Griffiths-Jones S. miRBase: integrating microRNA annotation and deep-sequencing data. *Nucleic Acids Res.* Jan 2011;39(Database issue):D152-157.

68. Griffiths-Jones S. miRBase: microRNA sequences and annotation. *Curr Protoc Bioinformatics.* Mar 2010;Chapter 12:Unit 12 19 11-10.

69. Griffiths-Jones S, Saini HK, van Dongen S, Enright AJ. miRBase: tools for microRNA genomics. *Nucleic Acids Res.* Jan 2008;36(Database issue):D154-158.

70. Griffiths-Jones S. miRBase: the microRNA sequence database. *Methods Mol Biol.* 2006;342:129-138.

71. Griffiths-Jones S, Grocock RJ, van Dongen S, Bateman A, Enright AJ. miRBase: microRNA sequences, targets and gene nomenclature. *Nucleic Acids Res.* Jan 1 2006;34(Database issue):D140-144.

72. Berezikov E, Guryev V, van de Belt J, Wienholds E, Plasterk RH, Cuppen E. Phylogenetic shadowing and computational identification of human microRNA genes. *Cell.* Jan 14 2005;120(1):21-24.

73. Harfe BD. MicroRNAs in vertebrate development. *Curr Opin Genet Dev.* Aug 2005;15(4):410-415.

74. Lee Y, Kim M, Han J, et al. MicroRNA genes are transcribed by RNA polymerase II. *Embo J.* Oct 13 2004;23(20):4051-4060.

75. Cai X, Hagedorn CH, Cullen BR. Human microRNAs are processed from capped, polyadenylated transcripts that can also function as mRNAs. *RNA.* Dec 2004;10(12):1957-1966.

76. Lund E, Guttinger S, Calado A, Dahlberg JE, Kutay U. Nuclear export of microRNA precursors. *Science.* Jan 2 2004;303(5654):95-98.

77. Diederichs S, Haber DA. Dual role for argonautes in microRNA processing and posttranscriptional regulation of microRNA expression. *Cell.* Dec 14 2007;131(6):1097-1108.

78. Chendrimada TP, Gregory RI, Kumaraswamy E, et al. TRBP recruits the Dicer complex to Ago2 for microRNA processing and gene silencing. *Nature.* Aug 4 2005;436(7051):740-744.

79. Kawamata T, Tomari Y. Making RISC. *Trends Biochem Sci.* Jul 2010;35(7):368-376.

80. Khvorova A, Reynolds A, Jayasena SD. Functional siRNAs and miRNAs exhibit strand bias. *Cell.* Oct 17 2003;115(2):209-216.

81. Calin GA, Sevignani C, Dumitru CD, et al. Human microRNA genes are frequently located at fragile sites and genomic regions involved in cancers. *Proc Natl Acad Sci U S A.* Mar 2 2004;101(9):2999-3004.

82. Bullrich F, Fujii H, Calin G, et al. Characterization of the 13q14 tumor suppressor locus in CLL: identification of ALT1, an alternative splice variant of the LEU2 gene. *Cancer Res.* Sep 15 2001;61(18):6640-6648.

83. McManus MT. MicroRNAs and cancer. *Semin Cancer Biol.* Aug 2003;13(4):253-258.

84. Gregory RI, Shiekhattar R. MicroRNA biogenesis and cancer. *Cancer Res.* May 1 2005;65(9):3509-3512.

85. Chen CZ. MicroRNAs as oncogenes and tumor suppressors. *N Engl J Med.* Oct 27 2005;353(17):1768-1771.

86. Esquela-Kerscher A, Slack FJ. Oncomirs - microRNAs with a role in cancer. *Nat Rev Cancer.* Apr 2006;6(4):259-269.

87. Calin GA, Dumitru CD, Shimizu M, et al. Frequent deletions and down-regulation of micro- RNA genes miR15 and miR16 at 13q14 in chronic

lymphocytic leukemia. *Proc Natl Acad Sci U S A.* Nov 26 2002;99(24):15524-15529.

88. Cimmino A, Calin GA, Fabbri M, et al. miR-15 and miR-16 induce apoptosis by targeting BCL2. *Proc Natl Acad Sci U S A.* Sep 27 2005;102(39):13944-13949.

89. Calin GA, Croce CM. MicroRNA-cancer connection: the beginning of a new tale. *Cancer Res.* Aug 1 2006;66(15):7390-7394.

90. Verhaak RG, Wouters BJ, Erpelinck CA, et al. Prediction of molecular subtypes in acute myeloid leukemia based on gene expression profiling. *Haematologica.* Jan 2009;94(1):131-134.

91. Jongen-Lavrencic M, Sun SM, Dijkstra MK, Valk PJ, Lowenberg B. MicroRNA expression profiling in relation to the genetic heterogeneity of acute myeloid leukemia. *Blood.* May 15 2008;111(10):5078-5085.

92. Calin GA, Croce CM. Chronic lymphocytic leukemia: interplay between noncoding RNAs and protein-coding genes. *Blood.* Nov 26 2009;114(23):4761-4770.

93. Zhou Y, Chen L, Barlogie B, et al. High-risk myeloma is associated with global elevation of miRNAs and overexpression of EIF2C2/AGO2. *Proc Natl Acad Sci U S A.* Apr 27 2010;107(17):7904-7909.

94. Gutierrez NC, Sarasquete ME, Misiewicz-Krzeminska I, et al. Deregulation of microRNA expression in the different genetic subtypes of multiple myeloma and correlation with gene expression profiling. *Leukemia.* Mar 2010;24(3):629-637.

95. Lionetti M, Biasiolo M, Agnelli L, et al. Identification of microRNA expression patterns and definition of a microRNA/mRNA regulatory network in distinct molecular groups of multiple myeloma. *Blood.* Dec 10 2009;114(25):e20-26.

96. Roccaro AM, Sacco A, Thompson B, et al. MicroRNAs 15a and 16 regulate tumor proliferation in multiple myeloma. *Blood.* Jun 25 2009;113(26):6669-6680.

97. Pichiorri F, Suh SS, Ladetto M, et al. MicroRNAs regulate critical genes associated with multiple myeloma pathogenesis. *Proc Natl Acad Sci U S A.* Sep 2 2008;105(35):12885-12890.

98. Livak KJ, Schmittgen TD. Analysis of relative gene expression data using real-time quantitative PCR and the 2(-Delta Delta C(T)) Method. *Methods.* Dec 2001;25(4):402-408.

99. Chim CS, Wong KY, Qi Y, et al. Epigenetic inactivation of the miR-34a in hematological malignancies. *Carcinogenesis.* Apr 2010;31(4):745-750.

100. Neri P, Ren L, Gratton K, et al. Bortezomib induced BRCAness sensitizes multiple myeloma cells to PARP inhibitors. *Blood.* Sep 13 2011.

101. Burnett JC, Rossi JJ. RNA-based therapeutics: current progress and future prospects. *Chem Biol.* Jan 27 2012;19(1):60-71.

102. Bommer GT, Gerin I, Feng Y, et al. p53-mediated activation of miRNA34 candidate tumor-suppressor genes. *Curr Biol.* Aug 7 2007;17(15):1298-1307.

103. Dijkstra MK, van Lom K, Tielemans D, et al. 17p13/TP53 deletion in B-CLL patients is associated with microRNA-34a downregulation. *Leukemia.* Mar 2009;23(3):625-627.

104. Lodygin D, Tarasov V, Epanchintsev A, et al. Inactivation of miR-34a by aberrant CpG methylation in multiple types of cancer. *Cell Cycle.* Aug 15 2008;7(16):2591-2600.

105. Wehner KA, Schutz S, Sarnow P. OGFOD1, a novel modulator of eukaryotic translation initiation factor 2alpha phosphorylation and the cellular response to stress. *Mol Cell Biol.* Apr 2010;30(8):2006-2016.

106. Kimball SR. Eukaryotic initiation factor eIF2. *Int J Biochem Cell Biol.* Jan 1999;31(1):25-29.

107. Shi L, Cheng Z, Zhang J, et al. hsa-mir-181a and hsa-mir-181b function as tumor suppressors in human glioma cells. *Brain Res.* Oct 21 2008;1236:185-193.

108. Debernardi S, Skoulakis S, Molloy G, Chaplin T, Dixon-McIver A, Young BD. MicroRNA miR-181a correlates with morphological sub-class of acute myeloid leukaemia and the expression of its target genes in global genome-wide analysis. *Leukemia.* May 2007;21(5):912-916.

109. Chen CZ, Li L, Lodish HF, Bartel DP. MicroRNAs modulate hematopoietic lineage differentiation. *Science.* Jan 2 2004;303(5654):83-86.

110. Guessous F, Zhang Y, Kofman A, et al. microRNA-34a is tumor suppressive in brain tumors and glioma stem cells. *Cell Cycle.* Mar 15 2010;9(6):1031-1036.

111. Chang TC, Wentzel EA, Kent OA, et al. Transactivation of miR-34a by p53 broadly influences gene expression and promotes apoptosis. *Mol Cell.* Jun 8 2007;26(5):745-752.

112. Welch C, Chen Y, Stallings RL. MicroRNA-34a functions as a potential tumor suppressor by inducing apoptosis in neuroblastoma cells. *Oncogene.* Jul 26 2007;26(34):5017-5022.

113. Gallardo E, Navarro A, Vinolas N, et al. miR-34a as a prognostic marker of relapse in surgically resected non-small-cell lung cancer. *Carcinogenesis.* Nov 2009;30(11):1903-1909.

114. Li N, Fu H, Tie Y, et al. miR-34a inhibits migration and invasion by down-regulation of c-Met expression in human hepatocellular carcinoma cells. *Cancer Lett.* Mar 8 2009;275(1):44-53.

115. Pichiorri F, Suh SS, Rocci A, et al. Downregulation of p53-inducible microRNAs 192, 194, and 215 impairs the p53/MDM2 autoregulatory loop in multiple myeloma development. *Cancer Cell.* Oct 19 2010;18(4):367-381.

116. Raver-Shapira N, Marciano E, Meiri E, et al. Transcriptional activation of miR-34a contributes to p53-mediated apoptosis. *Mol Cell.* Jun 8 2007;26(5):731-743.

117. Fabbri M, Bottoni A, Shimizu M, et al. Association of a microRNA/TP53 feedback circuitry with pathogenesis and outcome of B-cell chronic lymphocytic leukemia. *JAMA.* Jan 5 2011;305(1):59-67.

118. Kumar M, Lu Z, Takwi AA, et al. Negative regulation of the tumor suppressor p53 gene by microRNAs. *Oncogene.* Feb 17 2011;30(7):843-853.

119. Hermeking H. p53 enters the microRNA world. *Cancer Cell.* Nov 2007;12(5):414-418.

120. Chang H, Sloan S, Li D, Keith Stewart A. Multiple myeloma involving central nervous system: high frequency of chromosome 17p13.1 (p53) deletions. *Br J Haematol.* Nov 2004;127(3):280-284.

121. Gertz MA, Lacy MQ, Dispenzieri A, et al. Clinical implications of t(11;14)(q13;q32), t(4;14)(p16.3;q32), and -17p13 in myeloma patients treated with high-dose therapy. *Blood.* Oct 15 2005;106(8):2837-2840.

122. Guo Y, Li S, Qu J, et al. MiR-34a inhibits lymphatic metastasis potential of mouse hepatoma cells. *Mol Cell Biochem.* Aug 2011;354(1-2):275-282.

123. Hermeking H. The miR-34 family in cancer and apoptosis. *Cell Death Differ.* Feb 2010;17(2):193-199.

124. Issa JP, Kantarjian HM. Targeting DNA methylation. *Clin Cancer Res.* Jun 15 2009;15(12):3938-3946.

125. Fenaux P, Mufti GJ, Hellstrom-Lindberg E, et al. Efficacy of azacitidine compared with that of conventional care regimens in the treatment of higher-risk myelodysplastic syndromes: a randomised, open-label, phase III study. *Lancet Oncol.* Mar 2009;10(3):223-232.

126. Fenaux P, Mufti GJ, Hellstrom-Lindberg E, et al. Azacitidine prolongs overall survival compared with conventional care regimens in elderly patients with low bone marrow blast count acute myeloid leukemia. *J Clin Oncol.* Feb 1 2010;28(4):562-569.

127. de Lima M, Giralt S, Thall PF, et al. Maintenance therapy with low-dose azacitidine after allogeneic hematopoietic stem cell transplantation for recurrent

acute myelogenous leukemia or myelodysplastic syndrome: a dose and schedule finding study. *Cancer.* Dec 1 2010;116(23):5420-5431.

128. Gordon S, Akopyan G, Garban H, Bonavida B. Transcription factor YY1: structure, function, and therapeutic implications in cancer biology. *Oncogene.* Feb 23 2006;25(8):1125-1142.

129. Chen QR, Yu LR, Tsang P, et al. Systematic proteome analysis identifies transcription factor YY1 as a direct target of miR-34a. *J Proteome Res.* Feb 4 2011;10(2):479-487.

130. Baughn LB, Di Liberto M, Wu K, et al. A novel orally active small molecule potently induces G1 arrest in primary myeloma cells and prevents tumor growth by specific inhibition of cyclin-dependent kinase 4/6. *Cancer Res.* Aug 1 2006;66(15):7661-7667.

131. Epstein J, Yaccoby S. The SCID-hu myeloma model. *Methods Mol Med.* 2005;113:183-190.

132. Krutzfeldt J, Rajewsky N, Braich R, et al. Silencing of microRNAs in vivo with 'antagomirs'. *Nature.* Dec 1 2005;438(7068):685-689.

133. Orom UA, Kauppinen S, Lund AH. LNA-modified oligonucleotides mediate specific inhibition of microRNA function. *Gene.* May 10 2006;372:137-141.

134. Garzon R, Marcucci G, Croce CM. Targeting microRNAs in cancer: rationale, strategies and challenges. *Nat Rev Drug Discov.* Oct 2010;9(10):775-789.

135. Vester B, Wengel J. LNA (locked nucleic acid): high-affinity targeting of complementary RNA and DNA. *Biochemistry.* Oct 26 2004;43(42):13233-13241.

136. Ebert MS, Sharp PA. Emerging roles for natural microRNA sponges. *Curr Biol.* Oct 12 2010;20(19):R858-861.

137. Ebert MS, Sharp PA. MicroRNA sponges: progress and possibilities. *RNA.* Nov 2010;16(11):2043-2050.

138. Elmen J, Lindow M, Schutz S, et al. LNA-mediated microRNA silencing in non-human primates. *Nature.* Apr 17 2008;452(7189):896-899.